Processing of a multichannel seismic reflection survey in the Hebridean region with special emphasis on improvements in velocity analysis

Richard William Hobbs

Processing of a Multichannel Seismic Reflection Survey in the Hebridean Region with Special Emphasis on Improvements in Velocity Analysis

by

Richard William Hobbs

Volume I

A thesis submitted for the degree of
Doctor of Philosophy at the University of Durham

Graduate Society August, 1985

ABSTRACT

This thesis presents the results of a multichannel reflection survey conducted off of the Western Isles of Scotland in 1981 in the Sea of the Hebrides region. Ten profiles were acquired to 12 seconds two-way time using an air-gun source and a 2.4 km 24 channel receiver, yielding 24 fold coverage with a gather spacing of 50 metres. The data have been processed at Durham using the reflection seismic processing software developed there over the past six years. The interpretation shows that the Mesozoic basins lie unconformably on up to 5 km thickness of Torridonian sediments, which in turn lie uncomformably on Lewisian crystalline basement. The presence of eastward dipping events in the basement are associated with thrust faults and are probably of Caledonian age. The later reactivation of these faults has controlled the formation of the Mesozoic basins.

The thesis also contains details of the modifications made to both the computer hardware and the processing software of the Durham Seismic Processing System during the life-time of this project. The expansion of the facility has enabled a larger selection of faster algorithms to be written for the processing of multichannel reflection data. These include velocity filtering, autostatics and dip filtering routines. Particular attention has been given to the accurate determination of the velocity function used when processing the data and how this information may be used to help the geological interpretation.

ACKNOWLEDGEMENTS

I would like to thank Prof. M.H.P.Bott for allowing me the use the facilities in the Department of Geological Sciences and my supervisor Prof. G. K. Westbrook. Many thanks must also be given to all the memebers of staff, technicians and post-graduate students at Durham for their help and advice. In particular Dr. D. W. Wellby for help in re-writing the reflection seismic processing package and C. Uruski for his detailed knowledge of the sub-crop geology in the region.

Of my visit to the United States for six months, I must thank the staff and students at the Lamont-Doherty Geological Observatory. In particular the members of the Multichannel Seismic group, P. Buhl, J. Mutter, J. Ladd and G. Mountain. Special thanks must be extended to the last two for allowing me to use parts of their data as examples in this thesis. J. Ladd for the Aleutians data (NSF grant OCE82-08833) and G. Mountain for the Moroccan data (NSF grant OCE82-15430).

Thanks must go to the staff at Research Vessel Services who took part in the Farnella 1/81 cruise and for the use of their receiver array, air-guns, etc., J. Marr and Sons for the ship, and finally N.E.R.C. for the research grant.

CONTENTS

APPENDIX 1
Abridged watch keeper log
Positional fixes determined by Decca Co. Ltd.
Specifications of the SDS 1010 system
Sub-crop geology map (UTM) 1:250 000
Track chart (UTM) 1:250 000
Uninterpreted sections

APPENDIX 2
Computer software and documentation
(Separate volume 390 pp.)

LIST OF FIGURES

LIST OF TABLES

CHAPTER 1

INTRODUCTION

1.1 The Farnella 1/81 Cruise

During September 1981 a marine seismic reflection survey was conducted off of the Western Isles of Scotland. The area covered extended between Mull in the south east, to Skye in the north and to west of Berneray (Fig. 1.1). The interpretation of this data was to help define the tectonic evolution of the area, firstly identifying and tracing eastward dipping thrust faults formed during the Caledonian orogeny, then secondly by determining how the re-activation of these faults in the Mesozoic era, caused by the opening of the North Atlantic, influenced the formation and shape of the Sea of the Hebrides Basin.

The profiles shown in Fig. 1.1 can be broken into three separate regions. The first group lie to the south-west of Mull, these were intended to cross the line of the Moine thrust which is believed to pass between the Ross of Mull and the island of Iona. The second set cross back and forth across the southern extent of the Sea of the Hebrides Basin, the most northerly of these, between Tiree and Barra, follows the same line as that used in a refraction survey presented in Summers' Ph.D. thesis, (1982). The final two profiles were collected between Isle of Skye and Rhum, crossing the Kishorn and Moine Thrusts.

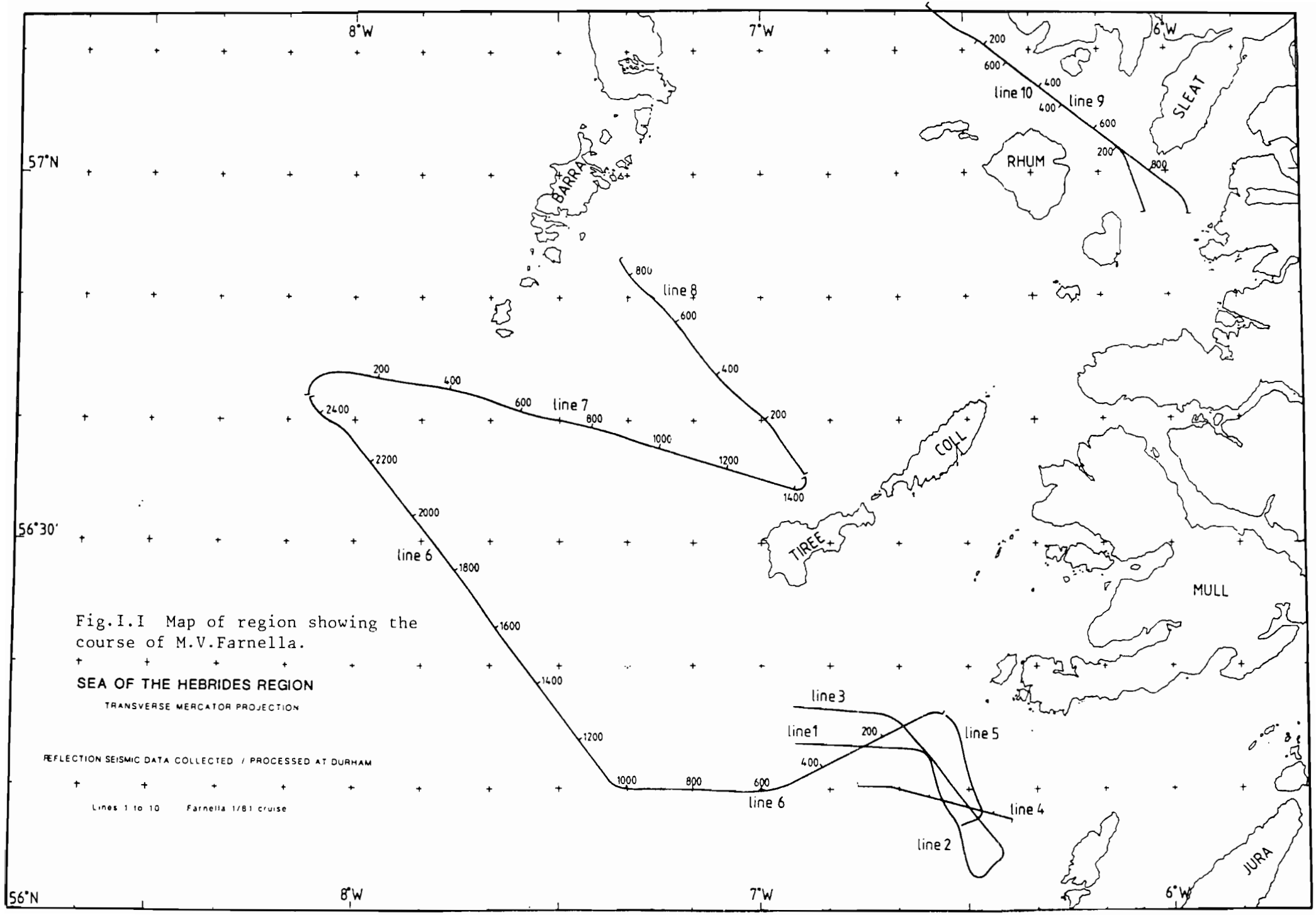

Fig.I.I Map of region showing the course of M.V.Farnella.

SEA OF THE HEBRIDES REGION

TRANSVERSE MERCATOR PROJECTION

REFLECTION SEISMIC DATA COLLECTED / PROCESSED AT DURHAM

Lines 1 to 10 Farnella 1/81 cruise

1.2 General Geological Regime

The near surface geology of this area is covered in an Institute of Geological Sciences Report 73/14 (1974) by Binns, McQuillin and Kenolty. The principle geological features (Fig. 1.2) show a north-east to south-west trend and are divided into two distinct areas by the Moine Thrust. This thrust represents the most major fault of a zone which runs down the west coast of mainland Scotland, across the Sleat peninsular of Skye then off of the coast probably passing between the Ross of Mull and Iona. Several smaller thrusts lie immediately to the west within the zone of which the Kishorn Thrust is the most westerly.

To the east of the Moine Thrust lie folded Precambrian and Palaeozoic rocks deformed by the Caledonian orogeny, some of the Moinian rocks in this area were probably already deformed in the earlier Grenvillian orogeny.

To the west of the Moine Thrust belt are half graben basins, fault-bounded on the western sides and filled with Mesozoic sediments sitting uncomformably on Precambrian Torridonian sediments, which, in turn, lie unconformably on crystalline Lewisian basement.

1.2.1 Basement

The Lewisian basement composed of highly metamorphosed rock probably underlies the whole of north west Britain, the most major exposures are to be found in the area to the west of the Moine Thrust belt. Here it is found to form platforms separating the later Mesozoic basins, e.g. the Tiree Platform, the Outer

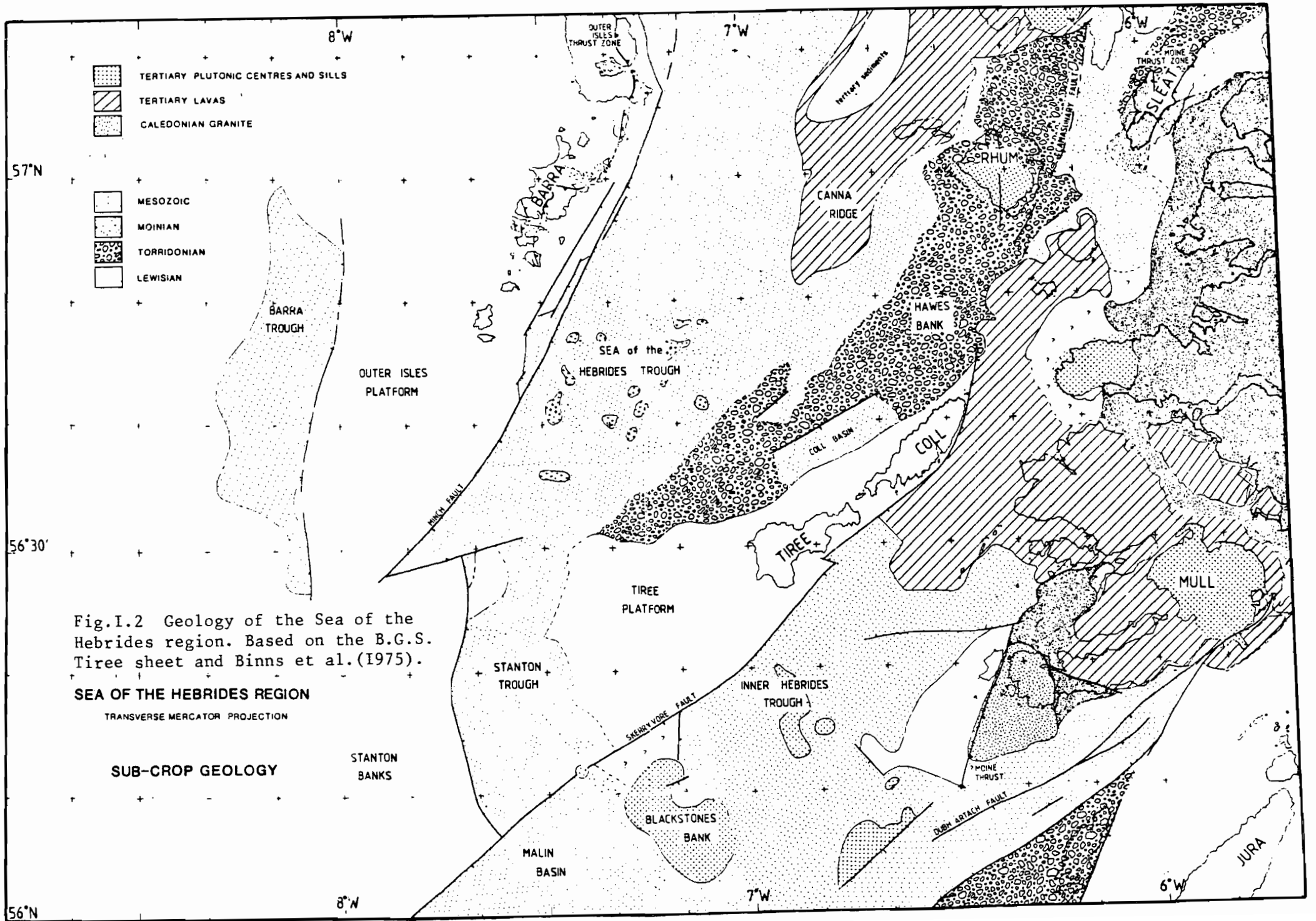

Fig.I.2 Geology of the Sea of the Hebrides region. Based on the B.G.S. Tiree sheet and Binns et al.(1975).

Isles Platform. The rocks have undergone two periods of metamorphism; the Scourian dated at about 2500 Ma, and the Laxfordian dated at 1600 Ma. A detailed account is given by Watson (1983). On shore exposures of the Lewisian show a hilly terrain which has been covered uncomformably by the Torridonian sequences.

1.2.2 Pre-Caledonian Orogeny Sediments

Within the area under review the Torridonian group outcrops on Skye, on Rhum, on Iona, forms the Hawes Bank to the west of the Camasunary-Skerryvore fault, and is believed to underlie the eastern edge of the Sea of the Hebrides Basin (Binns et al. 1975). It is composed of two main groups that were deposited with a 200 Ma separation. The earlier Stoer Group is about 2 km thick (Harris 1983), and the younger Torridon Group has a thickness of up to 7 km. Both sequences are predominantly made up of conglomerates and sandstones (Johnson 1983). Cambrian and lower Ordovician sequences may be found immediately to the west of the Moine Thrust belt some 20 km wide. The sequence ~~is carbonate in nature~~ includes quartzites and carbonates and may have a total thickness of about 1.5 km.

1.2.3 Post Caledonian Orogeny Sediments

During the Devonian and Carboniferous the Western Isles remained as a land mass, but there is evidence of erratics from this period in the Outer Hebrides (Jehu and Craig 1925).

The Permian and Triassic marked the start of a period which saw much deposition of sediments round Britain including the

Western Isles. Figure 1.3 shows the active basins around Scotland,although little on-shore outcrop now remains.Jurassic sediments may be found on Skye, Raasay, Mull and Ardnamurchan, those on Skye being some 600 metres thick. During the Jurassic period substantial thicknesses of sediments accumulated in the basins in this area. Land exposures of Cretaceous and Tertiary sediments are widespread, but only in thin sequences. These probablyrepresent the remnants of extensive deposits which have been subsequenty eroded to expose the older rocks beneath. Binns et al. (1974) suggest that there are up to 3 km of Mesozoic sediments in the deeper parts of the Sea of the Hebrides Trough.

During the Tertiary, igneous activity in the Western Isles region covered large areas with lava flows (Emeleus 1983). Evidence of these can clearly be seen on land with the plutonic centres of Skye, Rhum, Ardnamurchan and Mull, composed of both basic and acid igneous rock. The large positive gravity anomolies indicate that the Blackstones Bank is also underlain by an intrusive body with emplacement in the late Cretaceous (Durant et al. 1976) or early Tertiary (Mitchell et al. 1976). Modelling shows it to be a cylinder of about 5 km in radius and 16 km depth with a density of 3100 kg m^{-3} (Binns et al. 1974).

During the recent ice ages the whole area has been greatly eroded, and most of the off-shore geology is covered by Quaternary sediments of varying thickness.

The sub-crop geology,based on the map produced by Binns et al. (1975) and the British Geological Survey (1984) Solid Geology Tiree sheet compiled by Evans, is shown in Fig. 1.2. This

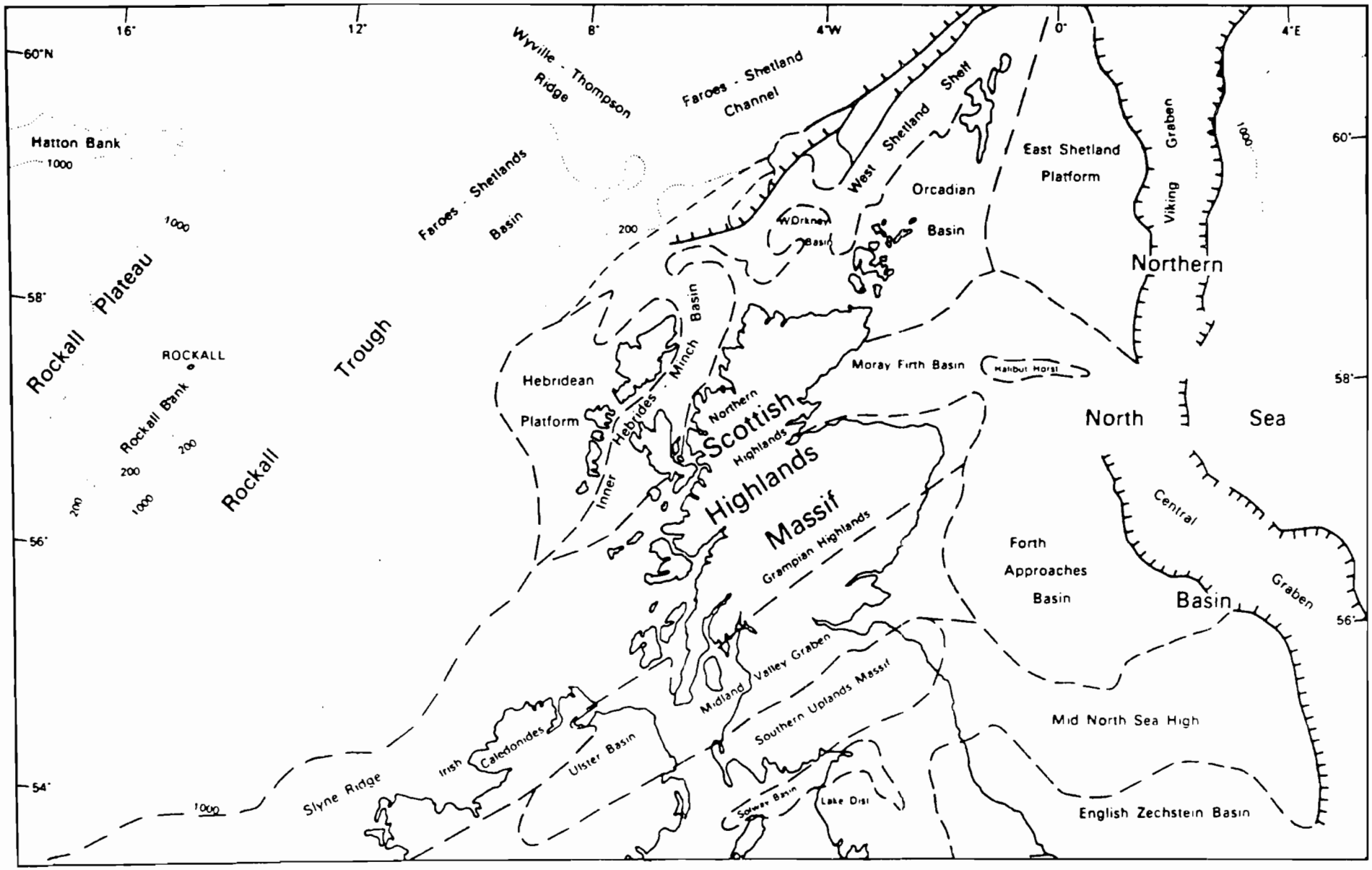

Fig.I.3 Mesozoic basins around Scotland. After Kent (1975).

interpretation is supported by subsequent work by C. Uruski.

1.2.4 Tectonic Evolution of the Western Isles

As mentioned above, the Caledonian Orogeny is believed to have been responsible for the shaping of this area (Watson 1984). It is accepted that the orogeny occurred on the closure between the Laurentia plate and the Baltica plate (Fig. 1.4a) (Dewey 1969, 1982, Phillips et al. 1976, McKerrow 1982), with subduction and dextral movement along the Iapetus Suture. Van der Voo et al. (1981) and others propose large sinistral displacement, during the mid-Devonian to Carboniferous, along the line of the Great Glen Fault of some 2000 km (Fig. 1.4b). However, Briden et al. (1982) show paleomagnetic evidence of polar wandering paths from igneous and metamorphic rocks either side of the Great Glen Fault, that no such major movement could have occurred and placed an upper limit of only one or two hundred kilometres. Dewey (1982) suggests that the 2000 km of stike-slip sinistral movement was distributed among ten or more faults with about 100 km of displacement on each. Some dextral movement along the Great Glen fault during this period is also proposed by Holgate (1969) but Dewey and Shackleton (1984) believe this to be Carboniferous.

A more recent model for the area proposed by Soper and Hutton (1984) put forward a three plate system (Fig. 1.5). Here the east west collision between Laurentia and Baltica forms the Caledonides, with the later accretion of the Cadomia etc. micro-continents onto the south eastern boundary. The metamorphism associated with the orogenic event in this region peaked during

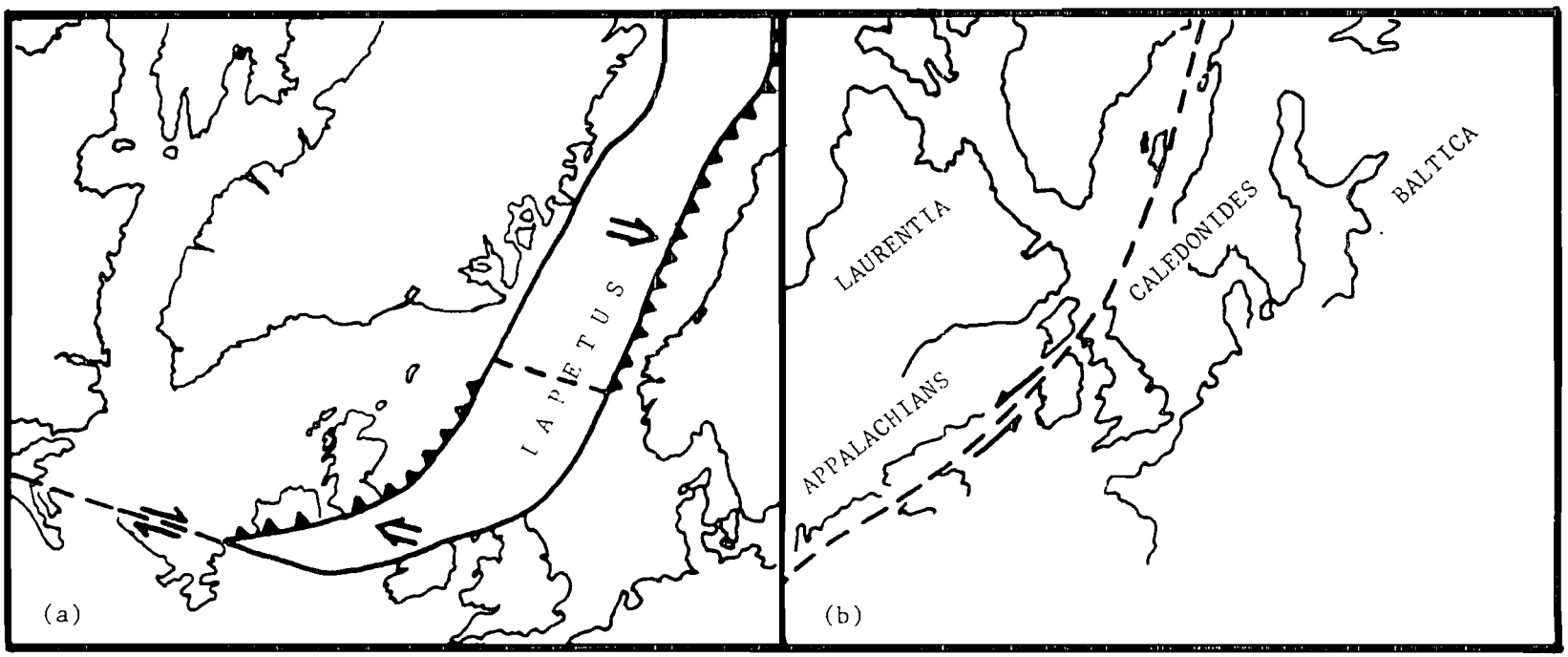

Fig.I.4 Tectonic evolution of the Caledonides.
(a) Closure of the Iapetus Ocean. After McKerrow (I982)
(b) Sinistral movement along the Great Glen Fault. After Ziegler (I982)

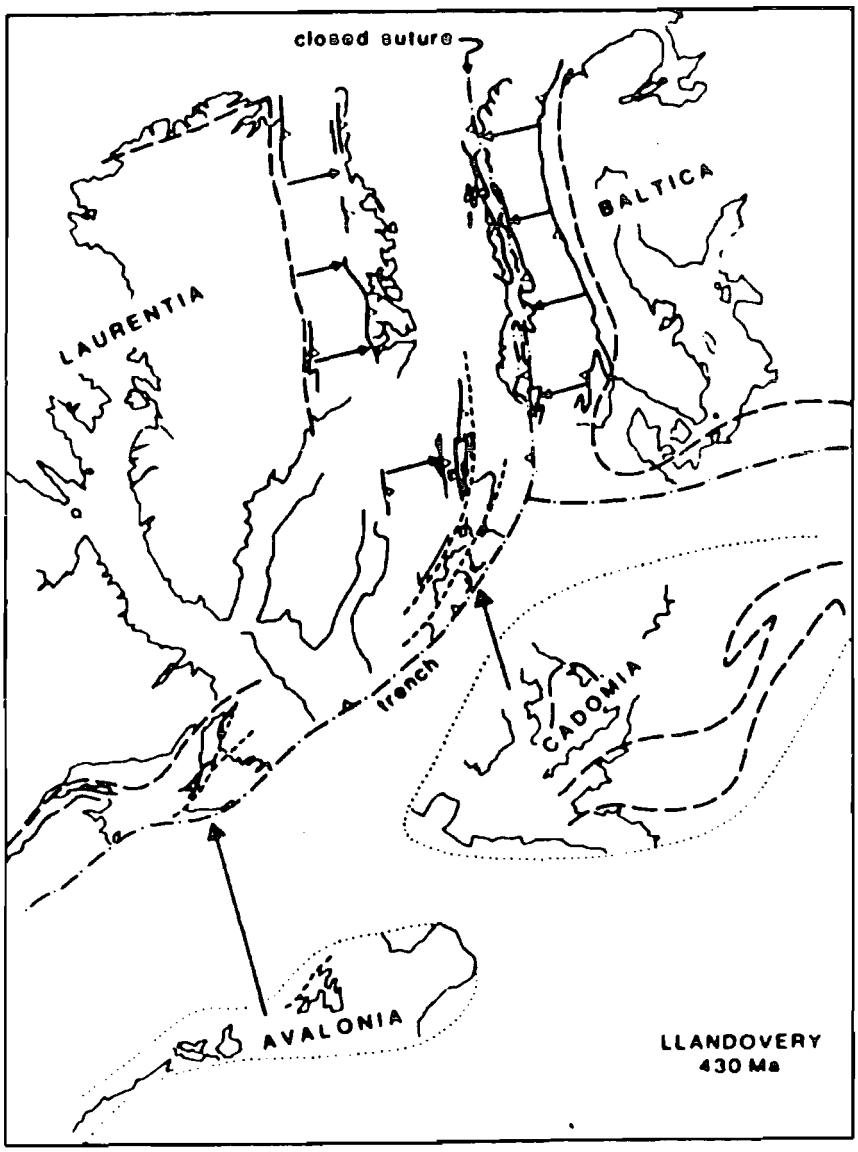

Fig.1.5 Reconstruction of the North Atlantic Caledonides. After Soper and Hutton (1984).

the mid-Ordovician. Crustal thickening probably started some tens of millions of years earlier further to the east along the Sgurr Beag Slide (Soper et al. 1984). Thrusting propagated westwards to the Moine Thrust and finally to the Outer Isles Thrust and Flannan Thrust. Butler et al. (1984) propose a total movement of 54 km along the Moine Thrust region with only a small displacement on the Outer Isles Thrust, Sibson (1977) estimates a movement of 10 km. By mid-Silurian times the orogeny was to have finished and cooling and erosion had begun. In late Silurian the Ross of Mull granite was emplaced (Harris 1983). Soper and Hutton (1984) futher propose that sinistral movement along north-east south-west faults, e.g. the Great Glen and the Highland Boundary faults, though representing a distinct period of stress within the region, did occur at the end of the Caledonian during the mid-Silurian and probably overlapped with the final stages of the main orogenic event.

Tensional stress was imposed on north-west Europe prior to the opening of the North Atlantic. This resulted in the graben collapse in the North Sea during the middle Jurassic, it also caused the reactivation of the Western Isles thrust faults, formed in the Caledonian , to act as low angle normal faults. How the reworking of earlier events may determine the geometry of later extensional or compressional phases has been investigated by Gibbs (1984a). This stress regime continued into the Cretaceous while the creation of the North Atlantic Ocean began. After the graben formation in the North Sea, an oceanic spreading axis appeared briefly in the Rockall Trough followed by a more major

speading phase forming the Labrador Sea west of Greenland, before settling between Rockall and Greenland in the Tertiary era.

1.3 Data Acqusition, Processing and Interpretation

Airguns were used to provide a repeatable acoustic source for the whole survey. The reflected seismic energy was picked up on a 2.4 km streamer towed behind the ship consisting of 24 receivers spaced at 100 metre intervals. The received data were sampled and digitally stored on magnetic tape using the acquisition system obtained by Durham from Western Geophysical in 1976. The processing of this data was to be done on the Durham Seismic Processing System set up by Poulter (1982).

The concept of using the reflection profiling techniques to determine middle and deep crustal structure has since been well proven by the British Institutions Reflection Profiling Syndicate, B.I.R.P.S, data (Smythe et al. 1982, Brewer et al. 1983, Brewer et al. 1984). The results from one of the surveys conducted in 1983 will be presented in later chapters.

1.4 Durham Seismic Reflection Processing System

The principles of reflection seismic processing are well documented in standard texts, Dobrin (1976), Telford et al. (1976) and Sheriff et al. (1983). The system set up at Durham (Poulter 1982) showed that it was possible to achieve an acceptable level of processing using a mini-computer provided with a small array processor, from the basic manipulation of the data during demultiplex to migration of final sections.

During this project the computer hardware has been upgraded. This has enabled improvements to be made to the original software, not only by the addition of extra processing routines but by making it quicker and easier to operate. It has also been possible to obtain many different data sets to test the system performance which was not possible with the original system, because of the non-standard data format used. This has meant that the verification of each stage of the processing sequence enabled the quick identification and removal of programming errors. Besides the 1980 Caribbean data and the 1981 Western Isles data, two profiles from the Lamont Doherty Geological Observatory, New York, have been processed. One of these profiles crosses the Aleutian accretionary prism, the other is a profile from the Morrocan margin which has been used for several processing examples included in this thesis. Data from a National Coal Board survey along with synthetic data from the AIMS package (Geoquest Inc.) have been processed and are presented by Jifon in his Ph.D. thesis (1984). Some of the algorithms have been tested using data acquired from a reflection seismic modelling tank in Durham (Sharp 1985).

1.5 Other Geophysical Data from the Western Isles Region

The Institute of Geological Sciences report 73/14 (1974) by Binns et al. includes data from several other geophysical techniques, namely gravity and aeromagnetics, as well as interpretations of reflection seismic lines produced by Seismograph Services Ltd. in 1969. Results from this report have

been used as a starting point for the interpretation of the Farnella 1/81 data. Shaw (1978) presented models of the sedimentary structure for the Sea of the Hebrides based on gravity, these models are reviewed with respect to the results of this project. A section of commercial speculative survey, currently in the possession of the British Geological Servey, which crosses the research area has been reprocessed in Durham. The B.I.R.P.S. WINCH (Brewer et al. 1983) profile passes through the south west corner of the area and approximately following part of one of the Farnella 1/81 profiles. Figure 1.6 shows all the reflection data used in the interpretation and the position of the five explosive charges fired in the Sea of the Hebrides Basin for the Western Isles (refraction) Seismic Experiment (WISE) (Summers 1982).

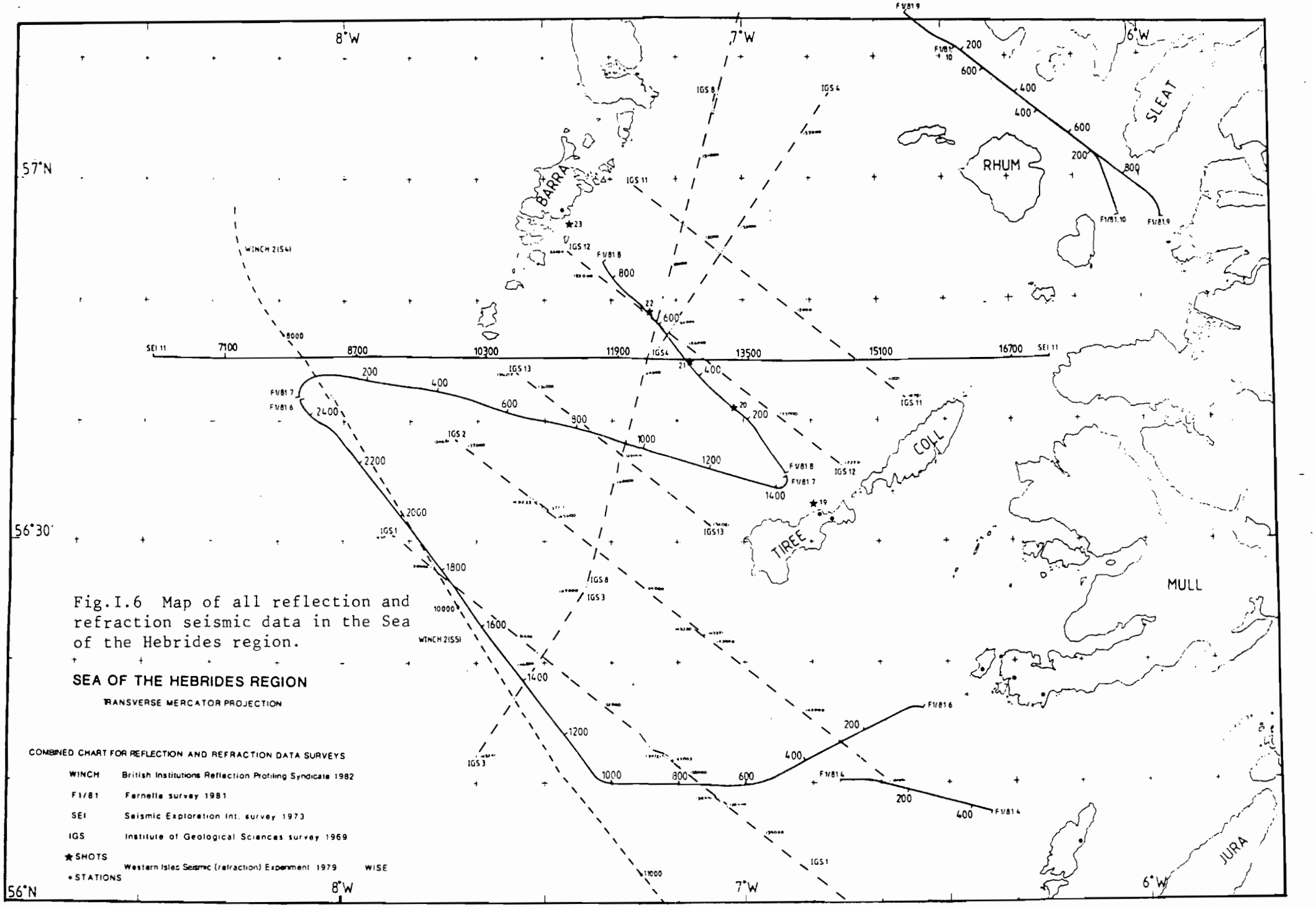

Fig.I.6 Map of all reflection and refraction seismic data in the Sea of the Hebrides region.

CHAPTER 2

DATA COLLECTION

This chapter deals with the description of the hardware used and the acquisition of the data used for this project, including the repairs and maintainance carried out to the Durham digital seismic recording system.

2.1 The Ship

The ship used for the experiment was a charter vessel from J. Marr & Sons of Hull. The M.V. Farnella was originally a stern trawler before conversion for marine data acquisition, the Hebrides project was the first to be conducted after the re-fit. Details of the ship and the work necessary to satisfy the scientific requirements can be found in an Research Vessels Services, R.V.S., report number 10 (1980).

On arrival at the ship to supervise the installation of the Durham seismic recording system, in the middle of August 1981, it was found that re-fit work was still underway. The laboratory, which was a ply-wood skinned box, was situated below the main deck where the fish processing plant used to be. Air-conditioning was provided by cooling and recirculating the air taken from the laboratory, there was no facility to ventilate the room with fresh air from outside. Space was more than adquate for the installation of the Durham system along with the R.V.S. computers and other navigation logging equipment. A gravimeter and

precision echo sounder were also fitted but these were not operational during this cruise. Storage for consumables; magnetic tape, paper, and spares; was in the fish freezing bays. Personnel access between the laboratory and the aft deck involved climbing round the large wooden fish gutting block, but large equipment was passed down the main fish chute.

2.2 Navigation

Navigation on the cruise was to be from two independent systems; the transit satellite system, Satnav, and the Decca Navigator radio-positioning system. Satnav calculated the position of the ship relative to a satellite by analysing the time difference and Doppler shift of a transmitted signal (Stansell 1978), typically a fix is obtained every ninety minutes in the region of this survey. The accuracy of these fixes was found to be suspect as positional errors increase when the ship is moving. The strong tidal currents caused by the islands meant that dead reckoning between the fixes, from gyro and speed measurements though the water, did not accurately reflect direction and speed over the sea-bed. The Decca system monitors the ship's position continuously, and is one of the several radio-positioning systems available around the coast of Britain. The system uses a master and three slave stations. Each master slave pair transmit continuous wave signals which create a hyperbolic interference pattern, the receiver on the ship computes the relative phase difference between the two signals and by knowing how many whole wavelengths the ship is away from

the transmitter, an accurate distance may be obtained. By using any two of the three possible pairs gives a position on the navigation chart with the Decca chain overprinting. The chain used by this experiment was the Hebridean Chain (8E). Decca Navigator Co. Ltd. publishes data sheets which give the operational area, accuracy and maps showing the fixed errors which can be compensated for when calculating the ship's position. Variable errors also occur, information on these effects must be obtained from Decca, but are normally small and have been considered negligible. Further information on the navigational aids can be found in Telford et al. (1976).

The final track charts were calculated from the Decca readings logged every two minutes, ignoring the Satnav fixes as being too inaccurate, and plotted on a Mercator projection to directly overlay the navigation charts. Due to errors in the R.V.S. Decca interpretation program some of the track was incorrectly drawn by the computer when passing between the master and slave stations, this section was later plotted by hand from the paper log kept by the Decca system. The computer output for the whole cruise is shown in Fig. 2.1. To verify the track charts produced twenty-four readings were sent to Decca for accurate conversion, the results are included in appendix 1. The track chart had to be transposed to the Tranverse Mercator projection for geological interpretation, this was done by hand correcting for the lost data, the result is shown in Fig. 2.2.

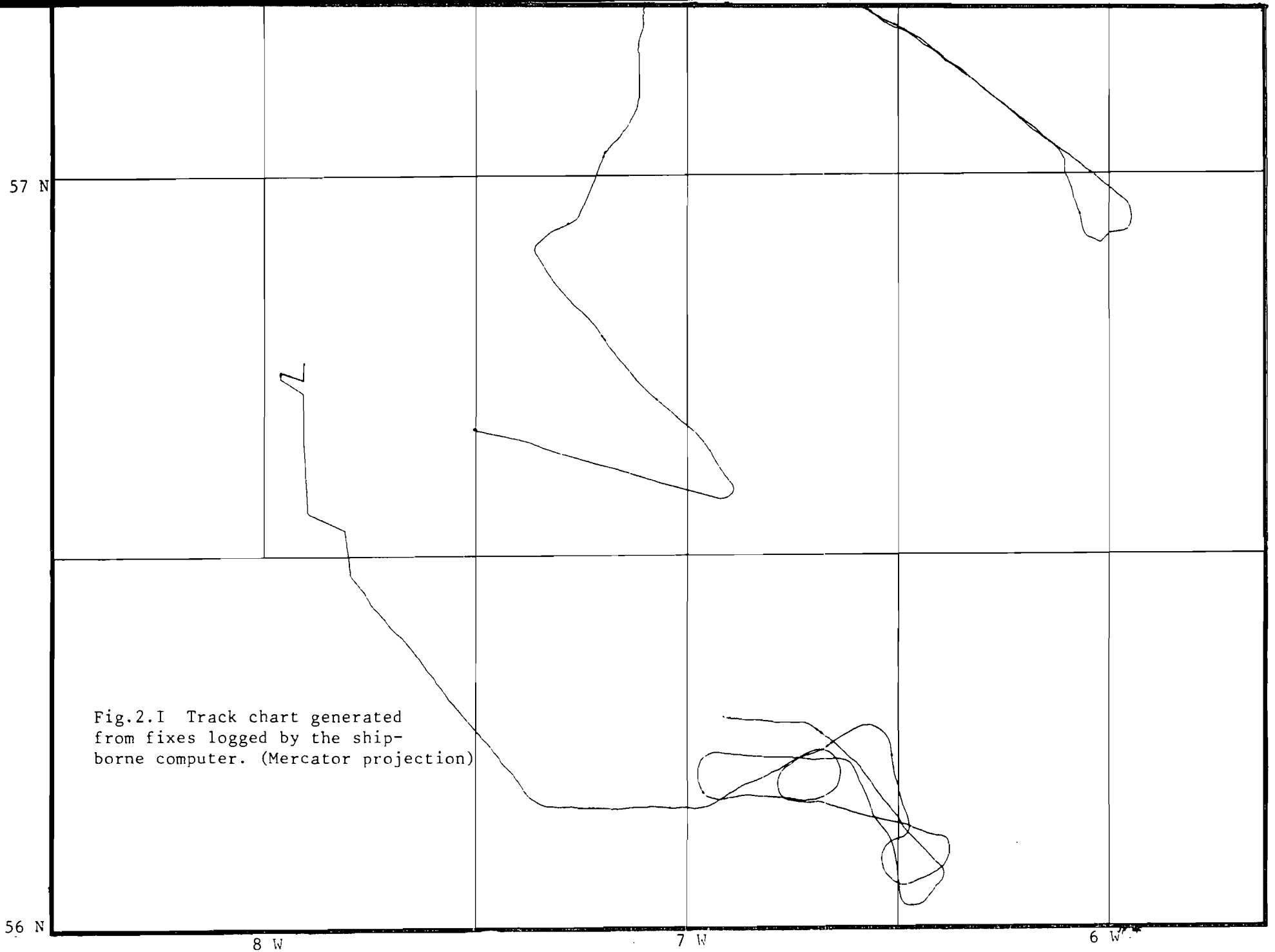

Fig.2.I Track chart generated from fixes logged by the ship-borne computer. (Mercator projection)

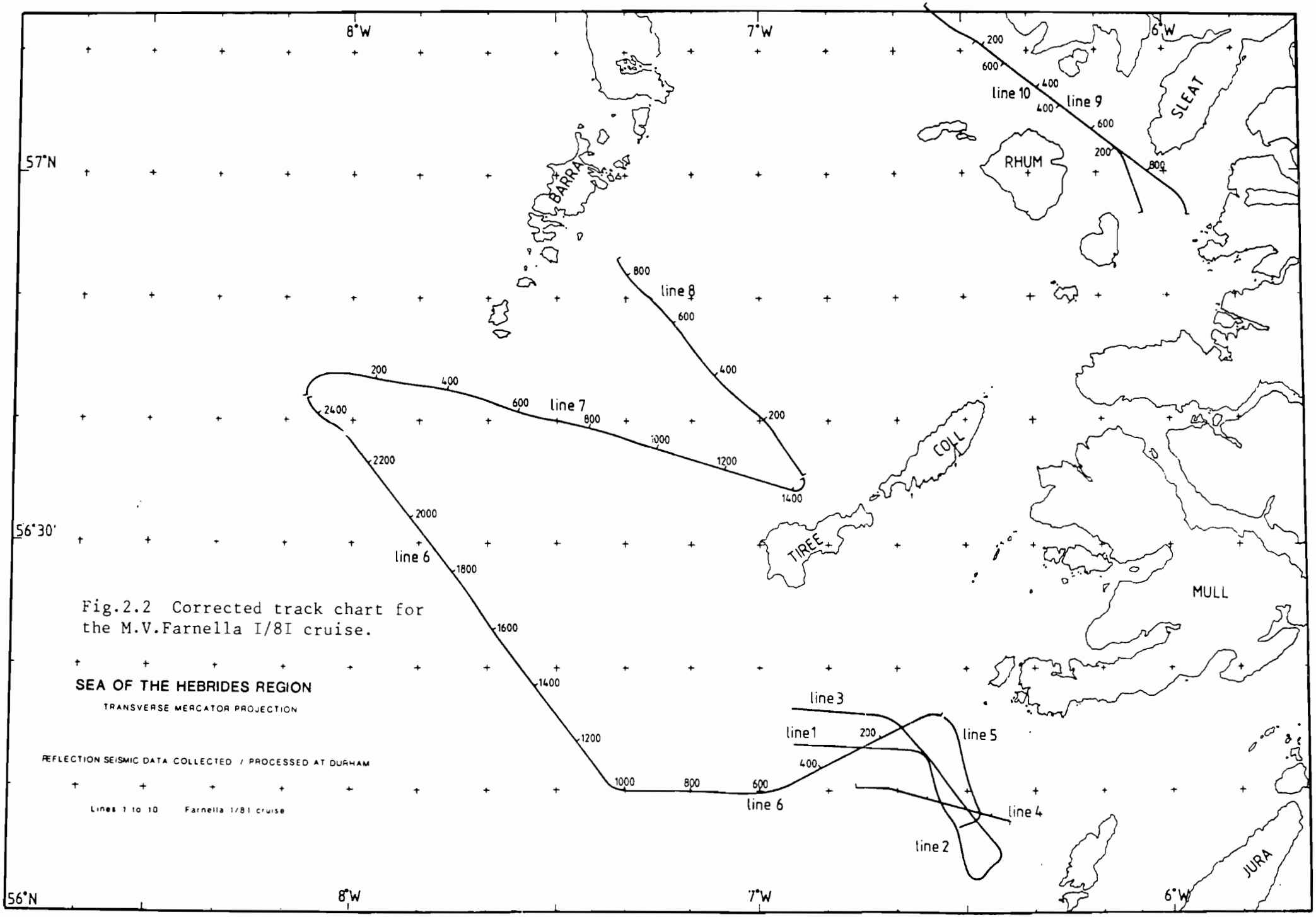

Fig.2.2 Corrected track chart for the M.V.Farnella I/8I cruise.

2.3 Bathymetry

The bathymetry was measured on an Atlas Fishfinder 800 sonar using a hull mounted transducer. When later analysing the records it was found that the instrument had not been accurately calibrated before the experiment. In areas of severe sea-bed topography parts of the record were lost because the range settings had not been adjusted correctly.

2.4 The Energy Source

As the orginal concept of the marine seismic reflection experiment was to resolve middle and lower crustal reflectors an energy source was required to generate large amplitude acoustic pulses over the frequency range of 10 to 40 Hz. The most convenient and reliable source availiable that fulfilled this need was the Bolt 1500C air-gun. The air-gun produces an explosive release of a measured quantity of compressed air from an attached chamber into the surrounding water. Once fired, the gun reseals the chamber which is then recharged with air via a hose from the ship board compressors. The firing of the gun may be as often as required provided the air supply is sufficient. The detailed operation of the air-gun can be found in Telford et al. (1976). R.V.S. supplied four air-guns for the cruise with six interchangable air chambers. The chamber size determines the power and the dominant frequency of the gun. Table 2.1 lists the chambers supplied.

Number	Size of chamber in cubic inches
2	1000
2	300
2	160

Table 2.1 Bolt air-gun chambers supplied by R.V.S.

Figure 2.3 shows a schematic diagram of the air supply, control and monitoring used for the air-gun array.

To provide compressed air for the operation of the air-guns two 2000 p.s.i. 70 cubic feet per minute compressors were fixed to the aft deck of the ship in container modules. These worked independently to supply air to a single high pressure air reservoir, switching on when the reservoir pressure fell below a pre-set value and off again when the pressure had been restored. Also each had a safety trip to cut the compressor off in the case of over heating.

A control board for supplying the high pressure air to the air-guns and necessary high pressure hoses and trigger cables were supplied by R.V.S.. The control board allowed the supply of air to each gun to be controlled individually, monitored the supply pressure and allowed the bleeding of the guns during deployment or retrieval.

2.4.1 Air-Gun Deployment

The original concept for the air-gun arrays was to tow two one metre bridles over the stern of the ship, one on the starboard side and one in the centre, with two guns on each

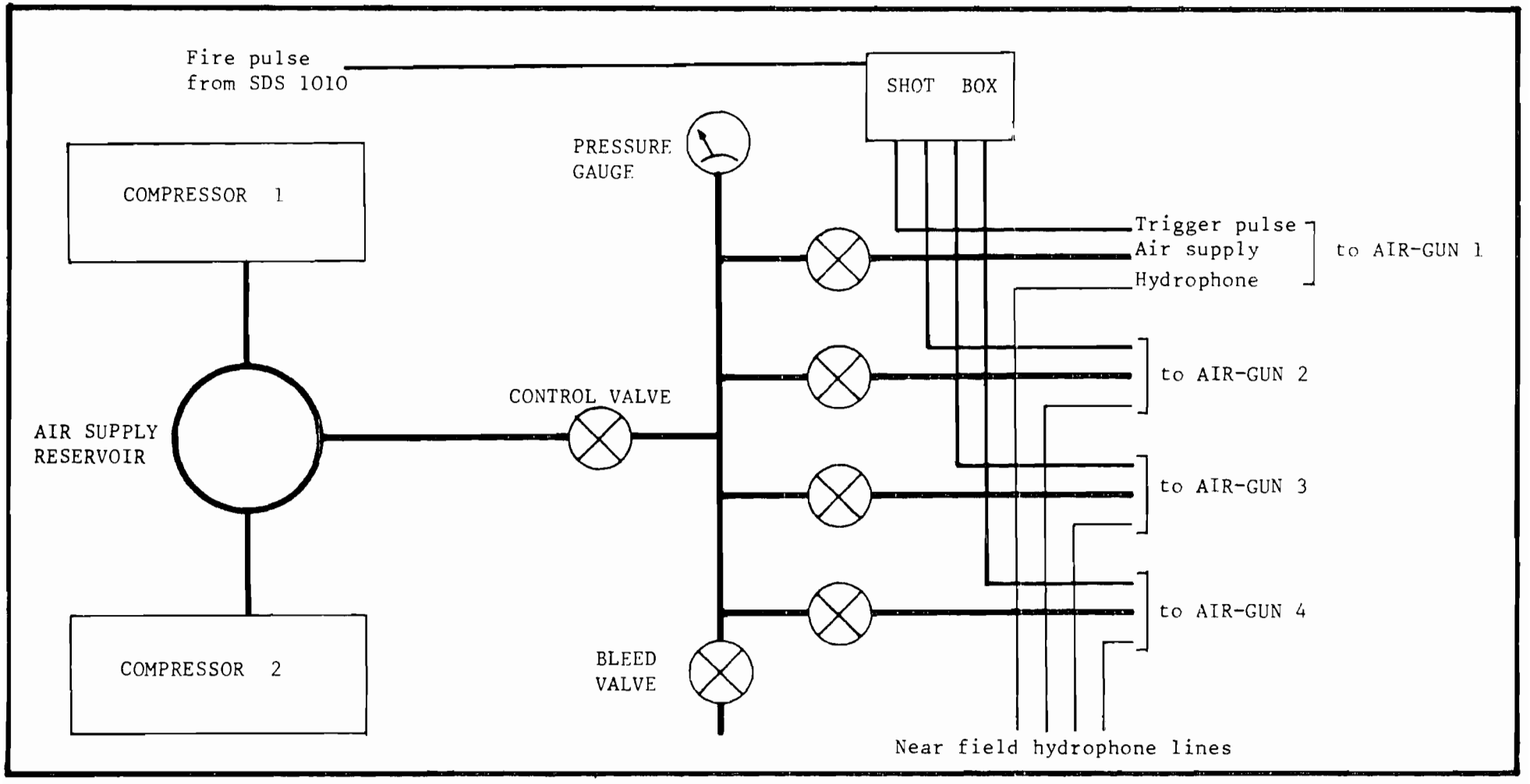

Fig.2.3 Schematic diagram of air supply, control and monitoring for the air-guns.

bridle, a 160 and a 300 in^3 (Fig. 2.4b). It was necessary to ensure the air-guns operated at a known depth so as to give as much contructive interference as possible between the directly down going wave and the ghost wave reflected from the sea surface, and also to enable a source depth correction to be applied to each seismic trace (section 4.3.1.). To determine the tow depth, the air-guns were towed with a sensitive pressure transducer attached whose output signal was calibrated for depth below the water surface. The array was towed at normal profiling speed, as speed affects how far the guns trail behind the stern of the boat, and the towing cable lengths were adjusted to give the towing depths required. Three depths where calibrated for the starboard array of 5, 7 and 9 metres, and two depths for the centre towed array of 10 and 12 metres, the towing cable lengths where marked with colour coded tape. After depth calibration the arrays were retreived and the depth transducer removed. The arrays were then finally deployed ready for use. Mounted on the towing bridles as close to the gun as possible were hydrophones to pick up the shot instant and signature of each gun.

2.4.2 Air-Gun Performance

During the early stage of the experiment one of the compressors kept tripping out at irregular intervals, therefore all the air had to be supplied by one compressor which was then in danger of over-loading. To ensure that the failure of one of the compressors would not interupt work the air-gun array was limited to that which could be supplied by a single compressor.

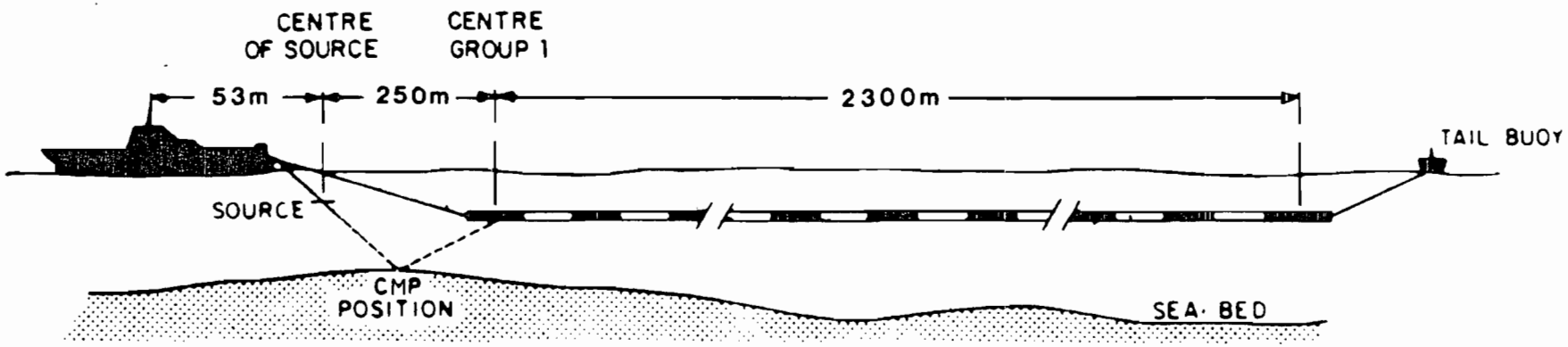

Fig.2.4a Towing geometry showing position of Decca navigation antenna, source array and receiver array.

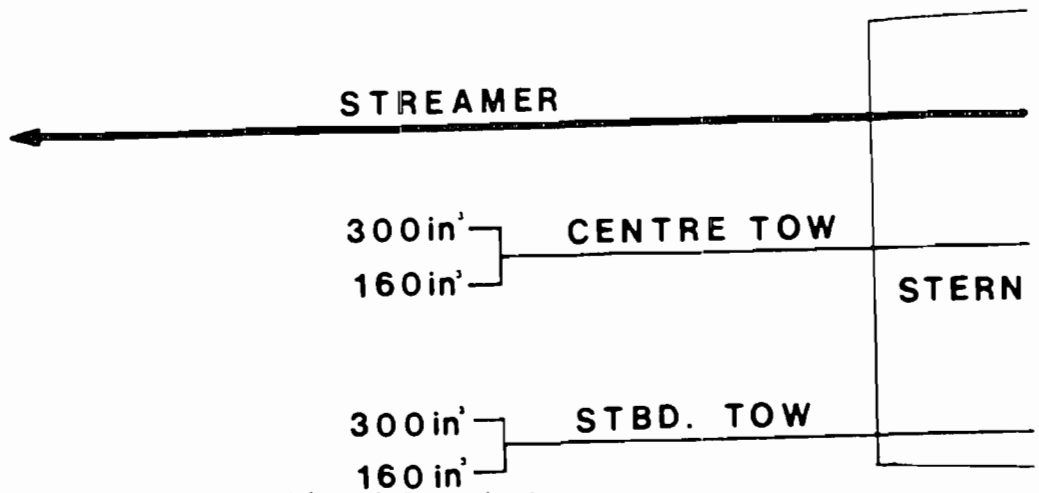

Fig.2.4b Towing arrangement from stern of ship. (Plan view).

Problems were also found in the firing mechanism for one of the guns which was removed from the array repaired and held as a replacement should one of the other guns fail. For all but one of the profiles acquired during this cruise the following array was deployed, a single 300 in^3 gun towed from the centre at a depth of 12 metres and a 160 in^3 and a 300 in^3 towed on a bridle from the starboard side at a depth of 7 metres. The final profile was different using just the 300 in^3 guns both towed at 10 metres depth.

It was found that where the 160 and 300 in^3 air-guns were attached to the same bridle the separation of one metre was not large enough to avoid the two air bubbles coalescing to form an effective 460 cubic inch gun (Fig. 2.5). This is not ideal for the subsequent processing of the data as the source is very monochromatic. Normally several guns are used to provide a source signature with unique character and with the energy concentrated in the first pulse giving a broad-band frequency response, (Telford et al. 1976). With the source array available this was not possible with most of the energy remaining in the oscillatory bubble pulse which followed the initial fire pulse.

The monitoring of the individual guns by the near field hydrophones allowed the exact timing of the array to maximize the first pulse energy. For the case where the towing depths were different an extra delay of 3.5 msec was added to the deeper guns to obtain maximum constructive interference with the down going wavefront from the shallower guns. This difference in towing depths and firing delay together produced a total of 7 msec delay

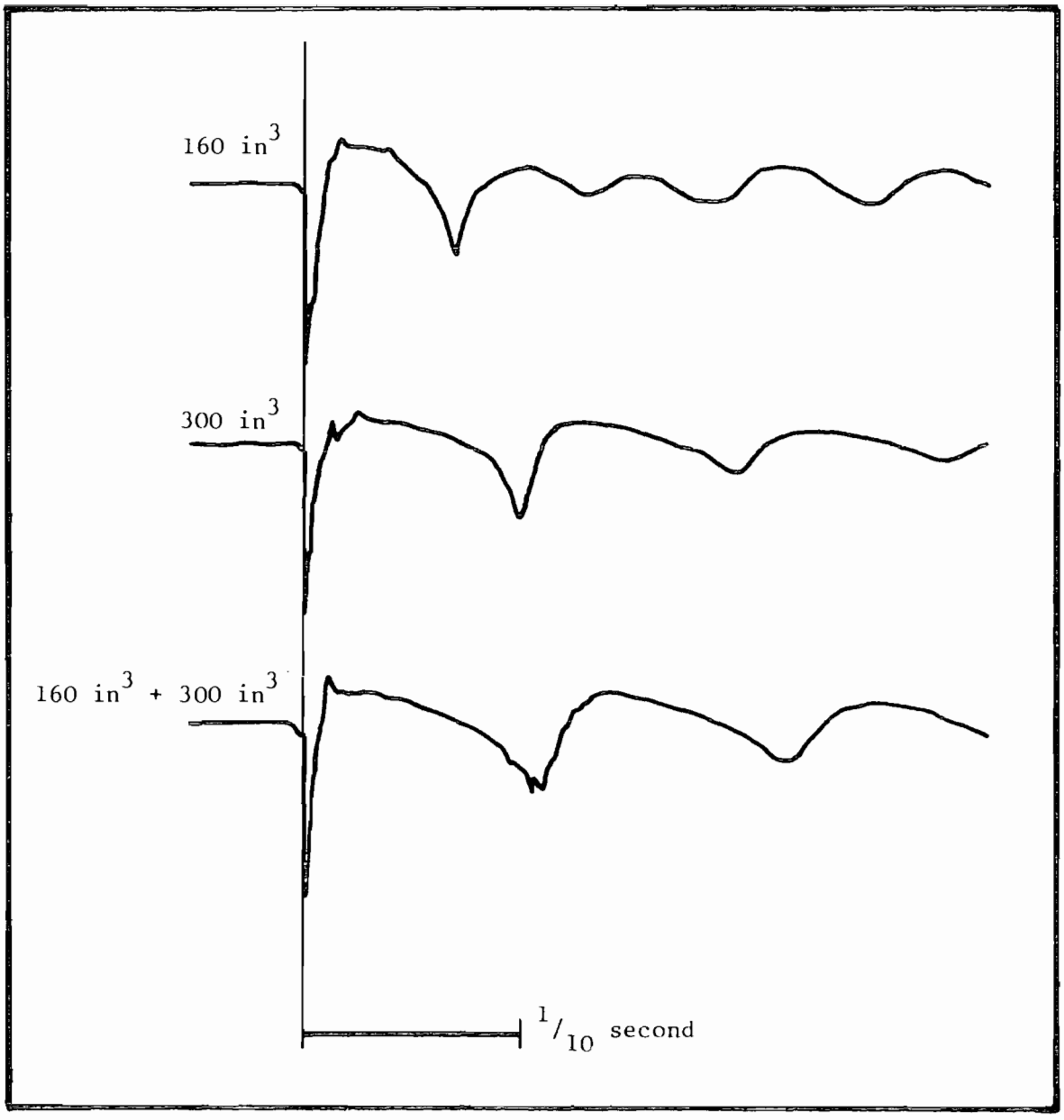

Fig.2.5 Effect of bubble coalescing for a 300 in^3 and a 160 in^3 air-guns towed 1 metre apart at a depth of 7 metres.

between the ghost arrivals which was hoped would produce a better cancellation effect in the far field.

Lines 4, 5, and 6 were shot using two air-guns, a 300 in^3 and a 160 in^3, both attached to the same bridle on the starboard side at a depth of 7 metres. As mentioned before the source acts like a single 460 in^3 air gun (Fig. 2.5).

Line 7 used an extra 300 in^3 air-gun from the centre towed bridle at a depth of 12 metres in addition to the two guns on the starboard bridle, giving the near field signature in Fig. 2.6a. After three hours profiling the 160 in^3 air-gun was shut down leaving only the two 300 in^3 firing. The different towing depths gave some bubble pulse cancellation (Fig. 2.6b).

Line 8 was shot with the same source configuration.

Line 9 was shot with the 300 in^3 air-gun towed from the centre at a depth of 12 metres and the 160 in^3 air-gun towed on the starboard bridle at a depth of 7 metres (Fig. 2.6c).

The start of line 10 used the same source array but was changed after an hour to the two 300 in^3 air-guns towed at 10 metres (Fig. 2.6d). The later part of this line took the same track as that used for the start of line 9, the use of the different array was to hopefully provide better penetration with the lower frequencies.

2.5 Receiver Array

The reflected acoustic energy was picked up on a 3 km streamer towed from the port side of the boat. The streamer is made up from a series of omni-directional hydrophones connected

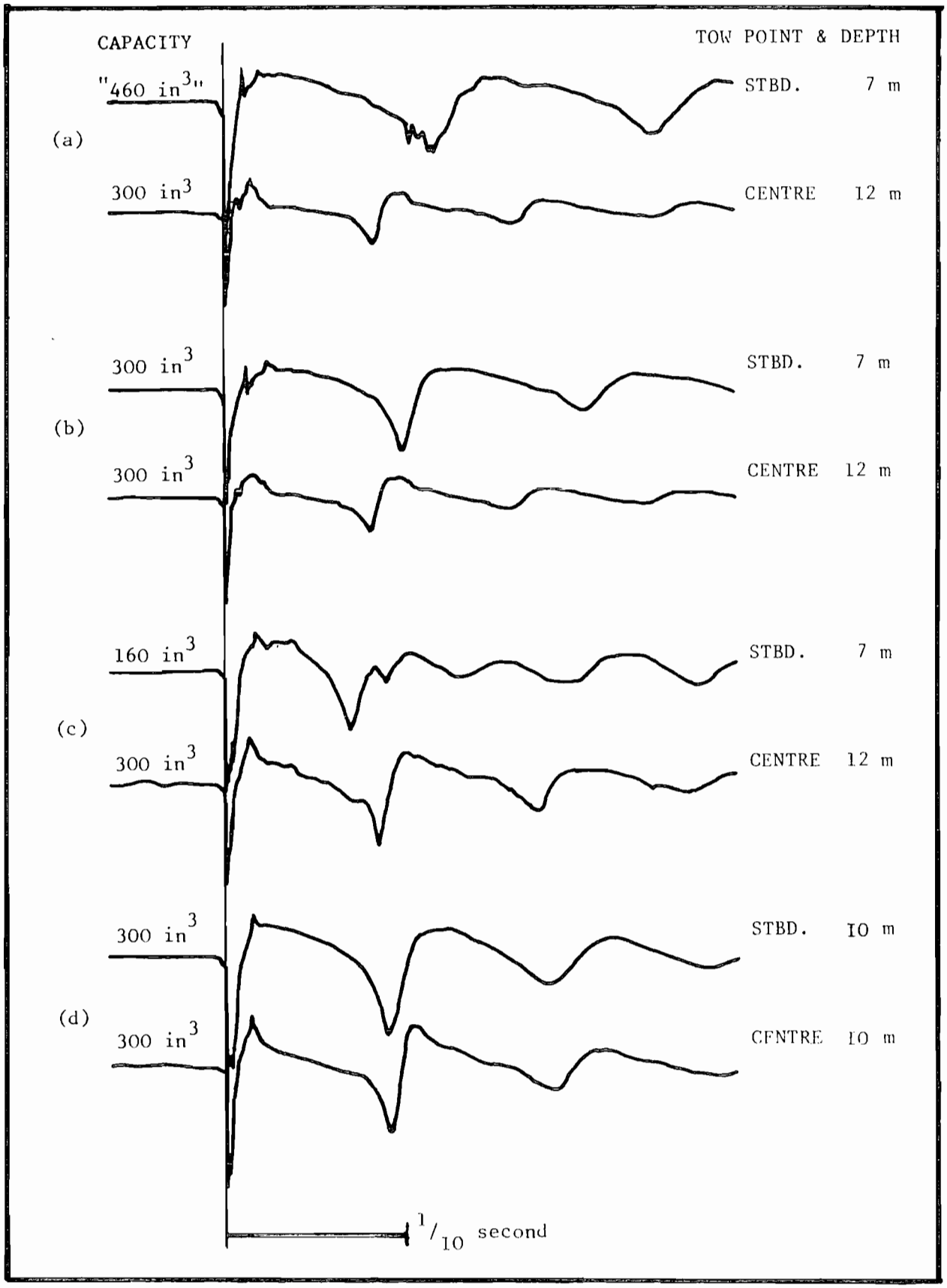

Fig.2.6 Near field source signatures for the air-gun arrays used during this survey.

together in groups down the length of the streamer to effectively give 24 separate received channels. Each group was made up of 50 hydrophones spaced evenly over 50 metres of cable. Typical contruction of seismic receiver streamer is explained in Telford et al. (1976). The full configuration of the streamer used for this experiment is given in table 2.2. Briefly, the streamer was made up from 24 active sections each of 50 metres length containing hydrophones; alternating with 24 passive sections each of 50 metres length not containing hydrophones. At intervals along the length of the streamer depth sections monitored the towing depth of the array. Spring sections at both ends of the streamer helped to decouple towing and wave noise from the ship and tail buoy.

2.5.1 Array Deployment

Due to the length of the streamer it was necessary to have a tail buoy, with both lights and radar reflector for safe navigation, as the end was to be nearly 3 km behind the towing ship. Launching this buoy proved to be less easy than expected as the heavy battery pack for the navigation lights was too far above the centre of bouyancy, hence the buoy was only stable when floating upside down in the water. Removal of the offending battery pack and lights cured the problem.

The streamer was deployed from a large winch under hydraulic control with an Ashbrooke depth control bird attached every 400 metres. These birds had been pre-set to keep the streamer at a depth of 10 metres at normal profiling speed. They work by

Notes: (i) All sections 50 metres except those mentioned below.
(ii) Adaptor sections - 1 metre.
(iii) Depth sensing sections - 1 metre.
(iv) Tail rope - 220 metres.
(v) Tow cable - 130 metres as measured from stern of ship.
(vi) Active - sections with hydrophones, Passive - sections without hydrophones.
(vii) Spring - sections without hydrophones that stretch to absorb movement by the ship or tail buoy.
(iix) Ashbrooke - indicates the position of the depth controllers.

Tow cable - Depth sensor - Spring - Spring - Active - Passive - Active - Passive - Active - Passive -
Ashbrooke Ashbrooke

Active - Passive - Adaptor - Depth sensor - Active - Passive - Active - Passive - Active - Passive -
Ashbrooke

Active - Passive - Active - Passive - Depth sensor - Active - Passive - Active - Passive - Active -
Ashbrooke

Passive - Active - Passive - Active - Passive - Depth sensor - Active - Passive - Active - Passive -

Active - Passive - Active - Passive - Active - Passive - Depth sensor - Active - Passive - Active -
Ashbrooke Ashbrooke

Passive - Active - Passive - Depth sensor - Active - Spring - Active - Spring - Tail rope - Buoy - Drogue

TABLE 2.2 Receiver Array Configuration

adjusting the angle of attack of a horizontal fin with the passing water flow. The control of the fin is by the effect of the ambient water pressure acting on a cylinder of compressed air, the pressure of which had been pre-set using a foot pump to that expected at the required towing depth. After the last of the streamer sections had been passed over the stern about 130 metres of towing cable was payed out to give a source to first active receiver group spacing of about 250 metres.

The source receiver lay out is shown schematically, both plan and elevation in Fig. 2.4.

2.5.2 Signal Conditioning

The acoustic energy is converted into small variations in electrical voltage by the hydrophone, all the hydrophones in each receiver group are connected in parallel hence any signal arriving in phase at all the hydrophones in a given group, e.g. a reflection with a high apparent velocity, contructively interfere to give a large electrical voltage; whereas acoustic energy travelling along the group, e.g. direct wave with low apparent velocity, would suffer destructive interference to produce a much smaller voltage even if the input energy is the same. The summed signal from each group is passed back along the steamer to the towing ship via an impedance matching transformer and twisted pairs of conductors. These wires passed down into laboratory onto a patch board which interfaced with the seismic acquisition equipment.

2.6 Seismic Acquisition Equipment

The purpose of the equipment is to take the small input analogue electrical signal from the streamer, amplify, low-pass filter to remove energy above the Nyquist frequency, sample, digitize and record onto magnetic tape in such a manner that the input signal can be regenerated by reading this tape on a computer.

The aquisition system used on this project was a SDS 1010, originally owned by Western Geophysical but given to Durham University in 1976. The system originally land based, was modified to convert it to the marine enviroment where it is necessary to fire the air-gun system repeatedly at fixed interval of time.

Despite its early design in 1969 the resolution achieved has not been improved upon by modern systems. Full specifications of the SDS 1010 are included in appendix 1. Over the last fifteen years the reliablity and scale of integration used in the electronics has changed drastically. Typical SDS 1010 circuit boards had very low level integrated circuits attached, e.g. board number FS10 has eight integrated circuit chips with a single J-K flip flop per chip. At the present time it is possible to obtain whole 32 bit computer processors on a chip.

2.6.1 Operation of the SDS 1010

The operation of a digital acquisition system may be read in Telford et al. (1976). The technical manual (Western Geophysical 1971) gives a full description of the SDS 1010 system. A brief

description follows to help with the understanding of the problems encountered with this system. A block diagram for the SDS 1010 is given in Fig. 2.7.

The SDS 1010 was built using a modular design, each module being responsible for a specific operation under the control of a master timing unit called the System Control Unit, except for the analogue to digital converter as explained below.

System Control Unit

This unit contains the master clock, a crystal controlled oscillator; the mode select logic, which interprets the control front panel switches hence the operation of the instrument; and a read after write error checking facility for the tape drives.

The Geophysical Amplifiers

As the input signal from a receiver array is typically in the millivolt range, it has to be screened from possible pick-up of spurious electrical signals, e.g. mains from the ship's generator. The signal first passes to a fixed gain input amplifier with an optional reject filter for mains hum if needed and a low-pass anti-alias filter. A switchable gain amplifier futher increases the signal amplitude to lie within the operational range of the analogue to digital converter. The gain of this stage is automatically varied by the instrument to keep the signal at the digitizer's optimum level. The record of any necessary gain changes is output to the digital tape which, along with the digitizer's output, enables the reconstruction of the

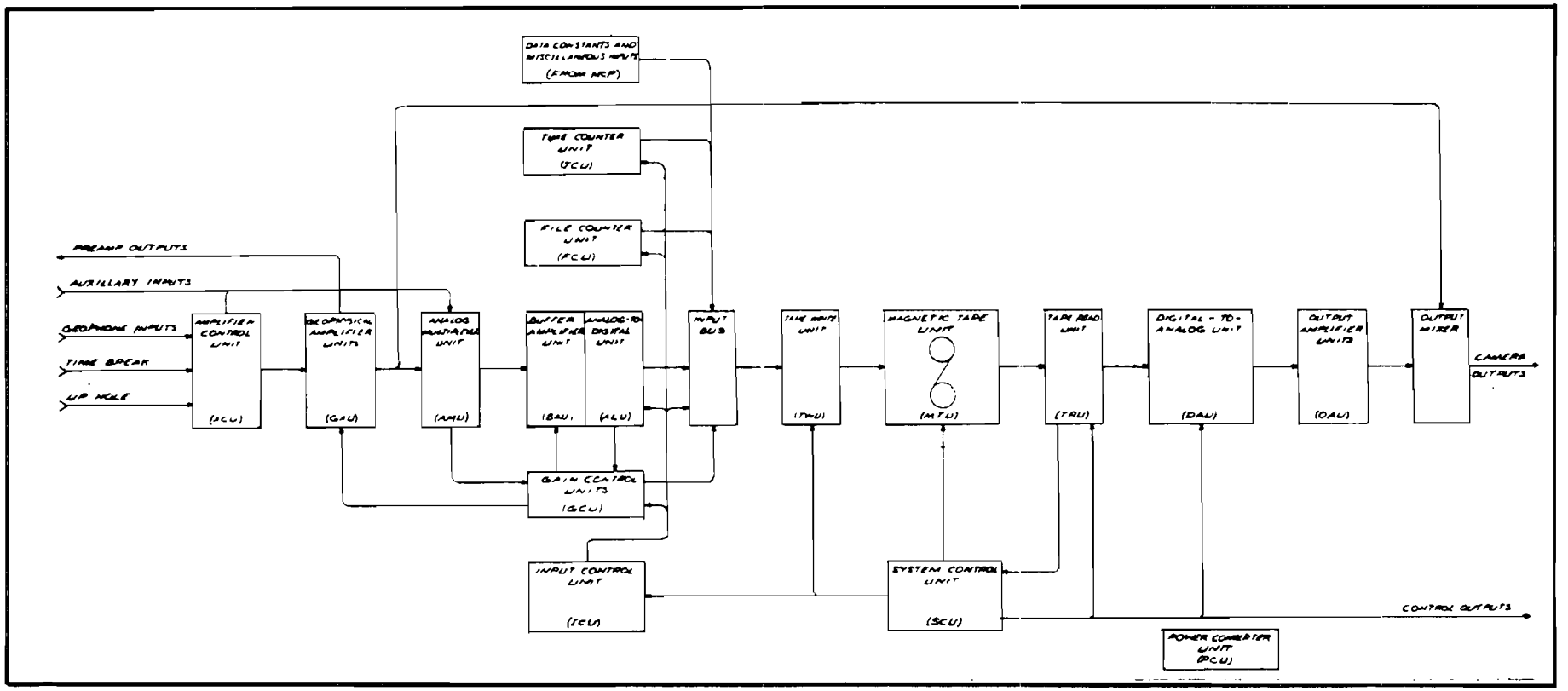

Fig.2.7 Schematic diagram for the SDS 1010 seismic recording system. After Western Geophysical (1971).

signal. There is an analogue amplifier for each active group in the receiver array.

Input Control Unit

The twenty-four Geophysical Amplifiers and six auxillary channel amplifiers continuously feed their receiver group's signal to the analogue multiplexer. The Input Control Unit scans each input channel in turn at a constant rate, reducing the thirty input signals to single stream of analogue levels which pass into the analogue to digital converter. After digitization the Input Control Unit then formats the number, gain code, and any necessary synchronization codes ready for output to tape via the Magnetic Tape Unit. At this stage each sample is checked for gain ranging purposes. If the number lies between 1/4 and 1/2 full scale no gain change is made for that channel. If the number is greater than 1/2, scale the amplifier gain is immediately reduced to prevent the digitizer saturating. The maximum rate of reduction of gain is by a factor of 2 every 2 samples on a given channel, for 4 msec sampling rates this is equal to 750 dB/sec, this process is called "burst out". If the number has fallen below 1/4 full range, then the system allows the gain to range up. To prevent the gain oscillating at the frequency of the input signal a pre-set time constant is selected which damps the rate of increase of the pre-amplifier gain to follow the envelope function of the received signal.

Analogue to Digital Converter

The Input Control Unit selects each receiver channel in turn via the analogue multiplexer. As soon as the voltage has stabilized a start pulse is sent to the converter. The digitization is done by a series of approximations to a given internal reference voltage. The input analogue signal is compared to this voltage. If it is greater or equal then this stage sets a flag and the difference of the two voltages is passed to the next stage. If it is not, then the flag is not set and the whole voltage is passed to the next stage. The reference voltage at the next stage is half that of the current stage. By repeating the process progessively builds up a binary number. For seismic signals where both positive and negative signals appear, two balanced reference voltages must be supplied. The Input Control Unit waits for a fixed time then scans the output digitization lines for which stages have their flags set. The resultant number can be directly handled by the digital control logic and can be recorded on computer tape. The internal timing of the analogue to digital converter is not under the control of the master clock and hence its operation is totally asychronous to the rest of the system. It is therefore imperative that the internal timing is exact otherwise digitization errors will occur.

Magnetic Tape Unit

Besides controlling the movement of the tape at either a slow speed for read/write operations or a fast speed for tape positioning, this unit also controls two futher sub-units, the

tape write unit and tape read unit. These are responsible for the encoding and decoding of the magnetic domains on the tape. The rate of data flow is also controlled to maintain the 800 bits per inch packing density used by this machine. Shot header information and sychronization patterns are also added at the start, and at fixed intervals during the data transfer and finally, the redundancy characters and tape mark at the end of each record. As the data is being continously acquired and the SDS 1010 has no internal memory it is necessary to continously output the data to tape, this results in all the data samples for a given shot being recorded as one long record on the output tape, error checking of such long blocks becomes very difficult and ambiguous, and there is no chance of re-recording data missed because of poor tape quality. To monitor errors on the output tape, a read after write facility is provided which reads the data from tape immediatedly after it has been written and compares it with the original input signal. Any differences cause an error to be flagged on the control panel of the instrument by the System Control Unit.

Output Amplifier Unit

This allows tapes, previously recorded by the instrument, to be replayed and converted by means of a digital to analogue converter, to a time varing output voltage which may be directly drive a pen recorder. During recording operations this unit is used to monitor the data as recorded on the tape.

2.6.2 Repairs to the SDS 1010

Since the system had been at Durham, little or no general maintainance had been carried out, and the condition of the system had been left to deteriorate. The components themselves do not usually fail due to lack of use but the circuit boards to which they are attached and the interconnecting cables and associated plugs and sockets do cause problems. The most severe effect is the oxidation of the bare metal edge connectors which run along the side of each printed circuit board, p.c.b., and the back plane socket into which they slot to make electrical contact with the rest of the system. If a system is in continual use then a single fault can quickly be traced but in a system which has not been used for a long period there will be many more faults to be identified. The problem is further compounded by the cross connection between different parts of the system to maximize the usage of the originally very expensive integrated cicuit chips. Secondary problems include the oxidation of the solder joints holding the electrical components to the p.c.b.'s and the effect due to time of the tin and lead alloy separating and crystallizing into their separate elements. Unfortunately tin tends to form a semi-conductor junction which operates perfectly in one direction but forms a barrier to any reverse voltage applied.

Thereforea complex system which is not used regularly with preventative maintainance conducted at regular intervals, is unlikely to meet its specifications, even if it works at all. The effect of deterioriation can clearly be seen between the quality

of data collected in 1976 (Fig. 2.8a) just after Western Geophysical had finished with the machine and the data collected in 1980 (Fig. 2.8b). Most of the channels exhibt major problems, e.g. mains pick-up totally obscuring the real data, or severe clipping of the signal at a very low amplitude, with the signal to noise ratio reduced to nearly sign bit recording. Some information may be regained by careful processing to remove the mains interference and spurious high frequency introduced by the clipping but a significant proportion of the data has been lost. With the high cost of running the ship to collect this data, the use of such ill-maintained equipment is short sighted.

For this cruise the original intention was to either borrow a modern system from I.G.S. Applied Geophysical Unit, or hire a system from the reflection seismic contracting industry. Unfortunately neither option came to fruition and so the only alternative was to repair the SDS 1010 system.

Repair work started on the system in July 1981 in preparation for the cruise in September of that year. Western Geophysical offered to examine a test tape recorded on the system using their diagnostic programs and report any detected faults. Due to the serious condition of the instrument it was only just prior to the cruise that it became possible to produce any recorded output tape and there was no time remaining for Western Geophysical to analyse the data.

Repairs to the system were slow and convoluted due to the design of the instrument, as mentioned above, and further hampered by the two sets of incomplete documentation which missed

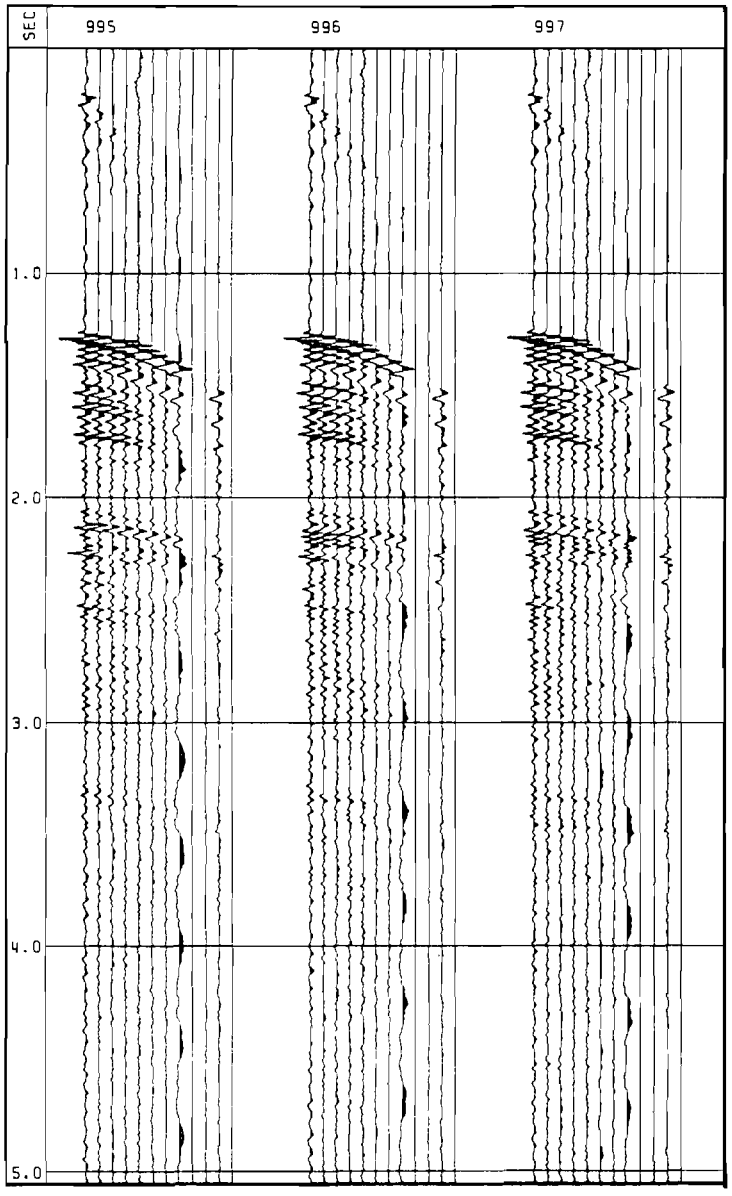

Fig.2.8a Data collected on the SDS 1010 in 1976.

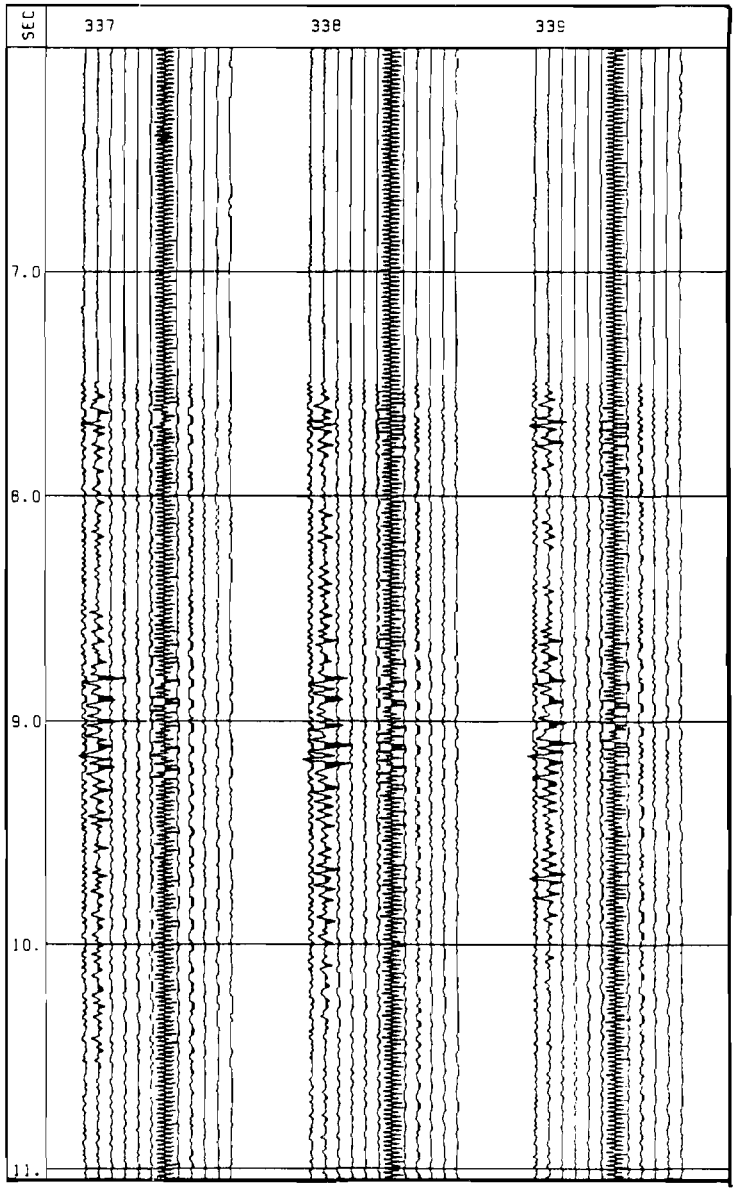

Fig.2.8b Data collected on the SDS 1010 in 1980.

whole sections and in places were totally different. This meant each fault had to be traced by working out each individual circuit from the p.c.b.'s themselves. Finally some of the modifications to create a marine system had not been properly documented.

After two months it was possible to record and play-back a synthetic signal produced by a sine-wave generator. Two major problems then became apparent: first the reason for the data quality on the 1980 cruise, namely the automatic gain control unit could not cope with burst out signals, secondly the sine-wave appeared to be severely distorted.

As mentioned before in the operation of the SDS 1010 if a large signal appears on the input amplifiers then the system should rapidly reduce the gain to prevent the analogue to digital converter running out of dynamic range and clipping the signal, this circuit had failed completely. In the 1980 data the gain ranged up to its maximum value during the period of no reflections from the water column and was unable to recover when the reflected signal did arrive back from the sea-floor and below. The distortion on the recorded signal was traced to the analogue to digital recorder referance voltages that should have been set at plus and minus 8 volts, these were found to be about +10 volts and -6 volts. As there was an abundance of spare parts available and time was pressing, all repairs where carried out by whole board replacement, this worked well in the case of the gain ranging unit, but having cured the reference voltage problem and replaced several digitizing stages in the converter the timing of

this sub-system was upset. The timing information sheet for the device was missing so the setting up was done to ensure the number would be ready well before the Control Unit interrogated the analogue to digital converter for the digitized output. Prior to the ship, the system appeared to work well in the laboratory where the operating temperature was controlled and the synthetic input signal was devoid of any sudden amplitude changes.

2.6.3 Commissioning

During transport and installation several more "dry" joints and bad contacts appeared, which were traced and repaired or replaced. The second tape drive, needed for continuity of recording while the other tape was rewound and a new tape loaded, was stripped down and repaired. The repair proved fruitless, as when profiling, the switch gear used to select the output tape failed. Due to lack of time and spares the Time Break Unit was not repaired. This outputs a spike on one of the six possible auxillary recorded channels to indicate when the fire pulse had been sent to the air-guns. Also this unit outputs a time code on the channel for checking during demultiplexing to aid error recover. Fortunately this unit was not essential to the workings of the rest of the system.

Continous repair and maintainance of the system was carried out during the first stage of the cruise to acquire refraction data for another Ph.D. (Summers 1982). Circuits that had been fully repaired and tested still kept failing as new bad contacts developed. To aggravate the problem, the air conditioning unit

failed causing the ambient temperature in the un-ventilated laboratory to regularly climb above thirty degrees Celsius. As the system was constructed of military specification integrated circuits, this did not cause any problems to the main logic operations, but this high temperature did cause synchronisation errors between the Input Control Unit and the Analogue to Digital Converter. The problem manifested itself as a very large read after write error. The cause was not tracked down until the end of the cruise, when it was found by disabling the automatic gain ranging facility, the error count was reduced to typically one or two per ouput record. After the end of the cruise, futher work indicated that the error was related to the automatic gain ranging unit which was being triggered too soon by the early arrival of the digitized signal from the analogue to digital converter. Realising the gain had to be changed, the unit reacted immediately, instead of waiting for the next sample, the amplifiers needing time to recover from the gain change. The effect of this change was directly passed into the analogue to digital converter as the Input Control Unit was still sampling that channel prior to accepting the digitized output. When the Input Control Unit took the digital code, the output represented an amalgam of original digitised signal in the lower bits, all ones in the middle bits, indicating the analogue to digital stage was busy, and new input analogue volage digitised into the higher bits. This resulted in totally spurious data samples on all but the first channel as the timing error appeared to be reset prior to each scan. As mentioned before this effect was temperature

related, as the error rate fluctuated during the day, being a minimum during the early morning when the laboratory was at its coolest.

2.7 Data Aquisition

An abridged version of the watch keepers log book is included in appendix 1. Reflection seismic profiling started on the 3rd August 1981 and continued for three days. The first three profiles have not been processed as the data quality is known to be very poor. Gain ranging problems with the SDS 1010 were further compounded by compressor problems resulting in the gun configuration continuously changing or being totally shut down; and on line no. 3 the file counter failed so that no record could be made of the shot number. Originally it was hoped to use both tape decks so as not to loose data at a tape change, by the end of line no. 2 use of the second deck had to be abandoned as problems were found when switching control between the tape decks. After a period of maintenance between lines 3 and 4 the file counter had been repaired and the tape deck switch over unit had been totally removed. However no progress was then made on discovering the cause of the high error rate encountered on each record. The system then ran with only one minor failure for the rest of the cruise, even so, a continuous maintenance programme was necessary to keep the SDS 1010 running.

2.8 Summary of the Farnella 1/81 Cruise

The data acquisition was disappointing with problems being found in all the systems installed on the ship during this cruise: the Durham seismic recording system (SDS 1010), the R.V.S. data logger, the high pressure air compressors, and the air-conditioning in the laboratory. Finally, the cruise was cut short by a day because the receiver streamer was broken. The parted tail section, however, was retreived after locating the tail buoy on the ship's radar.

Despite the problems outlined above a total of 43 hours of reflection seismic profiling generating 70 field tapes was done using a variety of air-gun arrays between 460 in^3 to 920 in^3. As the recording system was limited to the use of a single tape deck meant,that when it was necessary to change the output tape,data had to be missed. After the operators had become trained this only resulted in six or seven shots being missed each time.

CHAPTER 3

THE DURHAM SEISMIC PROCESSING SYSTEM

This chapter covers the hardware and the systems software incorpoated in the Durham Seismic Processing system. The first section describes the current configuration, while the second section shows how this relates to the original system described by Poulter (1982). The third section is a review of how the hardware improvements have expanded the seismic reflection processing capabilities at Durham.

3.1 The Current System

This is be explained as three sub-systems: the hardware, the operating system and the processing software. The first two are covered here with the processing programs described in chapters 4 and 5.

3.1.1 System Hardware

The schematic diagram in Fig. 3.1 shows the current hardware configuration. The central computer is a Digital Equipment Corporation (DEC) PDP-11/34. This has a 16-bit processor and a 18-bit address bus giving access to 256 kbytes of memory. Details are given in the PDP-11/34 Processor Handbook (DEC 1978a). The computer acts as a host to six peripheral devices which may be accessed through hardware controller circuit boards installed

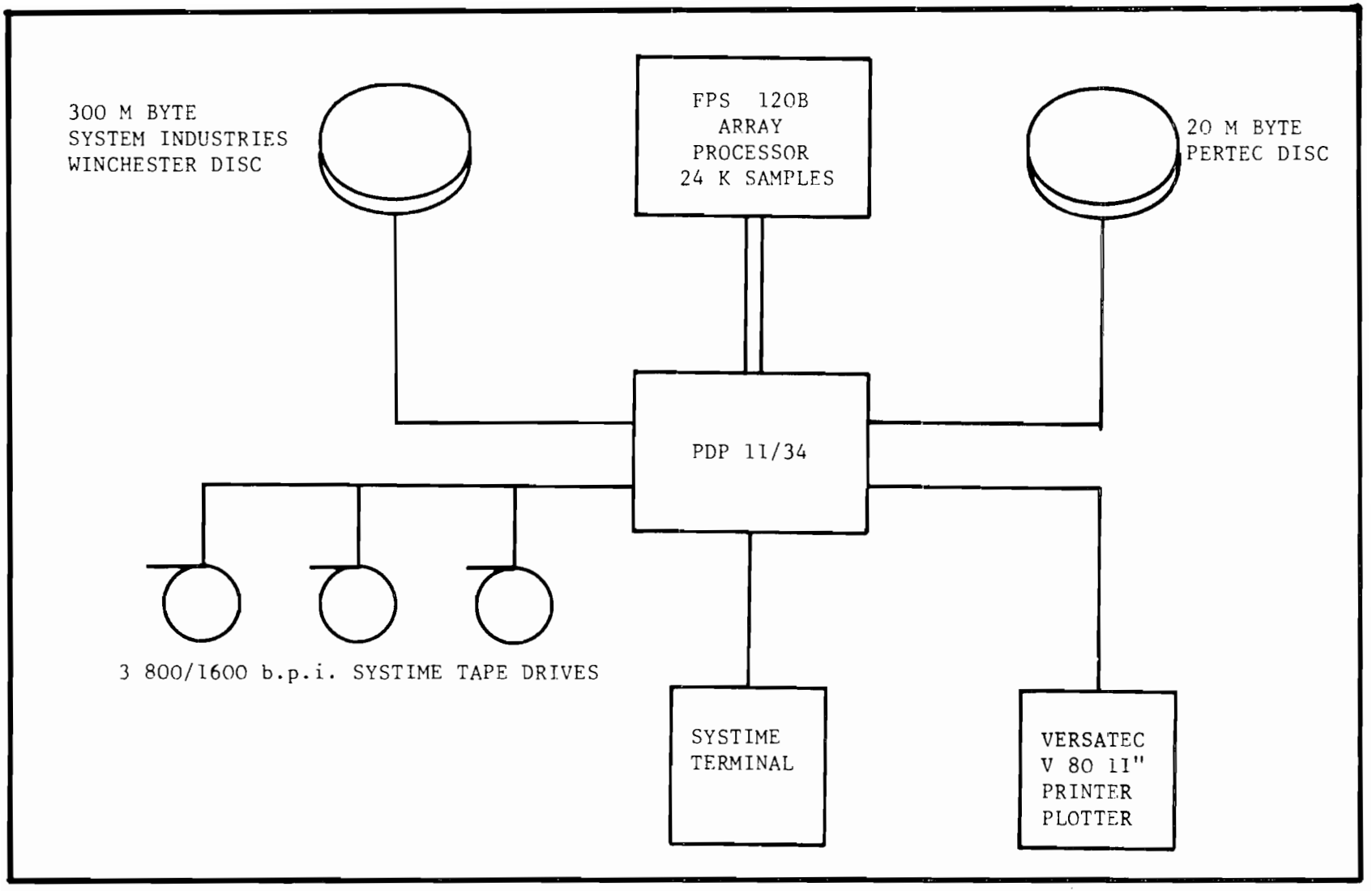

Fig.3.1 Schematic diagram of the current Durham Seismic Processing System

inside the PDP-11/34 unit, except for the array processor which has its own internal controller board and is connected directly to the PDP-11/34 UNIBUS, the computer contol and data bus. A visual diplay unit (VDU) manufactured by Systime gives the user control of the whole system to write or run programs.

The Floating Point Systems array processor, FPS 120B, is used as a high speed arithmetic device. All the seismic data manipulation is done by this unit. The processor has 24 k of floating point number memory, 2.5 k of table memory for floating point number constants and 1 k of program space. It operates by the PDP-11/34 loading in data and program code; it then runs asynchronously allowing the computer to work on other tasks until the computer is ready to retrieve the processed data.

The 20 Mbyte Pertec disc unit is divided into eight platters or discs; six are permanently accessible to all users and contain the operating system and the processing software, while the other two are contained in a removable cartridge pack. Each user has one of these packs and uses it to hold files containing processing parameters, program logs and software under development.

The 300 Mbyte Winchester disc unit is, like the Pertec unit, divided into eight discs. Its large capacity is used for seismic data storage by several of the programs where repeated access to the data base is needed, e.g. migration, velocity analysis, and for the generation of plot files.

The seismic data are recorded on magnetic tape. Storage of processed reflection seismic profiles are also on tape because of

the quantities of data involved. The three Systime tape decks allow these data to be accessed. The tape drives are dual density, 800/1600 b.p.i., and are driven by a single controller which limits operation to one drive at a time.

The Versatec electrostatic printer plotter, V80, is used to obtain listings of program, parameter files and log files, but with its 200 by 200 dots per inch resolution its main function is the output of seismic data in a raster format.

3.1.2 The Operating System

The operating system is the software package supplied by the computer manufacturer which allows the user to communicate with the computer, and it instructs the computer how to handle the peripheral devices. The system in current use is RT-11 3B SJ (DEC 1978b, 1978c). "RT-11" is the general name for the operating system supplied by DEC. Details may be found in the Introduction to RT-11 guide. "3B" is the version identity code this has now been superceded by version 4 and more recently by version 5. Change to a more modern system has not been implemented because it has been necessary to make several modifications to the operating system in order to accommodate reflection seismic processing on the PDP-11/34 computer. These modifications have been made to the peripheral instruction programs, called handlers, in order to extend the addessing capability to the full memory available in the PDP-11/34. The method is explained in detail by Poulter (1982). A new operating system would need similar modifications. "SJ" stands for the monitor type. The SJ,

or single job, monitor limits the computer to run only one program at a time. The choice was dictated by size. Other monitors supplied were the foreground background, FB, or the extended memory, XM, but both of these were significantly larger thus leaving less space for programs and data. With the standard SJ monitor, the programs, data and operating system are restricted to 64 kbyte of the 256 kbyte addressable PDP-11/34 memory, but the modifications mentioned above allow data to be transferred to or from the remaining 192 kbytes of memory. Of the 64 kbytes of program space, 8 kbytes are reserved for peripheral status and control words, about 32 kbytes are used by the RT-11 3B SJ operating system, leaving 24 kbytes for the seismic processing programs.

3.2 The Original System

A short description is given of the system configuration when starting this project, see Fig. 3.2. A more complete version may be found in Poulter (1982).

3.2.1 System Hardware

The original processing system was based on the PDP-11/34 computer connected to four peripheral devices and a DEC PDP-8E computer. The array processor only provided 8 k of floating point number memory, along with the 2.5 k of table memory and 1 k of program space. Storage of the operating system, processing programs and data relied on the 20 Mbyte Pertec disc. The Versatec electrostatic printer plotter was an earlier model,

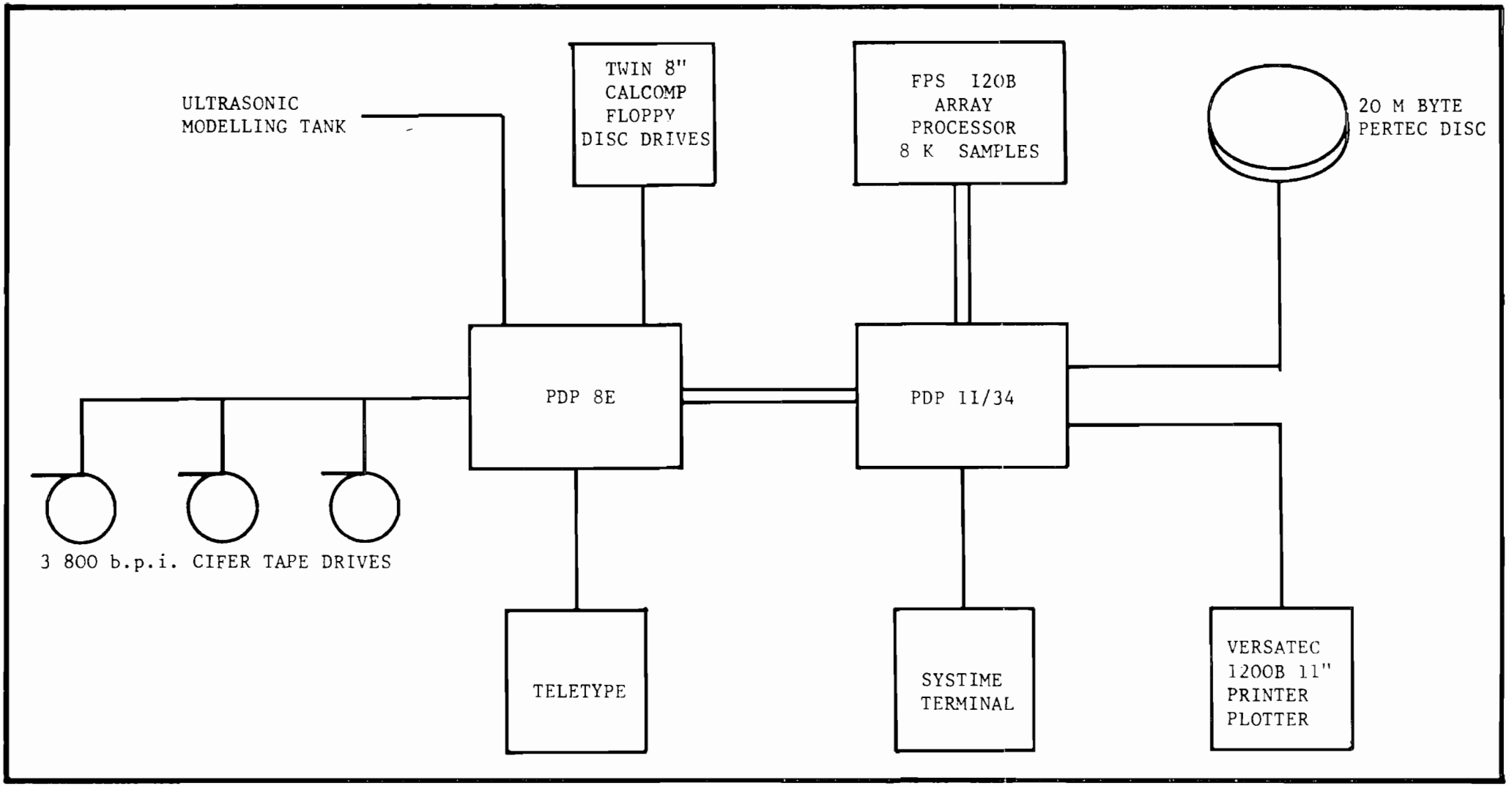

Fig.3.2 Schematic diagram of the original processing system set up by Poulter (1982).

1200B, but it still had the 200 by 200 dots per inch resolution. A parallel DMA interface connected the PDP-11/34 to an older DEC computer, a PDP-8E. This was only a 12 bit machine, and also much slower than the PDP-11/34. The PDP-8E sub-system was made up of three 800 b.p.i. Cifer tape drives, two Calcomp 8-inch floppy disc drives, used for storage of the PDP-8E operating system and local programs, and a Teletype terminal, used to control the operation of the PDP-8E. An ultrasonic modelling tank also interfaced with the PDP-8E.

3.2.2 The Original System Operation

The two computer systems had to be switched on and started independently. The PDP-11/34 worked under the RT-11 operating system, where as the PDP-8E used the more primitive OS/8 system. The PDP-8E then ran a single program which inspected the PDP-11/34 interface for a command to either read, write or move a tape mounted on the Cifer tape drives. To the PDP-11/34, the PDP-8E acted like an intelligent tape controller.

The data recorded on tape were read by the Cifer tape drives and passed via the PDP-8E and the PDP-11/34 to be stored on the Pertec disc unit for processing in the PDP-11/34 and array processor. After the data had been processed, the results were passed back from the disc via the same route to be recorded on to an output tape. The limited disc space meant that only small portions of the data set could be retained on the disc at any one time, e.g. a single CMP gather or part of a stacked profile.

3.2.3 Limitations and Problems with the Original System

With the machines, operating systems and user software available at the start of the project it soon became apparent that the system was too unreliable for long term reflection seismic processing. To minimize the interference from the unused seismic modelling tank the greater part of its associated electronics were disconnected. The majority of the major hardware problems encountered were from two devices, the Calcomp floppy disc drives attached to the PDP-8E and the interface between the two computers. The disc drives regularly failed to read the systems or program disc, usually due to some electronic component failure in the disc controller or the drive itself. As there was no maintenance contract with the disc drive manufacturer, repairs had to be done in house, normally by the author, and typically took several weeks.

The computer interface was made up of three parts: two printed circuit boards which plugged into the PDP-11/34 supplied by DEC, a box of electronics built at Durham to translate the 16-bit words used by the PDP-11/34 to the 12-bit words used by the PDP-8E, and the boards inside the PDP-8E. The communications channel proved to be very temperamental, particularly one connection, the slightest movement of which would cause communication between the computers to be lost.

3.3 System Improvements

The purchase of the Systime tape drives removed the dependence on unreliable components and obsolete computer hardware. It was hoped to complete the demultiplexing of the Farnella 1/81 data prior to the phasing out of the PDP-8E and its peripherals, by reading the field tapes using the PDP-8E and Cifer tape drives and writing the output common shot gathers to tape on the new Systime drives. This was not achieved because a major fault in the Calcomp floppy disc drives finally prevented operation of the PDP-8E system.

This marked the start of a complete rewriting of the processing software (Chapter 4 and 5), and the installation of a new operating system. Poulter (1982) states that the original system operated under RT-11 version 3B, but it actually appears to have been a mixture of versions 2 and 3. The advantages gained from the new operating system included a magnetic tape handler, the ability to handle more peripheral devices and an error logger to monitor the system.

The addition of a further 16 k of floating point number memory for the FPS array processor with a new extended software library gave a total data space of 24 k real numbers, and enabled far more number manipulation to be carried out in the device without the need to store intermediate results in the PDP-11/34. Also more options could now be included in the Time Sequence Analysis Program, e.g. time varying filters, velocity filtering of common mid-point gathers, and dip filtering of stacked sections (chapter 4).

The Pertec disc unit placed an upper limit on the quantity of data which could sorted from common shot to common mid-point gathers at a time. Other programs also needed more random access storage than was currently available, i.e. the velocity analysis, migration and plotting programs. To expand the disc storage the 300 Mbyte System Industries Winchester disc was purchased. The device has been configured to give 8 platters of 32 Mbytes per platter as opposed to the original disc system which only gave 2.5 Mbytes per platter. Even so, the original disc has been retained as the new disc can not be used as a system disc and has no facility for a removable platter cartridge, which can be used for backing up the system or for individual users to have a safe storage medium for their own programs and parameter files.

The latest hardware to be purchased is a new Versatec printer plotter, V80, of the same specifications as the previous machine as a direct replacement. As the original 1200B machine was obsolete, the likely cost of a badly needed overhaul could not be justified. The new machine is more compact, faster and cleaner to use.

3.4 Summary of the Current System

Most of the recommendations made by Poulter (1982) in his thesis have now been carried out: the purchase of new tape drives, the expansion of the array processor, the purchase of a mass storage Winchester disc system, and the replacement of the Versatec plotter.

These increased facilities available to the operator have

enabled many new and powerful algorithms to be added to the reflection seismic processing system. Efficiency has also improved: for example the migration of whole sections, upto 4 million samples per section, can now be done within ten hours. Using the original system this would have taken 32 runs of 128 thousand samples per section at three hours per run.

The possible throughput of the system may be seen in table 3.1 below. For the case of 50 metre CMP spacing this results in about 45 minutes processing time per kilometre of data. The times in table 3.1 do not include that needed for the choice of processing parameters by executing test runs. If a velocity analysis is done every 2 kilometres, each analysis taking typically 20 minutes, and the processing time is multiplied by a factor of one and a half to allow for optimizing the processing parameters, a total throughput of about 40 km. per week can be carried out.

Operation	Time taken per 100 gathers
Demultiplexing	120 mins.
Sorting	60 mins.
Deconvolution Before Stack and Stack	30 mins.
Deconvolution After Stack	2 mins.
Plot Generation, including minimum backgound	3 mins.

Table 3.1 Typical time taken for processing seismic data. For 24 fold data recorded to 8 seconds two-way time with a sampling interval of 4 msec.

CHAPTER 4

PROCESSING SOFTWARE

It was hoped that the data acquired on this project could be directly processed on the Durham seismic processing system using the available software. This was not possible because of reliability problems with some of the computer hardware coupled with limitations in the original processing package written by Poulter (1982). Poulter wrote 26 programs directly related to the processing of reflection seismic data. These proved to be slow in operation, difficult to use due to inadequate documentation, and imposed a maximum of 24 traces of 2048 samples per input gather. Further, many routines had been made obsolete by the purchase of the new hardware. It was therefore decided that a major overhaul of the software package was necessary. This was not only to enable the original algorithms to run more efficiently on the expanded system and provide a better standard of user documentation, but also to enhance the processing suite with new algorithms, to enable the handling of longer traces with higher folds of cover, and to output data in as near as possible the SEG-Y format (Barry et al. 1982). Of the 26 programs listed by Poulter (1982) only six now remain. This has been achieved by combining as many operations as possible into a single program, and chaining these programs together so that the user only needs to call a single routine to execute an entire program suite. For

example, the three programs used for pre-stack, stack and post-stack processing now form the Time Sequence Analysis Program, and the seven programs which were needed to output seismic data to the plotter, are now executed from one master Plot Program. In many cases the algorithms developed by Poulter (1982) have been retained, but the program structure and code have been greatly improved. The work was shared with a post doctoral research assistant, D. W. Wellby, with help on specific problems from other post graduate students and members of staff.

4.1 Demultiplexing.

The demultiplex program is designed to take the SEG-A (Northwood et al. 1982) tapes written by the SDS 1010 and write a "Durham SEG-Y" tape containing the shot gathers. The differences between the SEG-Y format described by Barry et al. (1982) and Durham SEG-Y are: the tape header is in ASCII characters, not EBCIDC, with file marks between each block written, standard SEG-Y has none, the use of DEC floating point numbers and DEC byte order as opposed to the IBM standard. The samples are floated into real numbers and sorted into trace sequential order so that the first trace written is from the receiver nearest the ship, and the last trace written is from the receiver furthest from the ship. This program has been completely re-written since the installation of the new tape drives and controller. The algorithm developed by Poulter (1982) has been retained but several errors have been corrected and more of the work of the program is now done in the array processor.

Under the DEC operating system it is not possible to read data blocks from tape which are more than 32k bytes long due to the 16 bit limitation of the computer. It has therefore been necessary to develop an in-house tape read routine which could handle the 200 kbyte blocks expected on the SEG-A field tapes recorded by the SDS 1010 for each shot record. The subroutine used, EXREAD, was written by D. Stevenson at the end of 1981. The computer memory is cleared of all program and system software to maximize the available space. A small routine then reads a whole tape block into the 256 kbyte computer memory by directly manipulating the tape drive status words. At the end of the read operation the same routine copies the data to a disc file before reinstating the computer operating system and the rest of the demultiplex program. The program processes and outputs the shot gather before clearing the memory again in preparation for reading the next record from the input tape. As the whole operating system is removed no error monitoring is performed and no check can be made for the successful copy of the program to and from disc, hence the whole process is extremely precarious. An attempt to implement a double buffering routine to continuously transfer the data in smaller blocks (by reading into one buffer while the other is copied to disc, then when the read buffer is full switching buffers, repeating until the whole input tape block is read) failed, as the Pertec disc drive could not keep up with the input data flow from the tape.

Much time was spent developing tape handling routines to deal with the Durham SEG-Y tape headers and the trace headers.

These routines were written so that they could be easily adapted to fit in any subsequent program as each was re-written.

This SEG-A demultiplex program has been documented by D. Wellby. A short note on the structure of the necessary parameter file used by the program is included in appendix 2.

4.2 Common Mid-Point Sorting.

The objective of the common mid-point (CMP) sort is to gather together all the individual traces which have the same source receiver mid-point into a single gather, i.e. a CMP gather. At this stage it is also convenient to provide a routine which can translate other demultiplexed formats to Durham SEG-Y.

Poulter (1982) developed a sort algorithm which could be used as a stand alone routine or be coupled to the demultiplex program to produce CMP sorted data directly from the field data tapes. The SEG-A demultiplex program is prone to fail occasionally during the transfer of the operating system and program in and out of memory. In order to ease the restarting of a crashed program, the sort routine has not been included at the demultiplexing stage, and is only available as a separate program. The algorithm developed by Poulter (1982) has been retained. The common shot gather is read trace by trace, each trace being output into the relevant CMP gather file on disc. Extra options have been added to enable the decimation of the input traces (i.e. to re-sample with a longer sampling period), to identify and remove traces with a severe noise problem such as large random spikes, and to allow the sorting of data acquired

with the receiver spacing less than twice the shot spacing (split sorting where each shot point gives rise to more than one CMP gather per shot gather).

A description written by D. Wellby for the running of the CMP sort program is included in appendix 2.

4.3 Time Sequence Analysis.

This is the major reflection seismic processing package, and again some of the algorithms follow from the work of Poulter (1982). The whole package has been completely re-written using a more powerful command structure to ease the operation of the very complex program which allows deconvolution before stack, stack, and deconvolution after stack to take place during a single pass. The intention of combining as much of the processing into a single program as possible is to minimize the tape input and output. Otherwise, as with the original programs, more time is spent transfering data to and from tape than processing. The first version of this program was written in conjunction with D. Wellby but it has since been greatly modified and expanded by the author to include several new routines and a new control structure. The most recent addition, and probably the most important, has been the writing of a full interactive input for ease of use by people not familiar with the DEC RT-11 computer operating system or the line edit program. A copy of the program manual is included in appendix 2. Table 4.1 shows the options now available.

Data Manipulation Routines.

Time Break correction

Source and Receiver Depth Correction, Field Statics

Sea-Floor Consistent Statics

Automatic CMP Consistent Statics

Whole or Part Trace Editing

Mute Functions at the Start and/or End of Traces

Polarity Reversal of Traces

Time Varying Gain Functions.

Assorted Time Ramps:

$T^n \exp(fT)$ where n = 0,1 or 2

TV^2 Time/Velocity Ramp

Automatic Gain Control

Trace Normalisation

One Dimensional Filtering Options.

Band-Pass Filter

Band-Reject Notch Filter

Time Varying Band-Pass Filter

Wiener Filter

Prediction Error Filter

Reflection Strength Transform

Two Dimensional Filtering Options.

Velocity Filter on CMP Gathers

Dip Filter of Stacked Profiles

Three Trace Mixing of Stacked Profiles

Horizontal Summation of Stacked Profiles

Miscellaneous Options.

Autocorrelation Fuction

Normal Move-out Correction Application and Removal

Horizontal Stack of NMO'ed CMP Gathers

Table 4.1 Processing Options

The new routines which have been added to the original system are decribed below.

4.3.1 Time Break Correction with Source and Receiver Statics.

The time break correction is coupled with the source and receiver depth correction in order to remove the known static errors from the data prior to any processing. These corrections are vital to set the zero two-way travel time to a specified datum level. For marine surveys this is usually chosen so that the zero time corresponds to the shot time with the source and receiver arrays at the sea surface. If this correction is not carried out then the timing errors may degrade the effectiveness of the stack. It is normal practice to start the acquisition record before the shot instant, so that the exact time of the source fire pulse may be recorded. This adds zero samples at the start of the trace, i.e. all the reflected energy will appear late; hence all the calculated velocities will be lower than expected. Similarly, if the source and receiver are not corrected back to the sea surface then the reflected energy will appear early giving correspondingly high velocities. The two-way time to the sea-floor reflector can be used as the gap for a prediction error deconvolution filter to remove multiples, any error in the water depth may cause this filter not to work, if the the design parameters are too narrow.

The time break correction is given in msecs while the source and receiver depths are defined in metres. The program assumes a velocity of 1.5 km/sec for the sea water to correct depths to travel times. The total correction time is computed accurate to

the nearest integer multiple of the sampling period and applied to the trace as a simple move operation in the array processor.

4.3.2 Sea Floor Consistent Statics for Deep Reflectors.

The sea floor consistent statics option is used to correct an input CMP gather for any large structures which may occur over the length of the receiver array. The routine applies a gross static correction assuming the water acts like a weathered layer, as in land data, by adding an unknown delay to the wave front. This delay is dependent on how deep the water is directly below the source and receiver. Using the bathymetry record from an echo sounder the water depths at the source and receiver are determined and compared to the depth at the CMP. From these values the correction can be calculated.

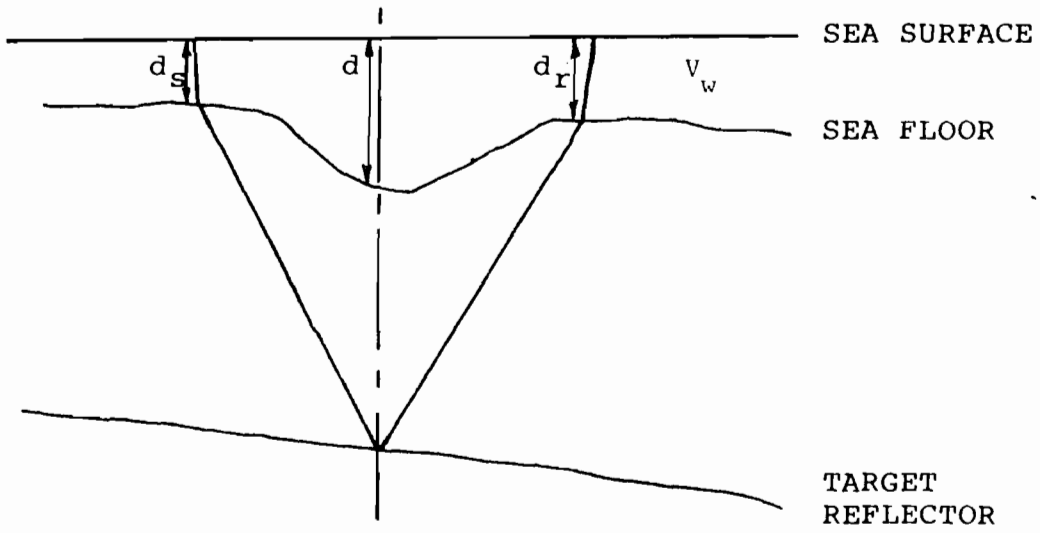

Fig. 4.1 Sea Floor Statics Geometry.

If the target reflector is very deep compared with the array

aperture then the acoustic energy may be assumed to be travelling vertically through the water column to a good approximation (Fig. 4.1)

If the zero offset two-way travel time in the water, which has seismic velocity V_w, at the CMP point is

$$T_{cmp} = 2 \left(d/V_w \right) \quad \ldots 4.1$$

and the travel time within the water below the source and receiver pair is

$$T_{sr} = d_s/V_w + d_r/V_w \quad \ldots 4.2$$

then the difference between the two travel times is given by

$$dT = T_{sr} - T_{cmp} \quad \ldots 4.3$$

$$= \left(d_s + d_r - 2\, d \right) / V_w. \quad \ldots 4.4$$

This correction, accurate to the nearest sample interval, is applied to the trace in the same way as the time break correction.

4.3.3 Automatic CMP Consistent Statics.

The automatic CMP consistent statics may be used for removing any residual static corrrections left within each CMP gather after the removal of any gross static corrections mentioned above. The program was developed from work done by Loveridge (1981). The gather is corrected for normal move-out but not stacked, each trace is then cross-correlated with a pilot trace. The pilot trace may be an individual trace or group of

traces summed together. The position of the maximum value in the cross-correlation function represents the optimum delay for that particular trace, and is applied as a static correction. After the static shifts have been applied to the gather it may be directly stacked without the need to remove the move-out correction. However, if muting or velocity filtering is to be applied or the gather is to be used for velocity analysis then the move-out correction must be removed. Care must be exercised when using this routine as it is necessary to apply the future stacking velocity move-out correction to the gather before the static shifts are applied to align the primary reflectors. If there is an error in the stacking velocity picks then the program will align the primary reflectors to the given false velocity structure or may even choose non-primary events. The most robust reflector in a marine data set for this correction is found to be the sea floor, where this is not obsured by refracted energy. The other advantages are that the sea water velocity is known and the reflector from a flat lying sea floor is truly hyperbolic and so fits the move-out equation exactly. An example of the effectiveness of this routine can be seen in Fig. 4.2. The data is taken from the 1980 Discovery cruise to the Caribbean where there were problems with the receiver array not maintaining a constant towing depth in the water, which caused unknown delays to be added to the further offset data traces. Figure 4.2a shows a velocity analysis done on an uncorrected CMP gather. Note the poor definition of the velocity function on the semblance diagram and the 1.7 km/sec velocity for the sea water. Figure 4.2b shows

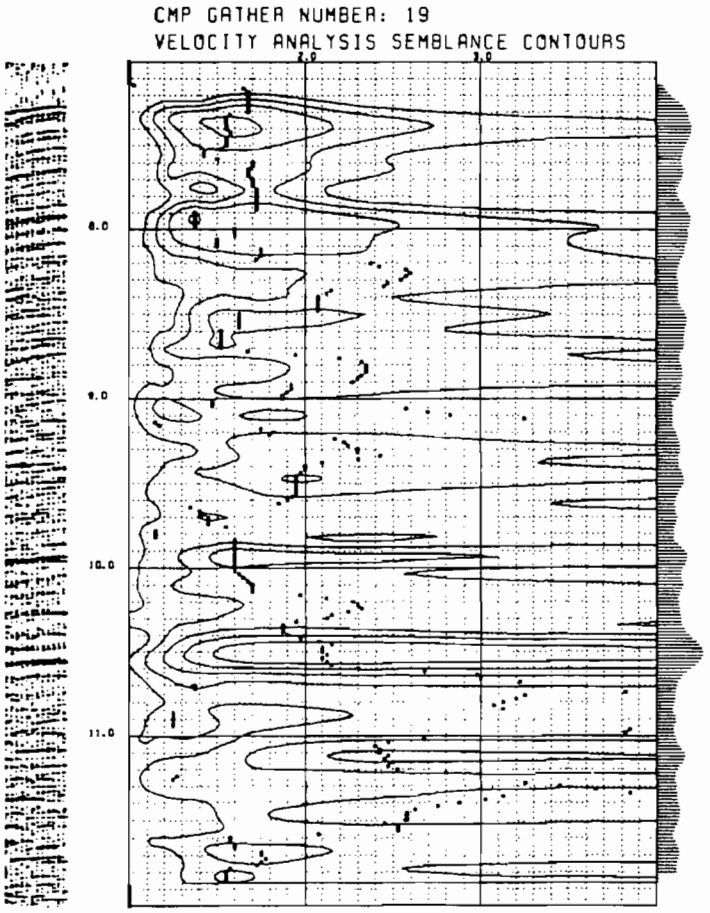

Fig.4.2a Velocity analysis before the application of CMP consistent statics.

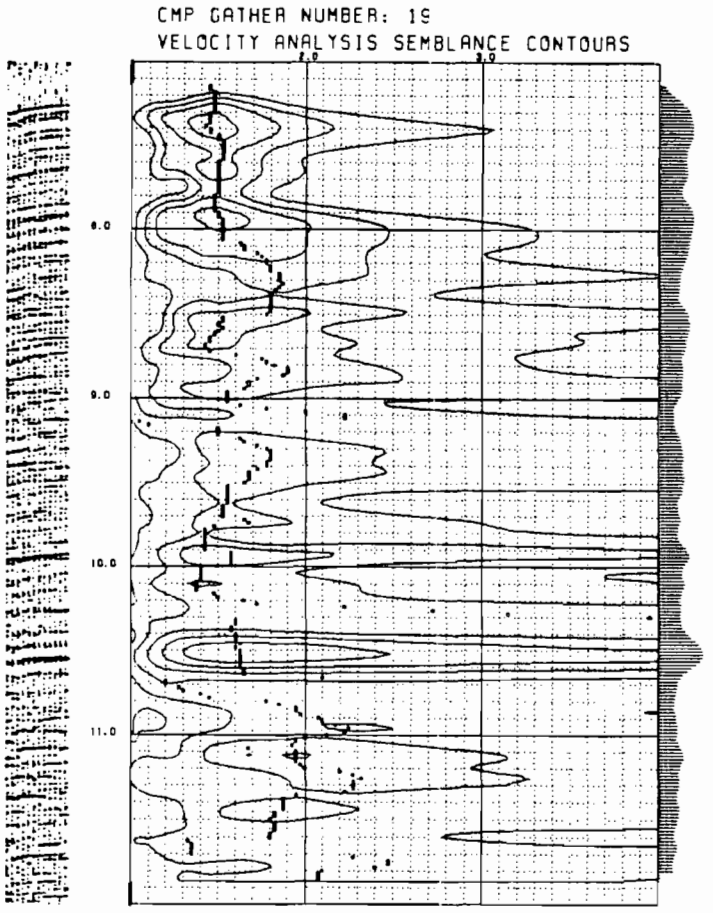

Fig.4.2b Velocity analysis after the application of CMP consistent statics.

PROCESSING PARAMETERS

NO. OF CHANNELS = 12
SAMPLES PER CHANNEL = 2048
TRACE DELAY MS = 4000.0
LEVEL OF INTERPOLATION = 4
CHANNEL 1 OFFSET M = 220.0
CHANNEL SPACING M = 100.0
SAMPLING INTERVAL MS = 4.0
START OF ANALYSIS MS = 7000
END OF ANALYSIS MS = 12000
TIME STEP MS = 20.0
OPERATOR GATEWIDTH MS =256
START VELOCITY KM/S = 1.00
END VELOCITY KM/S = 4.00
VELOCITY STEP KM/S = 0.03
MIN. CONTOUR VALUE = 0.20
CONTOUR INTERVAL = 0.10

the same gather after auto-statics have been used to remove the unknown delays assuming a water velocity of 1.5 km/sec. The effect of the shift applied can be seen in the gather and the correponding improvements in the velocity analysis.

4.3.4 Autocorrelation Function.

Autocorrelation output enables short sections of the line to be processed with the autocorrelation output written to disc. This file may be plotted to show any periodicities within the data before and after deconvolution. The function may be used to help in the design of deconvolution filters or to check how good a given filter has been at removing periodic signals from the data. The disc file is written in a form which can be read directly by the plot program (section 4.4).

Figure 4.3a shows a short section from a profile collected by Lamont-Doherty Geological Obsevatory from off of the Moroccan coast. Its autocorrelogram before deconvolution is shown below. Figure 4.3b shows the same section after deconvolution with its autocorrelogram. As expected, the periodicity in the section has been removed.

4.3.5 Time Varying Band-Pass Filter.

The time varying band pass filter is taken from a paper published by Nikolic (1975). Most seismic processing applies an approximation to a time varying filter by using several constant filters over short windows and then merging these windows together. If the filter characteristics change abruptly, the

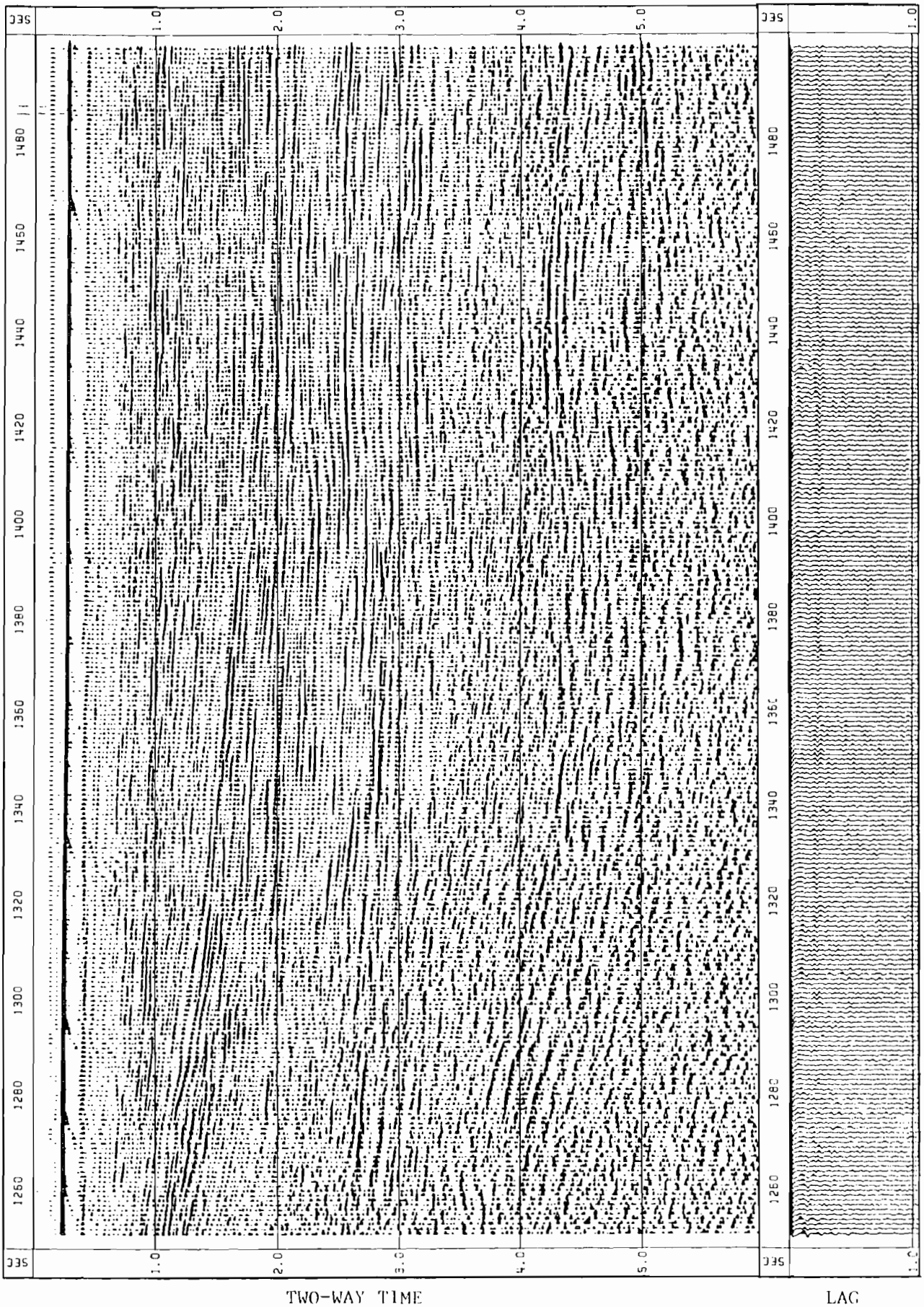

Fig.4.3a Raw stacked section with its autocorrelogram showing the presence of the sea floor multiple at a lag of 250 msec.

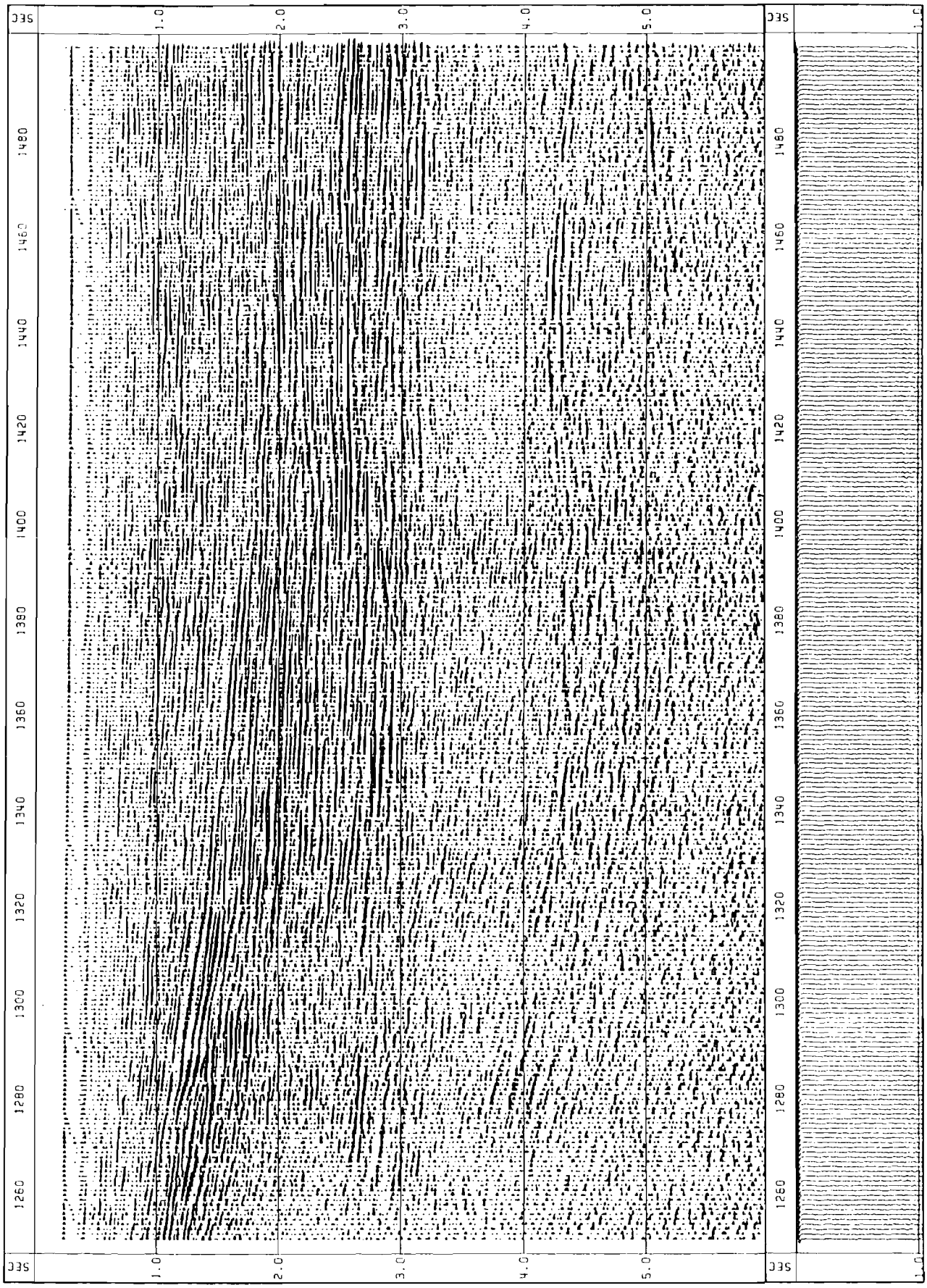

Fig.4.3b Processed stacked section with prediction error filtering applied to remove sea floor multiple.

final section will contain sudden changes in signal shape which may mislead the interpreter. The advantage of the Nikolic approach is that the filter is truly time varying so the areas merge smoothly together.

The basic filter used is a simple Butterworth band-pass filter (Lynn 1977), with the following transfer function $P_a(s)$ in the s-plane is given by

$$P_a(s) = B\ s\ /(\ s^2 + B\ s + \omega_0{}^2) \qquad \ldots\ 4.5$$

where: s is the Laplace transform variable

$B = \omega_h - \omega_l$

$\omega_0{}^2 = \omega_h . \omega_l$

$\omega_h = \tan (T\pi f_h)$ is the upper -3dB point

$\omega_l = \tan (T\pi f_l)$ is the lower -3dB point

T is the sampling interval

f_l is the lower cut off frequency of the analogue filter

f_h is the upper cut off frequency of the analogue filter

As shown by Nikolic, if $s = j\omega$ then the filter is not zero phase. This may be overcome by applying two filters, with the second having the opposite phase characteristics to the first. By using half the amplitude of each filter the final gain of the combined results is unity.

$$P_a(\omega) = 1/2\ P_a(j\omega) + 1/2\ P_a(-j\omega) \quad \ldots 4.6$$

By applying a bilinear transform (Rader and Gold, 1967) of the following form where $z = \exp(j\omega T)$

$$s = (z - 1)/(z + 1) \quad \ldots 4.7$$

a corresponding digital filter may be produced.

$$1/2\ P_d(z) = 1/2\ P_a(s) \quad \ldots 4.8$$

$$1/2\ P_d = a_0(1 - z^{-2})/(1 - a_1 z^{-1} - a_2 z^{-2}) \quad \ldots 4.9$$

where: P_d is the digital filter response

$$a_0 = B / 2 (1 + B + \omega_0^2)$$

$$a_1 = 2 (1 - \omega_0^2)/(1 + B + \omega_0^2)$$

$$a_2 = 4\ a_0 - 1$$

This filter may be applied by a forward recursion formula

$$y_n^F = a_0(x_n - x_{n-2}) + a_1 y_{n+1}^F + a_2 y_{n+2}^F \quad \ldots 4.10$$

Similarly for the second case where the (-s) term is equivalent to a reverse recursion formula

$$y_n^R = a_0(x_n - x_{n+2}) + a_1 y_{n-1}^R + a_2 y_{n-2}^R \quad \ldots 4.11$$

To obtain the final band-passed trace the resultant forward and reverse recursion traces are added together

$$y_n = y_n^F + y_n^R. \quad \ldots 4.12$$

The coefficients a_0, a_1 and a_2 may be solved for any given frequency range f_l to f_h. To achieve the time varying characteristic two frequency ranges are chosen, one for the upper part of the section down to a two-way travel time t_1 and one for the lower part of the section starting at two-way travel time t_2, such that t_2 is greater than t_1. Above and below these times the band pass characteristic is constant with the specified values but between these times the filter coefficients, a_0, a_1 and a_2 linearly change from one band pass filter to the other. This variation is not strictly linear in the frequency domain but it does provide a smooth change as shown in Fig. 4.4, which is the same section as Fig.4.3b with the time varying band-pass filter applied. Also by writing the routine in the array processor assembler language, APAL (Floating Point Systems 1982), the implementation of the filter in the processor has been made extremely fast (see TVBP in appendix 2).

4.3.6 Reflection Strength Transform.

This reflection strength transform R is a simple envelope detection problem which may be solved by finding the quadrature component using the Hilbert transform H [a] and summing the squares of the amplitudes of the real and quadrature signals and taking the square root of the result (equation 4.13).

The resultant is used to show "bright spots" in the seismic section. These are used in the oil industry as an indication of a gas/liquid interface in a reservoir, but in general the technique may be used to high-light any strongly reflecting interface.

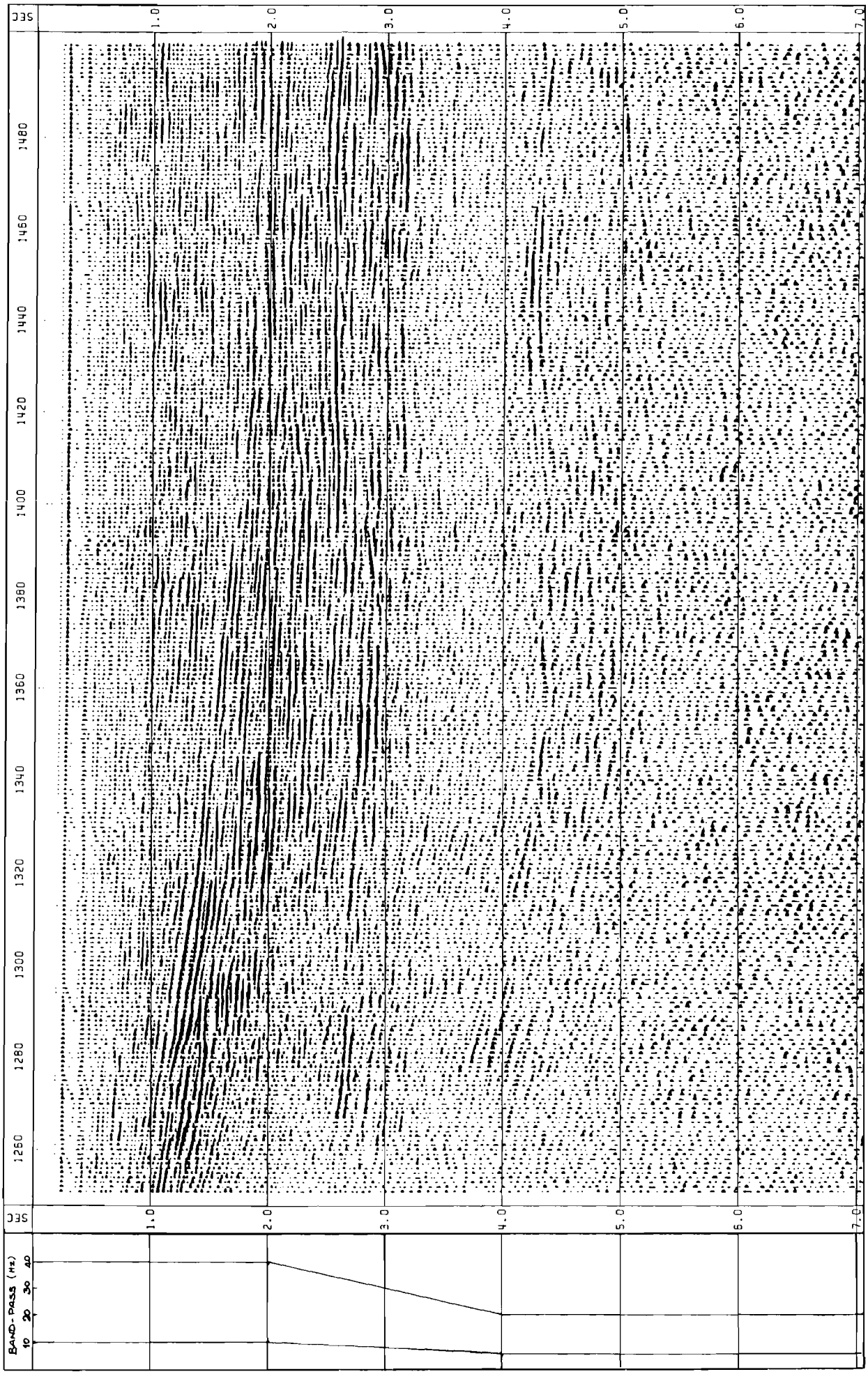

Fig.4.4 Post stack processed section with time varying band-pass filter applied.

Having determined the Hilbert transform the routine may be expanded to produce instantaneous frequency and phase in the seismic section.

$$R_i = (a_i^2 + (H [a_i])^2)^{1/2} \qquad \ldots 4.13$$

where: R_i is the reflection strength coefficient at sample i

a_i is the amplitude of the i th sample

$H[a_i]$ is the quadrature signal amplitude

if $a(t) < F.T. > A(\omega) = R(\omega) + j\, X(\omega)$

then $H\,[a(t)] < F.T. > H\,[A(\omega)] = X(\omega) - j\, R(\omega)$

Figure 4.5 shows the section displayed in Fig. 4.4 as a reflection strength plot.

4.3.7 Velocity Filter.

The velocity filter has been developed from work by Ryu (1982), where a simple-distance time, x-t, domain operator could be applied by two dimensional convolution with a CMP gather which has had a false move-out correction applied. This move-out correction is chosen so that the wanted primary and unwanted multiple coherent arrivals are separated into different quadrants in the frequency- wavenumber, f-k, domain, i.e. have opposite apparent velocities in the x-t domain. Then by applying a reject filter in the f-k domain the unwanted arrivals may be suppressed. This filter has a simple form and may be directly designed in the

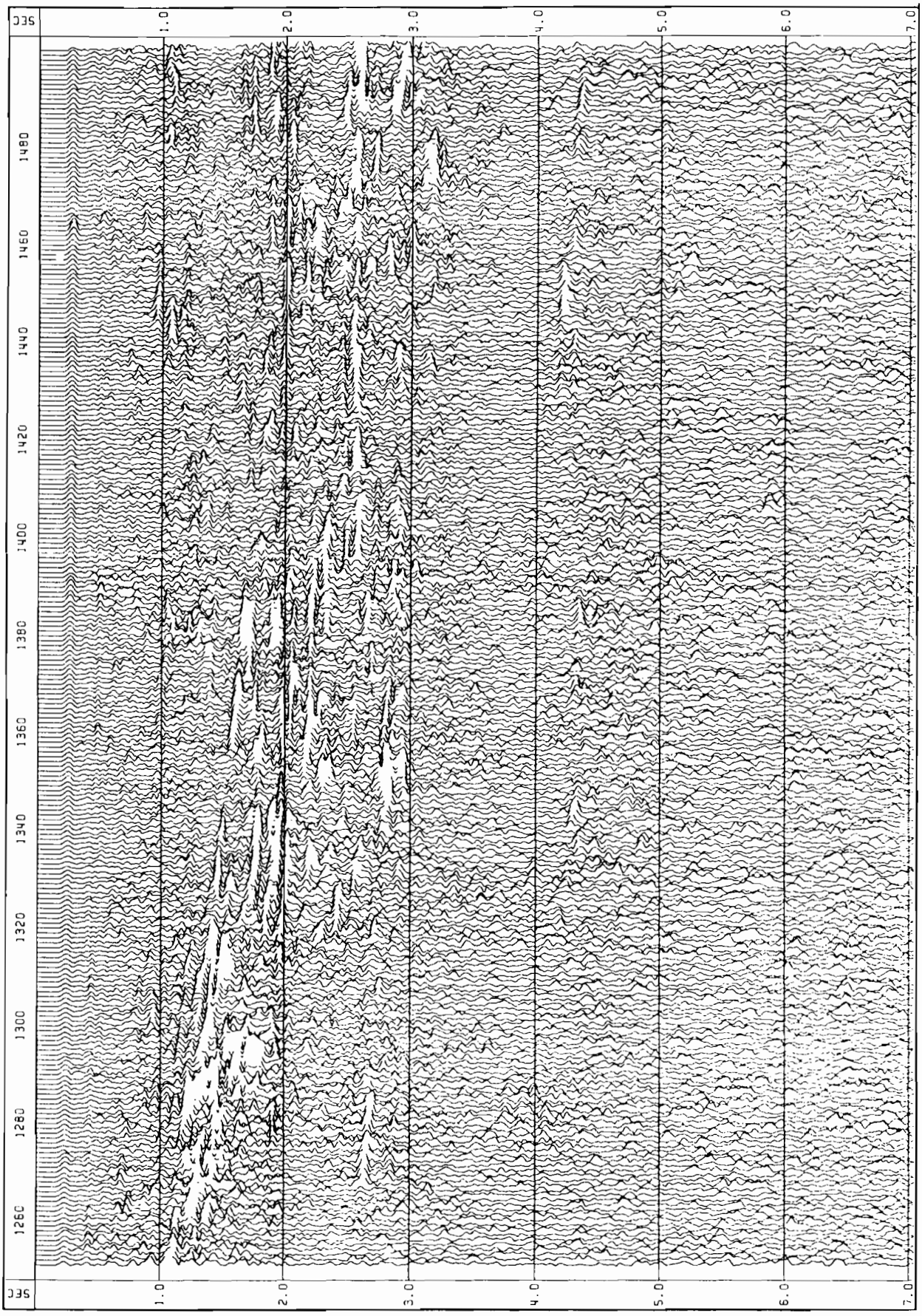

Fig.4.5 Reflection strength transform on a post-stack processed section.

x-t domain. Figure 4.6 shows the basic principles involved. The CMP gather (Fig. 4.6a) contains primary reflections P which are partially obscured by multiples M. It can be seen that the multiples have a lower apparent velocity than the primary events. By choosing a false velocity function so that when the move-out correction is applied the primary reflections are over-corrected and the multiple arrivals are under-corrected (Fig. 4.6b), the crossing events are separated in the f-k domain. A double Fourier transfrom would produce the result indicated in Fig. 4.6c, where the multiple events appear in the positive quadrants and the primary reflections appear in the negative quadrants. The filter to remove the multiple energy, shown in Fig. 4.6d, is of a simple form so that the double Fourier integral may be solved. The resulting x-t domain operator may be applied directly to the false moved-out gather by two dimensional convolution. This avoids the need to transform the whole data set into the f-k domain. The result of such a process is shown in Fig. 4.6e, where the unwanted multiple has been suppressed. Figure 4.6f shows the final CMP gather after the false move-out function has been removed.

The process works well where there is considerable move-out difference between the primary and multiple energy, but care must be exercised not to set the false move-out velocity too high; otherwise primary energy will be lost. The filter also has the tendency to colour the noise so that it may appear as a coherent arrival at the false move-out velocity function. It has been found that the velocity filter is best used in the velocity

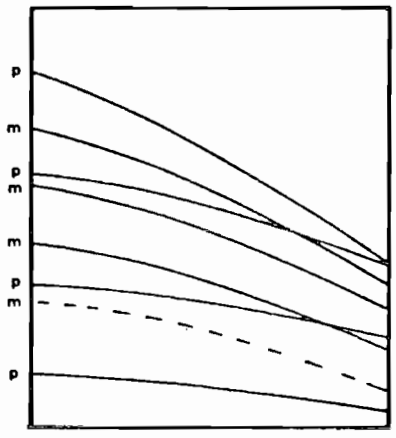

(a) Input CMP gather
p is a primary arrival
m is a multiple arrival

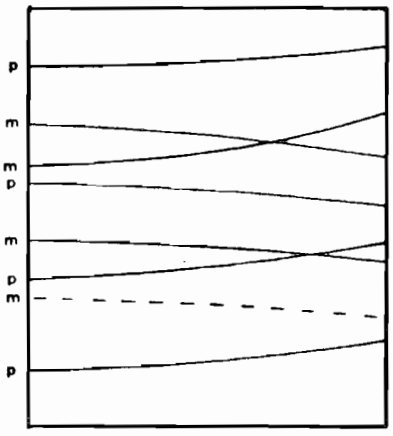

(b) Gather with false move-out applied.

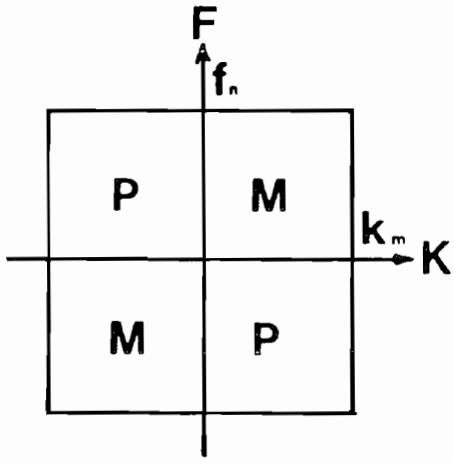

(c) False moved-out gather transformed into the f-k domain

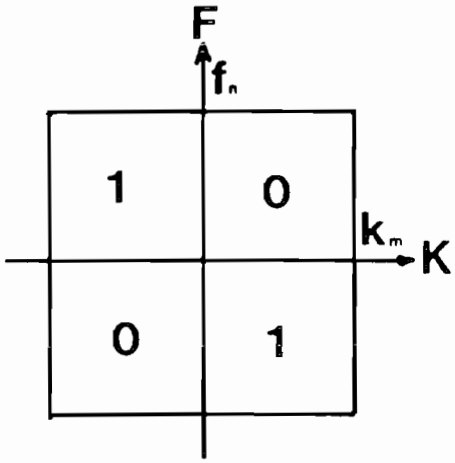

(d) F-k domain filter to remove multiple arrivals

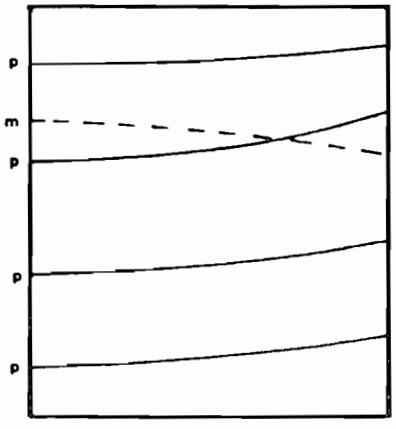

(e) Filtered gather transformed back into the t-x domain

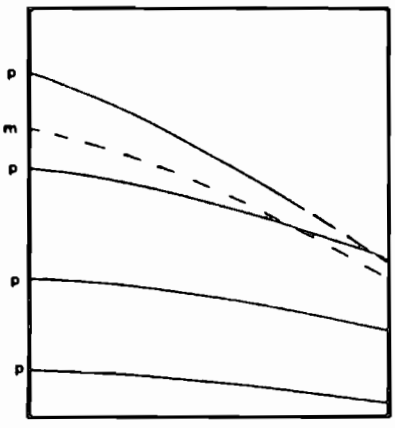

(f) Filtered gather with the false move-out removed

Fig.4.6 Principles involved in velocity filtering CMP gathers. Redrawn from Ryu (1982).

analysis routine to obtain the optimum stacking velocity function. Its use during routine processing before stack did not greatly reduce multiple energy in the final section over and above that obtained through the normal stacking process. It is not effective in areas of deep water with small aperture arrays as the normal move-out corrections are too small.

The space time operator shown in Fig. 4.6d is the solution to the Fourier integral

$$L(x,t) = \left[\int_{0}^{f} \int_{-k}^{0} + \int_{-f}^{0} \int_{0}^{k} \right] \exp(-j2\pi(ft+kx)) \, df \, dk \quad \ldots 4.14$$

The solution to this equation for discrete sampling on both the x and t axes is as follows

$$L(m\Delta x, n\Delta t) = \frac{1}{2 \, mn \, \Delta x \, \Delta t \, \pi^2} \left(1 - (-1)^m - (-1)^n + (-1)^{m-n} \right) \quad \ldots 4.15$$

To apply the above filter needed the development of a two dimensional convolution routine from the following formula

$$a(i,j) = \sum_{n=1}^{N} \sum_{m=1}^{M} s(i-n, j-m) \, f(n,m) \quad \ldots 4.16$$

For efficient array processor usage a practical limit of a 29 by 29 operator is imposed and a specialist APAL routine CSQ2D has been written, see appendix 2.

Figures 4.7 show the effectiveness of the filter on real data. Figure 4.7a is a velocity analysis taken fron a shallow marine environment and Fig. 4.7b is the velocity filtered

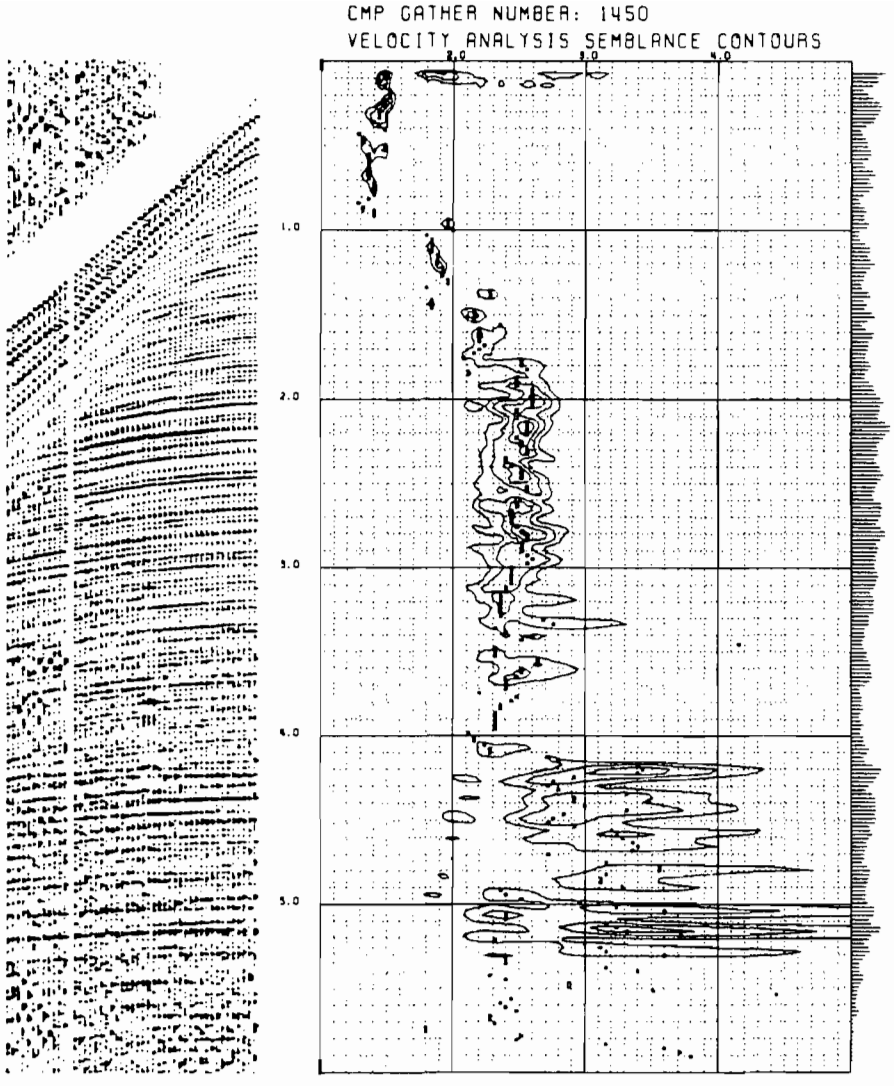

Fig.4.7a Velocity analysis of a CMP gather without prior velocity filtering.

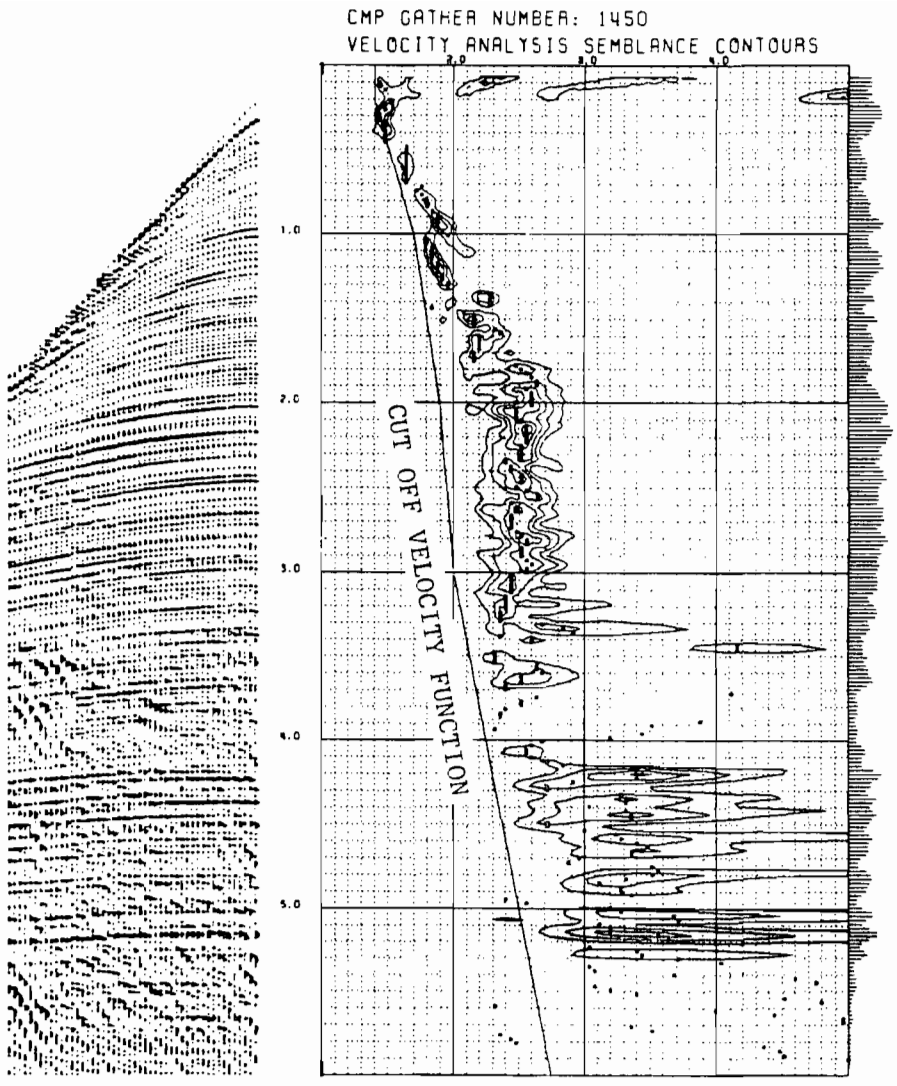

Fig.4.7b Velocity analysis of a CMP gather with prior velocity filtering.

version. Note the improved resolution of the velocity structure in the upper two seconds of the record. The improvement in the estimate of the stacking velocity function will give the better resolution in the final processed section.

4.3.8 Dip Filter

The dip filter for stacked data sections is an extension of the x-t domain velocity filter. Here the filter is designed in the f-k domain and transfomed back into the x-t domain and applied by the same APAL routine, CSQ2D. The cut off dip is determined by the minimum apparent velocity.

Figure 4.8 shows the same section as Fig. 4.3b after dip filtering. The processed section shows a better continuity in the reflectors in the upper 4 seconds of the profile, but as can be seen at the bottom of the example, where the signal to noise ratio is low, the result is a "wormy" appearance of crossing lines at the cut-off velocity.

4.3.9 Horizontal Summation

The horizontal summation of stacked traces allows the changing of the horizontal sampling interval without the loss of any data. If each output trace is the sum of N input traces, then the spacing is increased by a factor N and the effective fold of cover for each trace is also increased by a factor N. The advantages of such a process are the improvement in signal to noise by the suppression of coherent arrivals with large apparent

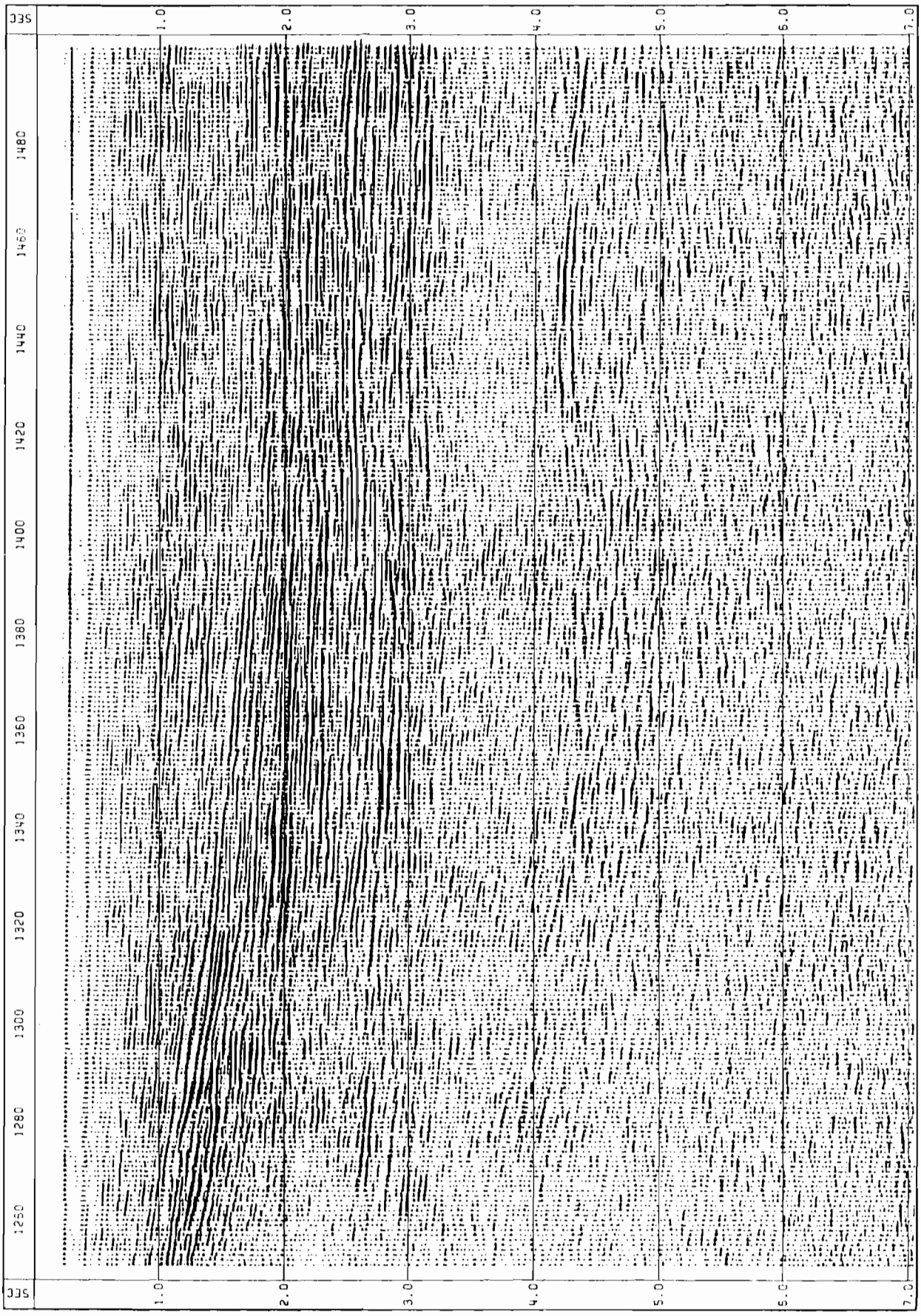

Fig.4.8 Dip filtered post-stack processed section.

dips, such as side-swipe for off-line reflectors and diffraction energy trapped in the water layer. The same effect may be achieved by dip filtering, but this does tend to leave a blurred effect to sharp edges and introduce coherent noise at the cut-off velocity of the filter. Unfortunately, this type of process may only be used where the target reflectors are reasonably horizontal over the N traces to be summed. The disadvantage is the loss of lateral resolution but this may be discounted if the width of the summed traces at the target horizon is less than that of the first Fresnel zone at that depth for unmigrated data. The effect of horizontal summation on the section of Fig.4.3b can be seen in Fig. 4.9.

4.3.10 Normal Move-Out Correction and Vertical Stack.

The move-out correction and vertical stack were originally part of a separate program. This meant handling the data at least three times to produce even a brute stack. As tape transfers were the slowest operation more time was spent reading or writing tapes than processing. It was therefore beneficial to incorporate the stack process into the main processing package. This also enabled both the autostatics correction and velocity filter algorithms to be included. The move-out correction algorithm written by Poulter (1982) worked by interpolating the input trace to a higher sampling frequency using the approach of Lu and Gupta (1978), and then calculating the nearest interpolated sample to the ideal move-out hyperbola. This was satisfactory provided that a high enough interpolation level was used to avoid serious

Fig.4.9 Post-stack processed section with horizontal summation.

waveform distortion. Originally, when the size of the array processor was limited to 8 k samples, the interpolated data samples had to be stored in the PDP-11/34 memory which greatly slowed down the operation. The addition of more array processor memory and the writing of a faster normal move-out algorithm in APAL, NMO (appendix 2), enabled the whole process to be done in the array processor, the stack routine has been transformed from a stand alone program to a small subroutine within the Time Sequence Analysis Package. In addition, correction can now be made for a mute function at the start of the trace and to account forany totally zero traces which might have been included in the gather. The resulting stacked trace therefore now represents the true amplitude of an ideal stacked gather with no zero traces and no mute function. The new algorithm works by calculating the moved-out sample value by the linear interpolation between the two nearest samples on an interpolated input trace to give least possible distortion. The reverse move-out routine, OMN (appendix 2) also written in APAL, was originally written as part of the development of the velocity filtering routine.

If the standard move-out formula is given by

$$T_x^2 = (T_0^2 + X^2/V_{rms}^2) \quad \ldots 4.17$$

where: T_x is the move-out time at trace offset X

T_0 is the time at the zero offset trace

X is the offset

V_{rms} is the rms velocity at time T_0 defined at zero offset.

The reverse move-out equation is given by

$$T_0^2 = (T_x^2 - X^2/V'^2_{rms}) \quad \ldots 4.18$$

where: T_0 is the move-out corrected time at the zero offset trace

T_x is the time at the at trace offset X

X is the offset

V'_{rms} is the rms velocity at time T_0 defined at offset X.

4.4 The Plot Program.

The plotting routines written by Poulter (1982) were not only slow but very inconvenient to use. Only one of the routines produced any annotation on the output plot and that had to be merged onto the seismic section at the time of plotting. The trace spacing on the plots could be varied up to a tenth of an inch or fixed at half an inch. Different programs had to be run if control was to be interactive or to come from a parameter file. The frequency analysis only produced amplitude and phase plots. The phase was not unwrapped to remove the discontinuities from the solution of the arctangent calculation.

The new plot program incorporates all of the Poulter (1982) programs in a single suite. The range of output formats has been increased to include variable area (either positive or negative lobe) and wiggly line plots with trace spacing which may be set to any value up to one inch. Also there is more flexibility in choosing the time window and time scale of the plot. Every plot produced has a limited header added automatically which includes a time scale, details of the plot parameters used, and a title to minimize the risk of confusion when many plots are produced at one time. The frequency analysis option produces power, amplitude and unwrapped phase. Figure 4.10 shows part of the frequency analysis of a post-stack processed trace taken from the section shown in Fig. 4.3b. The main input routine is interactive but the program may also execute from a data file. The users manual for Plot Program is included in appendix 2.

To speed the raster conversion of seismic data use was made

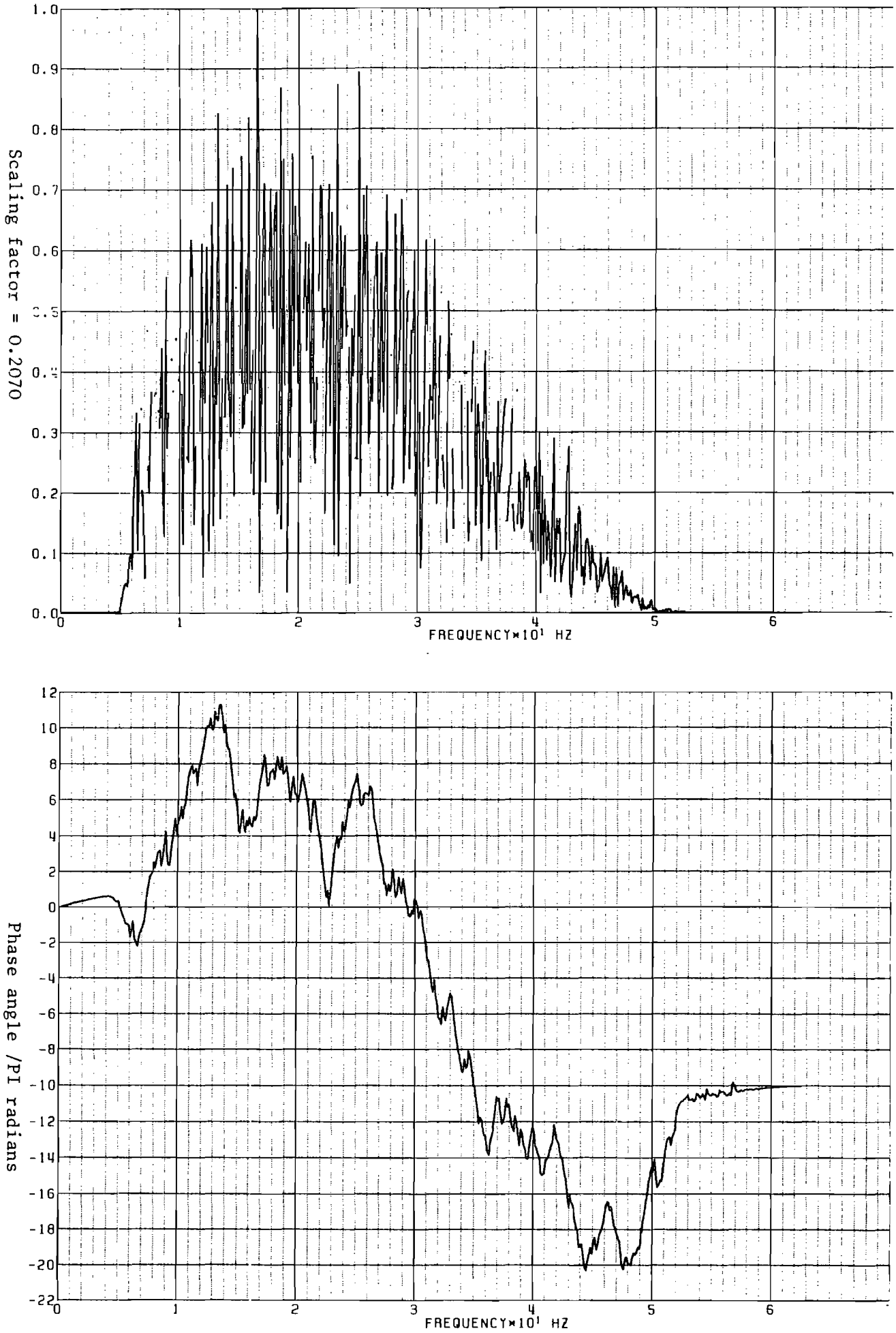

Fig.4.IO Spectral analysis showing amplitude and phase as a function of frequency.

of the expanded facilites now installed at Durham. The data to be plotted are read in to a file on the Winchester disc. The 16-bit limitation of the PDP-11/34 computer imposes a maximum size of 4 M samples per plot, e.g. 4096 traces of 1024 samples per trace. For profiles larger than this the plot has to be produced in sections. The rasterized plots files are also generated on the Winchester disc and may be up to 26 feet in length. Four APAL routines have been written (RASTER, LOR, WLINE and LINE, see appendix 2) to convert the seismic data to raster format using the speed of the array processor.

4.5 Summary

The software package now operating on the Durham Seismic Processing System is faster and easier to use than that written by Poulter (1982). To achieve this has meant the individual programs are now far more complex and make better use of the hardware facilities, i.e. wherever possible all data manipulation is done by the array processor, leaving the PDP-11/34 as a host responsible for control and data transfer only. The penalty for the level of efficiency obtained is that the programs and computer operating system have become entwined, and it will be impossible to make major changes to one without modifying or rewriting the other.

CHAPTER 5

VELOCITY ANALYSIS

This chapter deals with the improvements made to the velocity analysis program on the Durham Seismic Processing System, and the work carried out while visiting the Lamont-Doherty Geological Observatory, New York, to obtain more accurate velocity determination using statistical techniques.

The basic principles for velocity analysis were first investigated by Dix (1955), who found that stacking velocities are approximately the r.m.s. values of the interval velocities (Fig. 5.1a). The coherence methods of Taner and Koehler (1969) and Neidell and Taner (1971) give an indication of how good a particular r.m.s. velocity is at giving a constructive stack for a given two-way travel time (Fig. 5.1b).

The single most important part of the processing of multichannel seismic reflection data is the estimation of stacking velocities. These are used for the normal move-out correction when collapsing the common mid-point, CMP, gather to a single zero offset trace. If the velocity structure is wrong then the primary reflection information will be suppressed and can not be recovered by subsequent processing.

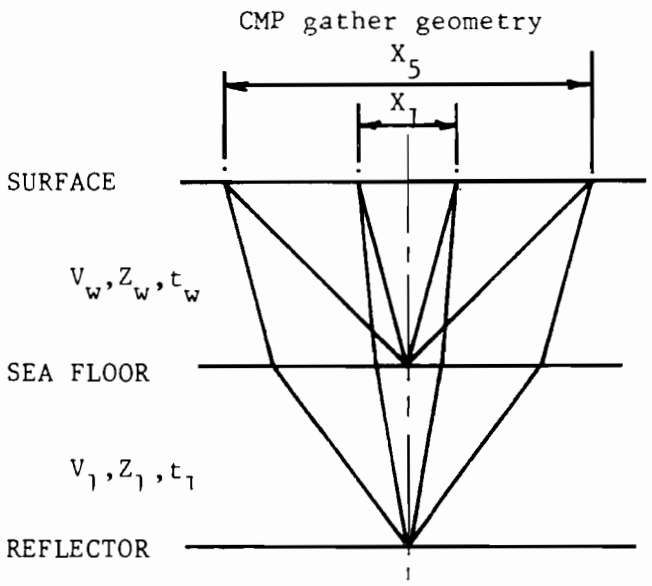

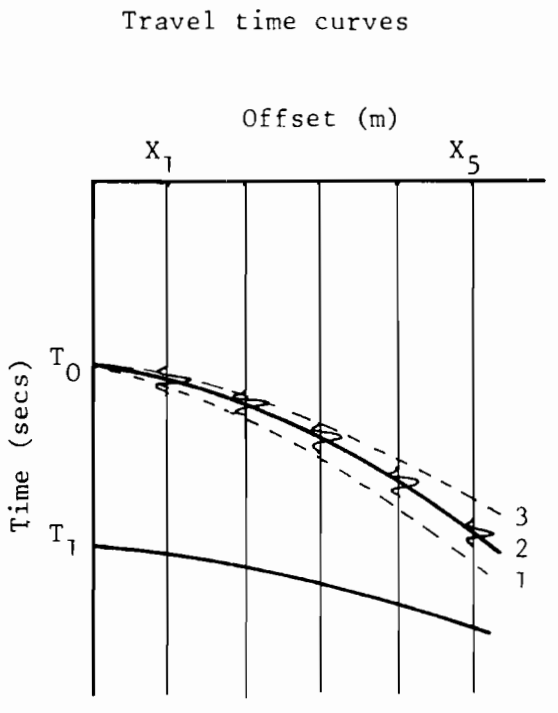

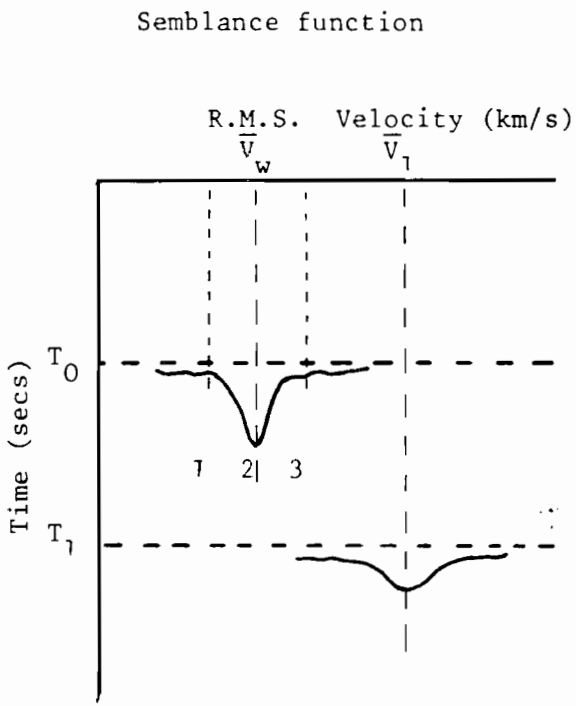

Travel time equation for the sea floor reflector $T^2 = T_0^2 + \frac{X^2}{\overline{V}_w^2}$

Travel time equation for the target reflector $T^2 = C_1 + C_2X^2 + C_2X^4 + \ldots$

$= T_1^2 + \frac{X^2}{\overline{V}_1^2}$

(Dix formula) ... where $\overline{V}_1^2 = \frac{V_w^2 t_w + V_1^2 t_1}{t_w + t_1}$

(a)

Semblance = $\frac{\text{Output energy}}{\text{Input energy}}$

Velocity "2" correct r.m.s. velocity
- - "1" too low
- - "3" too high

(b)

Fig.5.1 Principles involved in velocity analysis.

5.1 The Velocity Analysis Program

Poulter (1982) installed on the Durham Seismic Processing System a program developed by Nunns (1978) which provided a stacking velocity versus two-way travel time contoured semblance map. To obtain the analysis of any given CMP gather, four programs had to be run: one to copy the gather file from tape to disc, one to perform the analysis, one to contour the semblance output and add the annotation, and finally RASM, a Versatec (1976) routine, to convert the vector file to a raster image with output to the plotter. These routines have been combined into a single program suite, VELAN, which includes three other routines. These enable velocity filtering of the gather prior to analysis, a statistics package and a fast plot routine to output the CMP gather on the final plot. The manual for the suite is included in appendix 2. After defining the parameters, interactively or in a parameter file, the whole sequence runs from tape to final plot without any further user intervention. The suite incorporates several of the faster and more accurate array processor, APAL, routines written for the Time Sequence Analysis package.

The input routine to the velocity analysis package takes the data from tape and stores it on disc. As each trace has to be read many times the gather must be stored on a random access device. This routine allows the summing of several adjacent CMP gathers to improve the signal to noise ratio. This assumes that the primary reflecting horizons are relatively flat and exhibit the same reflected waveform over the summed gather window. Also up to 20 summed CMP gathers may be output into a single disc file

for the statistical analysis package desribed in section 5.2.1.

The velocity filtering routine, the principles of which were explained in the previous chapter (section 4.3.7), is optional and may be included to suppress unwanted multiple arrivals.

The velocity analysis scans all the input gathers at each velocity step requested, calculating the stacked trace energy and the total input trace energy for every sample. The semblance function is then calculated (Fig. 5.1b). It is standard practice to smooth the semblance plot along each trace to show the envelope function, rather than individual peaks which may arise from seperate cycles of a reflected wavetrain. The smoothing operator originally used by Nunns was a simple box-car function which produced a linear sum over a window of input values. This has been replaced by a Hanning window function as this was found to produce an equally smooth response, and for a given window length reacted earlier to rapid amplitude changes because the output value is weighted to the centre of the window.

At the end of the analysis the output data file contains smoothed semblance values for each CMP gather as a function of two-way travel time and velocity. There are several methods to display the data: using a wiggly line where semblance amplitude is proportional to the deflection of a line, as a contoured map with either lines or colours representing different semblance intervals, or where there are several analyses close together then some form of statistical distribution map may be produced.

At Durham, for a single anaysis the final result is presented as a contoured plot. This gives a clear display

allowing accurate determination of the velocity time function. Unfortunately, the contouring routine is very time consuming, but at present there is no facility to obtain colour plots which would give equal resolution far quicker. A typical final velocity analysis plot is shown in Fig. 5.2. The plot contains the input CMP gather used, with an automatic gain control applied so the whole trace may be seen, and the contoured semblance map of stacking velocity against two-way travel time. To the right of the map the maximum semblance values for each time step are plotted, their positions being indicated on the map by dots, and the annotation gives the analysis parameters used.

Figure 5.3 shows a similar analysis calculated at Lamont-Doherty Geological Observatory, which uses the wiggly line display for semblance values. Again the input CMP gather and the maximum semblance values are plotted.

5.2 Presentation of Multiple Velocity Analyses

When there is more than one analysis then the result may still be output as contoured plots, but an alternative is to compute the statistical distribution which presents all the information from all the input analyses on a single plot. Instead of summing the ajdacent CMP gathers prior to the velocity analysis, analyses are performed on each gather and the results are then combined at the interpretation stage. The assumption that the target horizons need to be flat made when summing the gathers is no longer necessary, provided the overall velocity structure remains constant, i.e. there are no gross structural

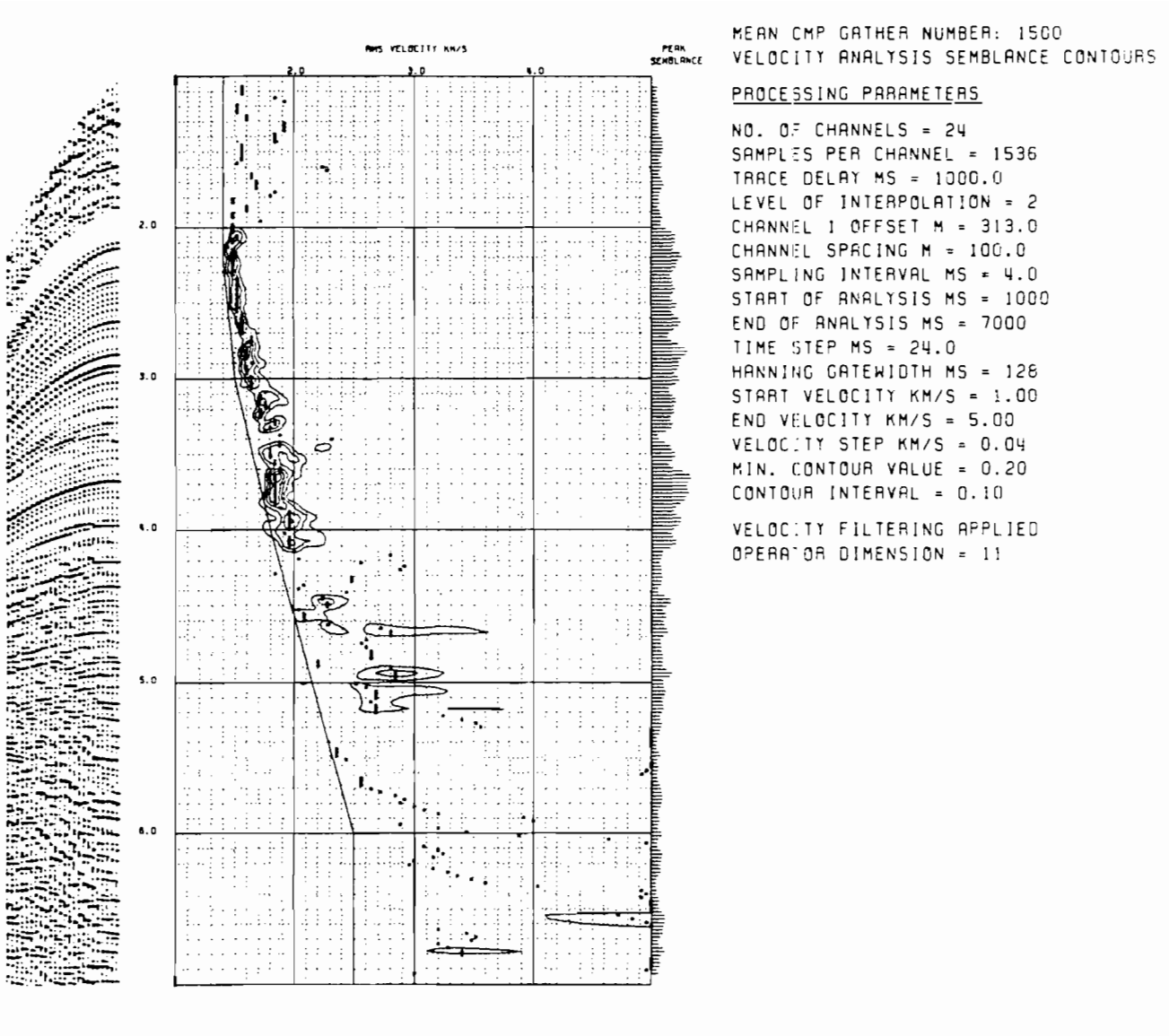

Fig.5.2 Output plot from the Durham velocity analysis program.

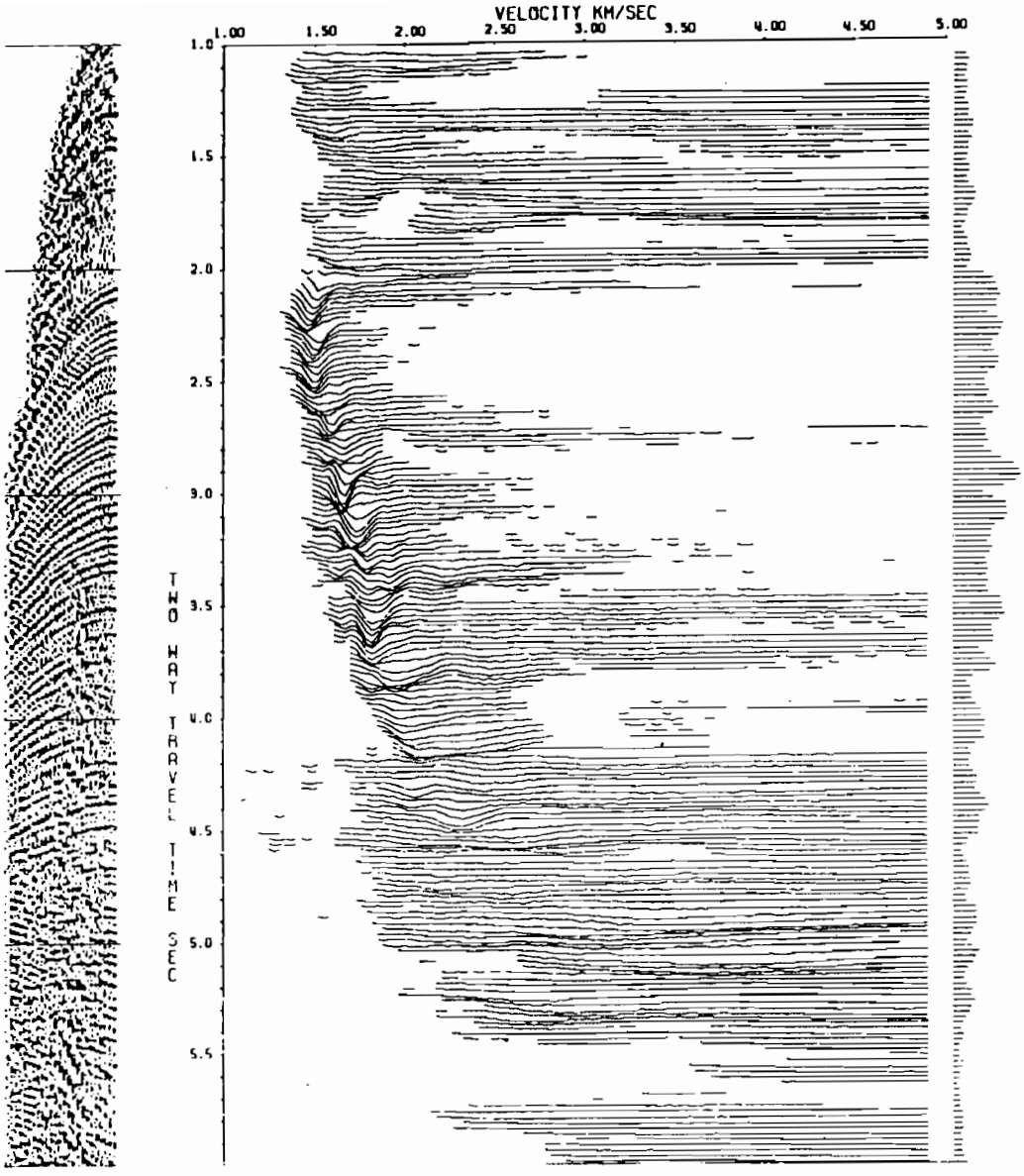

Fig.5.3 Output plot from the Lamont-Doherty velocity analysis program.

discontinuities such as faults within the set of CMP gathers. Two modes of presentation have been tried: one treats each velocity analysis as an independent sample of a process and uses the normal Gaussian distribution statistics to combine the results, whereas the other sums the output semblance values to form an average semblance function.

5.2.1 Gaussian Statistics

The routine for this type of analysis was developed at Lamont and has since been implemented at Durham. The program combines the results from several input analyses using a Gaussian distribution weighted by the individual values of semblance to give a mean semblance function. For any given time slice the optimum stacking velocity may be taken as the position of the mean of the distribution, with the standard error as a measure of the accuracy of its determination (Barford 1967, Topping 1972).

The mean value of velocity, $\bar{V}$, for a particular time slice is given by

$$\bar{V} = \frac{\sum_{i=1}^{N} S_i \; V_{i\ rms}}{\sum_{i=1}^{N} S_i} \qquad \ldots 5.3$$

where: S_i is the semblance value from the ith analysis

$V_{i\ rms}$ is the stacking velocity giving S_i

N is the total number of analyses included.

The value of the mean semblance is given by

$$\bar{S} = \sum_{i=1}^{N} S_i \; / \; N \qquad \ldots 5.4$$

The variance of the distribution is

$$\sigma^2 = (\sum_{i=1}^{N} S_i \; (\; V_{i\ rms} - \bar{V} \;)^2 \qquad \ldots 5.5$$

The standard error s.e. of the mean velocity

$$s.e. = (\frac{\sigma^2}{\bar{S} \; (\; N - 1 \;)})^{1/2} \qquad \ldots 5.6$$

A measure of the stacking velocity resolution at particular time slice may be obtained by calculating the aspect ratio of the semblance peak,

$$\text{Aspect ratio} = \frac{\text{maximum value}}{\text{width of peak at half maximum value.}} \qquad \ldots 5.7$$

A sharp narrow peak indicating a well defined stacking velocity has a high aspect ratio, whereas, a broad peak of equal amplitude has a low aspect ratio and shows that the stacking velocity is not well constrained.

Figure 5.4 shows the final display produced by this program from the analysis of twenty velocity filtered common mid-point gathers including the gather used in the previous examples. The gathers used are displayed on the left hand side of the plot. The program reads the output of each individual velocity analysis,

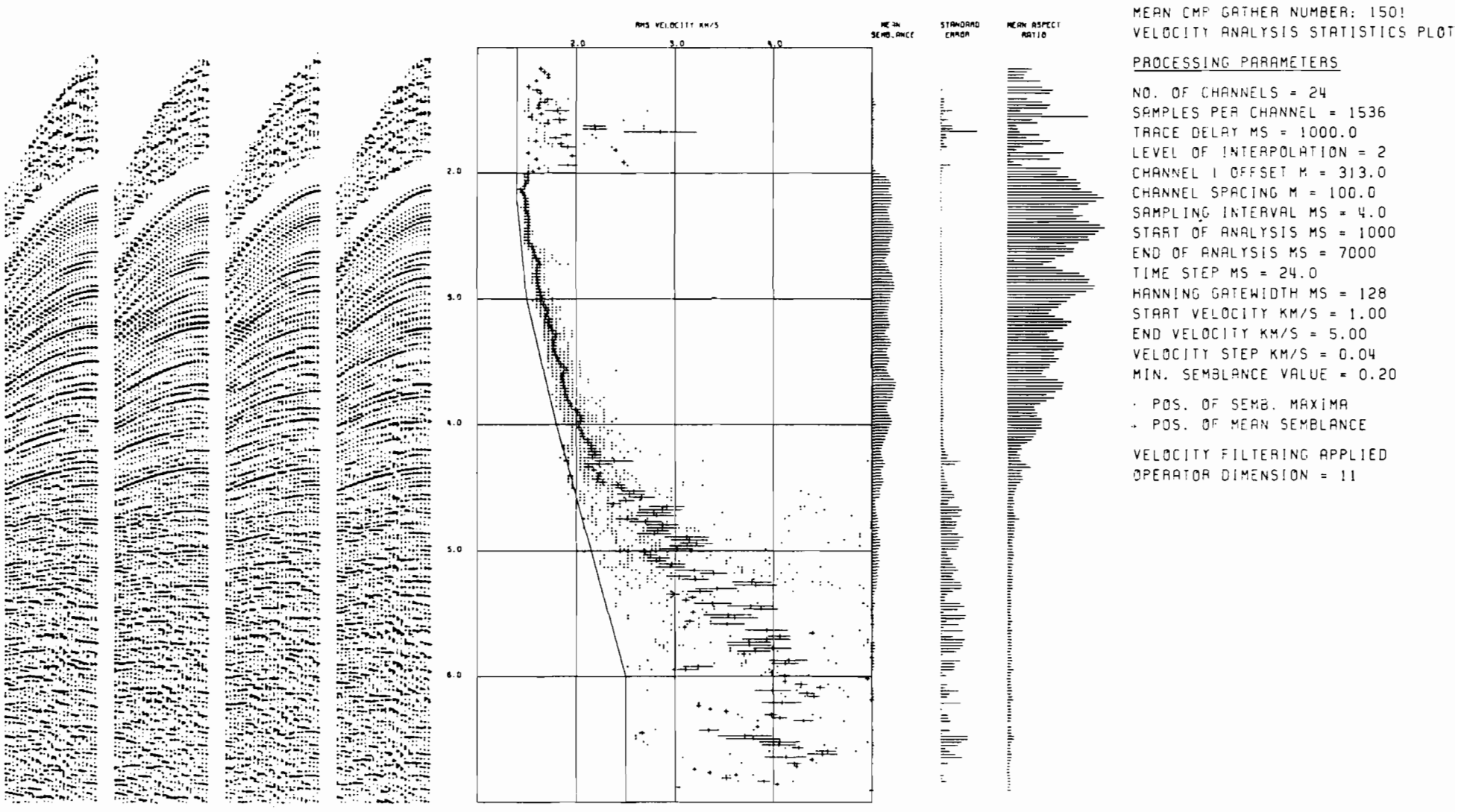

Fig.5.4 Gaussian Distribution of the velocity function determined from 20 velocity analyses. (Only four of the 20 input CMP gathers are shown on this diagram).

then scans each two-way travel time slice at which semblance has been calculated and picks off the stacking velocity at the maximum value of semblance while noting the amplitude of the semblance peak. The individual maxima are marked by a dot. This is repeated for every gather to be included in the statistical analysis and the results for each time slice are combined. To avoid small semblance peaks due to noise a minimum threshold has been imposed. The position of the mean is represented by a small cross on the horizontal line whose length represents one standard error either side of the mean. To the right of the display are plots of the of the mean semblance value and standard error and the mean aspect ratio.

The interpretation of this plot not only gives a stacking velocity function but also give some quantitative indication of its accuracy. Where the mean semblance is high with low standard error and large aspect ratio, the velocity function is well defined and constant over the analysis window. Where the opposite is found, with large standard error and low values of aspect ratio and mean semblance, the velocity function is poorly defined. This will usually be associated with broad semblance peaks in the input analyses, e.g. for events at a large two-way travel time, where there is little move-out for accurate velocity determination. Other special cases may also be identified. The situation where the mean semblance and aspect ratio are high with a large standard error, shows the presence of isolated random semblance peaks on the input analyses and should be ignored. The case where the standard error is zero indicates that only one

input semblance value exceeded the minimum threshold for that time slice, and the results for this time slice should also be ignored.

The combination of velocity filtering and statistics also works in the situation where the water multiple completely overwhelms the velocity analysis (Fig. 5.5a). Multiples from a strong reflector at 900 msec obscure all the deeper events and hence the velocity information. The record is further complicated by interference from refractions and low frequency noise from the direct arrival on the larger offset traces. The record can be improved by velocity filtering the CMP gather prior to analysis (Fig. 5.5b). Extra muting of the larger offset traces is also used to avoid problems of spatial aliasing. Applying the statistical package to twenty adjacent CMP gathers results in stacking velocity function shown in Fig. 5.6. Again this shows more clearly the overall function than that possible with a single gather (Fig. 5.5), and enables a better picking of stacking velocities than was possible from the original record.

5.2.2 Summing the Semblance Values

An alternative to the statistical approach is to average the semblance functions from each input analysis. The maximum semblance for each time slice can be found along with the aspect ratio for the peak (Fig. 5.7). As only a single peak is found the standard error is set to zero. The main advantage of this type of averaging is that isolated random peaks in the input semblance functions are suppressed. The semblance noise level is also

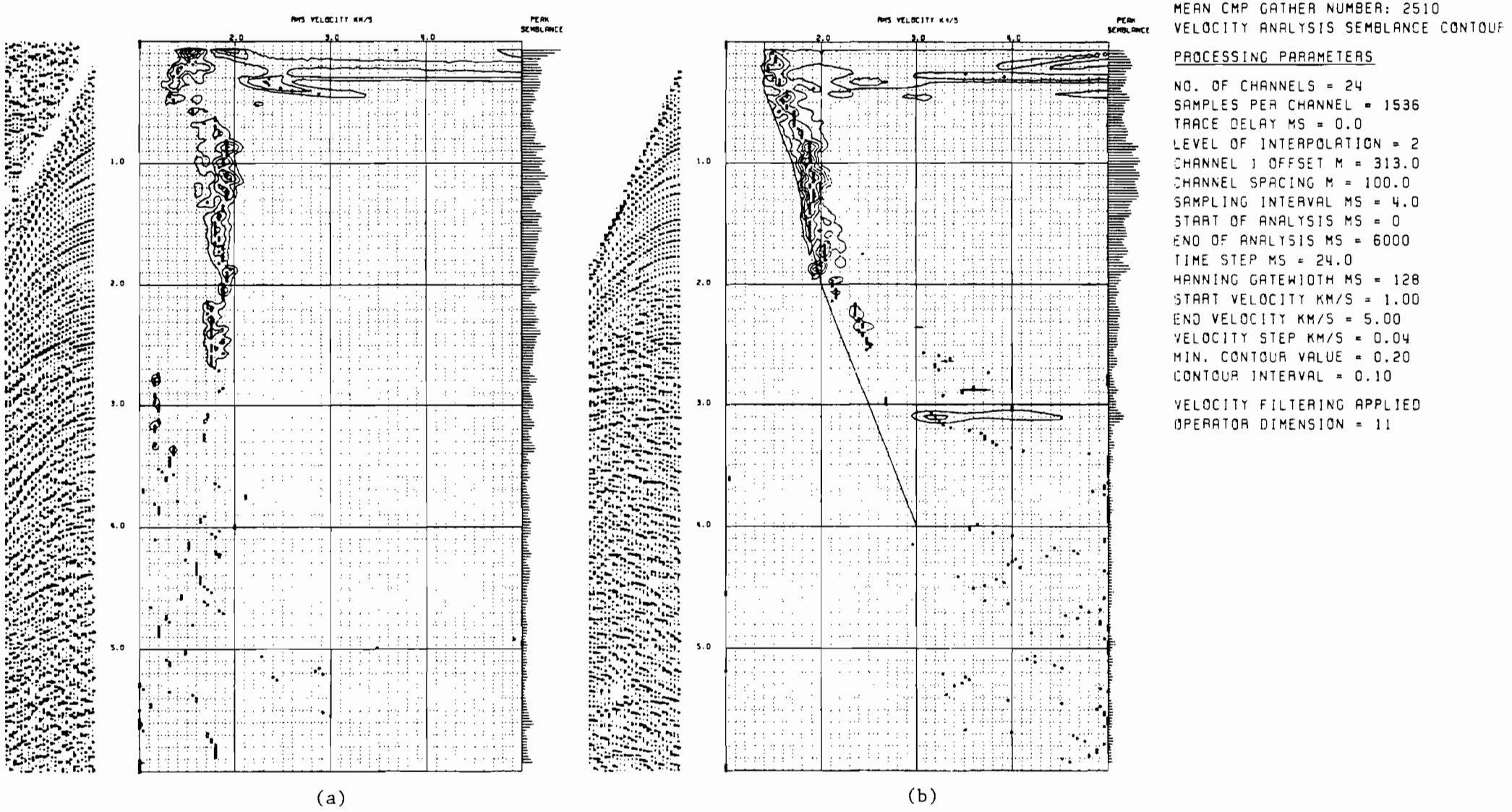

MEAN CMP GATHER NUMBER: 2510
VELOCITY ANALYSIS SEMBLANCE CONTOUR

PROCESSING PARAMETERS

NO. OF CHANNELS = 24
SAMPLES PER CHANNEL = 1536
TRACE DELAY MS = 0.0
LEVEL OF INTERPOLATION = 2
CHANNEL 1 OFFSET M = 313.0
CHANNEL SPACING M = 100.0
SAMPLING INTERVAL MS = 4.0
START OF ANALYSIS MS = 0
END OF ANALYSIS MS = 6000
TIME STEP MS = 24.0
HANNING GATEWIDTH MS = 128
START VELOCITY KM/S = 1.00
END VELOCITY KM/S = 5.00
VELOCITY STEP KM/S = 0.04
MIN. CONTOUR VALUE = 0.20
CONTOUR INTERVAL = 0.10

VELOCITY FILTERING APPLIED
OPERATOR DIMENSION = 11

Fig.5.5 Velocity analysis of a CMP gather from a shallow marine enviroment before and after the application of velocity filtering.

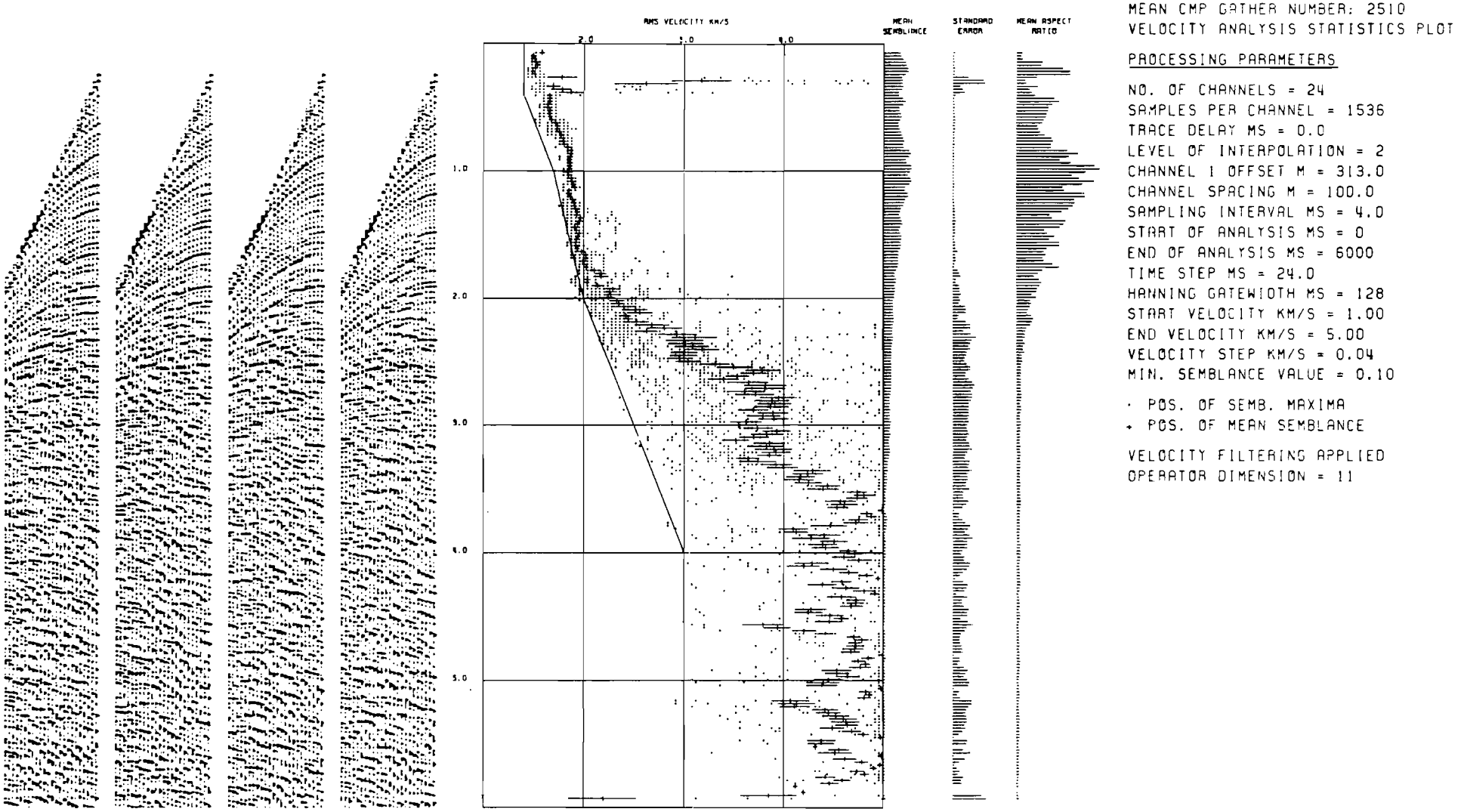

Fig.5.6 Gaussian Distribution of the velocity function determined from 20 velocity analyses from a shallow marine enviroment. (Only four of the 20 input CMP gathers are shown on this diagram).

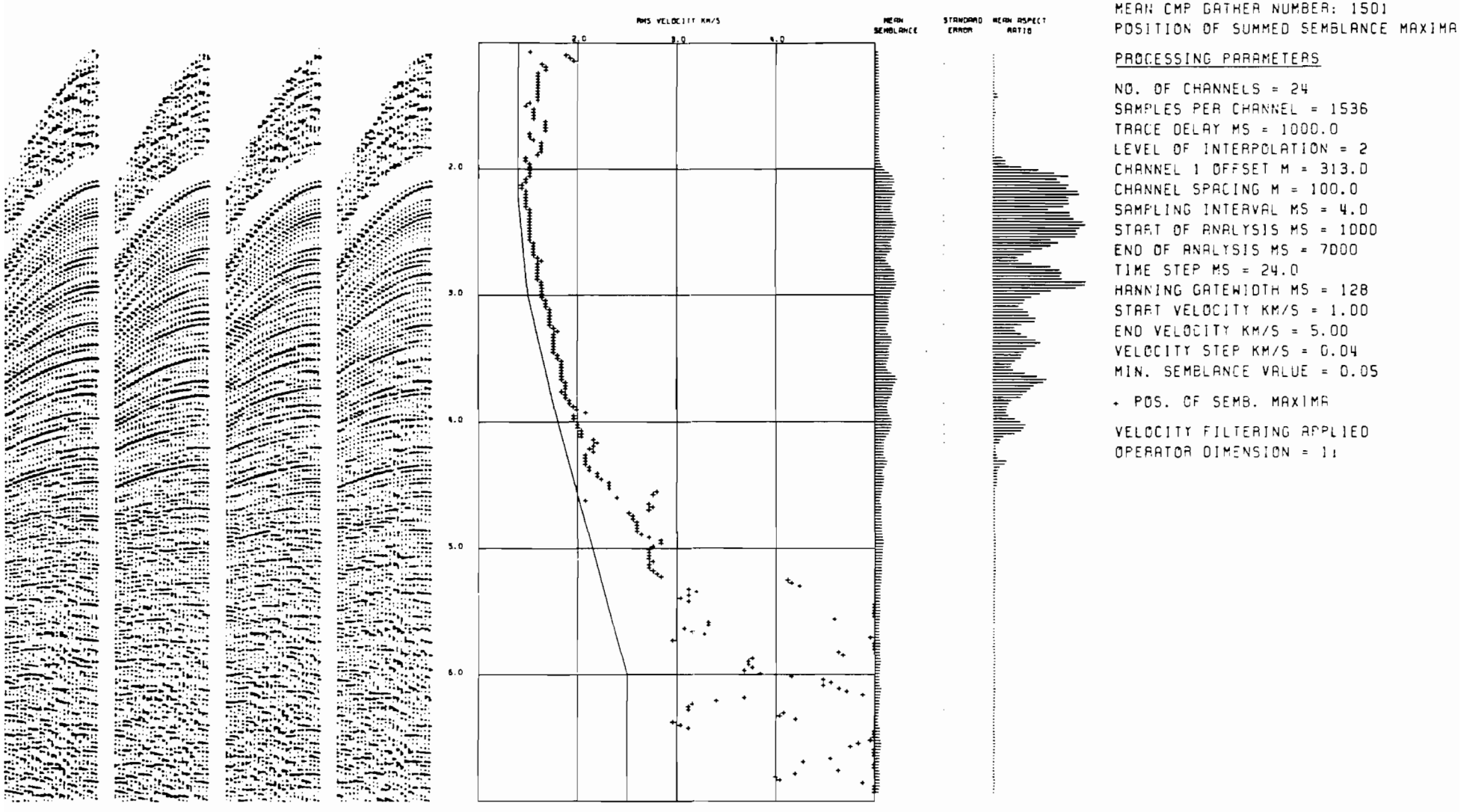

Fig.5.7 The velocity function as the result of picking the maxima from the summation of 20 velocity analysis semblance functions. (Only four of the 20 input CMP gathers are shown on this diagram).

reduced enabling a lower threshold to be used when picking the maxima.

5.2.3 Summary

The results from the two techniques can be seen to be similar, the same set of gathers having been used as input for both Fig. 5.4 and Fig. 5.7. The Gaussian distribution routine shows how well constrained the velocity function is where there is a high signal to noise ratio, i.e. in the upper part of the analysis. The summed plot gives the same result but does not show how the individual input semblance peaks have contributed. Lower on the plot the summed semblance output gives a clearer indication of the velocity function, as it is more immune to the effects of random semblance peaks in the input analyses. One of the uses of the statistics plot is that two analyses from different parts of a profile may be compared to see if there is any significant difference in velocity structure. A difference in velocity functions would be considered significant at two-way times for which the standard error window on each of the velocity functions do not overlap.

5.3 Determination of Receiver Aperture

The aspect ratio measurement may be used to determine the optimum length of the array of receivers, the receiver aperture, for a given target reflector. If the aperture is too narrow then the move-out correction is too small to give an accurate velocity function. If the aperture is too wide then the hyperbolic

approximation made when calculating the normal move-out correction is inadequate. To obtain the maximum ammount of information from a given survey it is necessary to design the acquisition parameters to suit the conditions expected. Using some synthetic aperture profile data acquired by Lamont-Doherty Geological Observatory (Buhl et al. 1982) it was possible to simulate three different array lengths for a particular common mid-point yet keeping the fold of cover the same at 48 traces per gather. The use of real data as opposed to synthetic data was preferred as this produced a seismic gather with all the possible sources of noise included.

Figure 5.8 shows the results for three different apertures. The input gather with the value of peak semblance and its aspect ratio are plotted for each time slice. Figure 5.8a shows the result for a 2.4 km array. In particular note the value for the reflector at 7.9 seconds two-way travel time of about 3.9 sec/km. Figure 5.8b shows the analysis for a 5.4 km array, for the chosen reflector the semblance value has fallen from 0.88 in the previous figure to 0.71, but the aspect ratio has doubled to 8.9 sec/km. Finally Fig. 5.8c shows the effect of increasing the array length to 7.2 km. The aspect ratio has now fallen to 5.2 sec/km indicating that the hyperbolic move-out approximation is now failing. From the three arrays tested the 5.4 km array gives the best velocity definition for this particular target in a region of 2 km water depth.

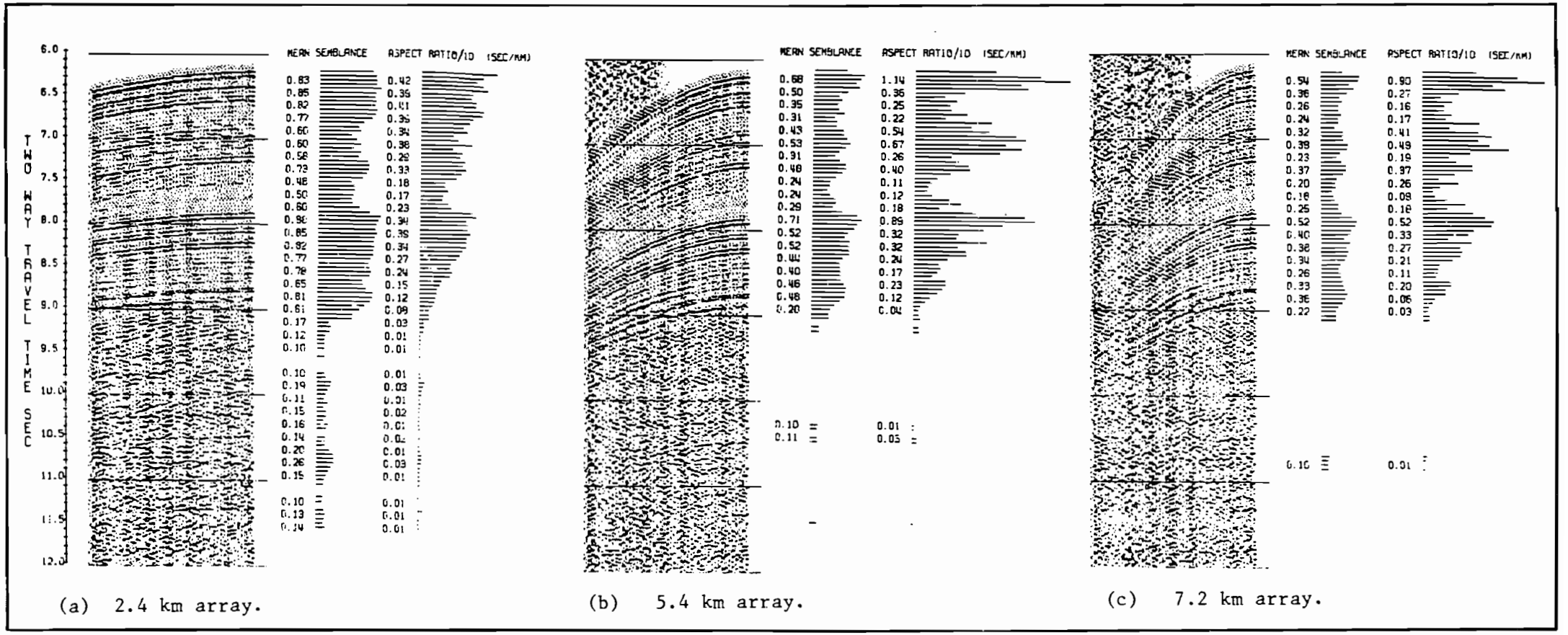

Fig.5.9 Effect of receiver aperture on the accuracy of velocity determination.

5.4 Semi-Automated Velocity Picking

The statistical analysis program was taken a stage further at Lamont to provide a semi-automated stacking velocity determination. The routine takes in an approximate model of the interval velocity distribution, estimated from what is known about the geology. The Dix formula (Fig. 5.1a) is then used to find the stacking velocity function for the model. This function is then corrected to be consistant with the velocity function calculated from the analysis of the real data. This routine is then repeated at every velocity analysis point along the profile. The input model may be either the result from the previous analysis or may be a new model input by the user. The amended models are then used to find average interval velocities between reflectors along the whole profile. The resultant interval velocity map can then be used as input to the CMP stacking routine or can be used to detect any changes in facies between prominent reflecting horizons which cause significant changes in the interval velocity structure.

CHAPTER 6

PROCESSING OF THE REFLECTION SEISMIC DATA

This chapter covers the processing parameters used in obtaining the section plots included in this thesis. Section 6.1 explains the processing of the Farnella 1/81 data, and section 6.2 the processing of the commercial profile.

6.1 Processing of Farnella 1/81 data

6.1.1 Demultiplex

Of the ten profiles collected only seven were demultiplexed, the first three having large data gaps caused by air-gun problems, SDS 1010 failures or lack of operator experience in tape changes. The demultiplex program added dummy shot gathers with traces in which all the samples had been set to zero to replace the gathers lost. Gathers with zero traces were also substituted for field records which were un-readable due to tape errors. Data errors due to the SDS 1010 gain range unit were not corrected at this stage.

6.1.2 Common Mid-Point Sort

As the common mid-point, CMP, sort program could not handle true navigation, the Poulter (1982) algorithm would only correct for the situation where the ship was consistently fast or slow,

it was assumed that the ship maintained an ideal course and speed of 9 km/hr, about 4.8 knots. From the track charts it could be seen that this was not true, but when averaged over a whole profile the errors were found to be small. Of the seven demultiplexed profiles, six were sorted into CMP gathers. Line 5 was not included as it was only a short connecting profile and started with two sharp turns which meant the bearing of the tail buoy was at 41^{o} to port at the start of the line. Half an hour later this had swung to 2^{o} to starboard, but shortly after this time the turn was started to the course for the next profile.

The sort program presented in chapter 4 was modified to identify and remove digitization errors by the addition of a special routine, GLITCH. The erroneous samples always had the the higher bits in the mantissa set, the GLITCH routine searched the whole trace for any value within narrow windows centred on the binary fraction series: half, quarter, eighth, etc.. On finding such a value the sample was set to zero and a record of the total number of samples lost was incremented by one. At the end of the search a check was made to ensure no more than a quarter of the data has been lost, if this was exceeded then the whole trace is zeroed as much of the useful information in that trace had been lost. After the errors had been removed the trace was band-pass to smooth any edges where samples had been lost. The main routine was written in the array processor language (APAL) to run in the processor, see GLITCH appendix 2. This dramatically improved the data as can be seen in Fig. 6.1 but could not replace the lost information. At this stage between 15 and 20 per cent of the data

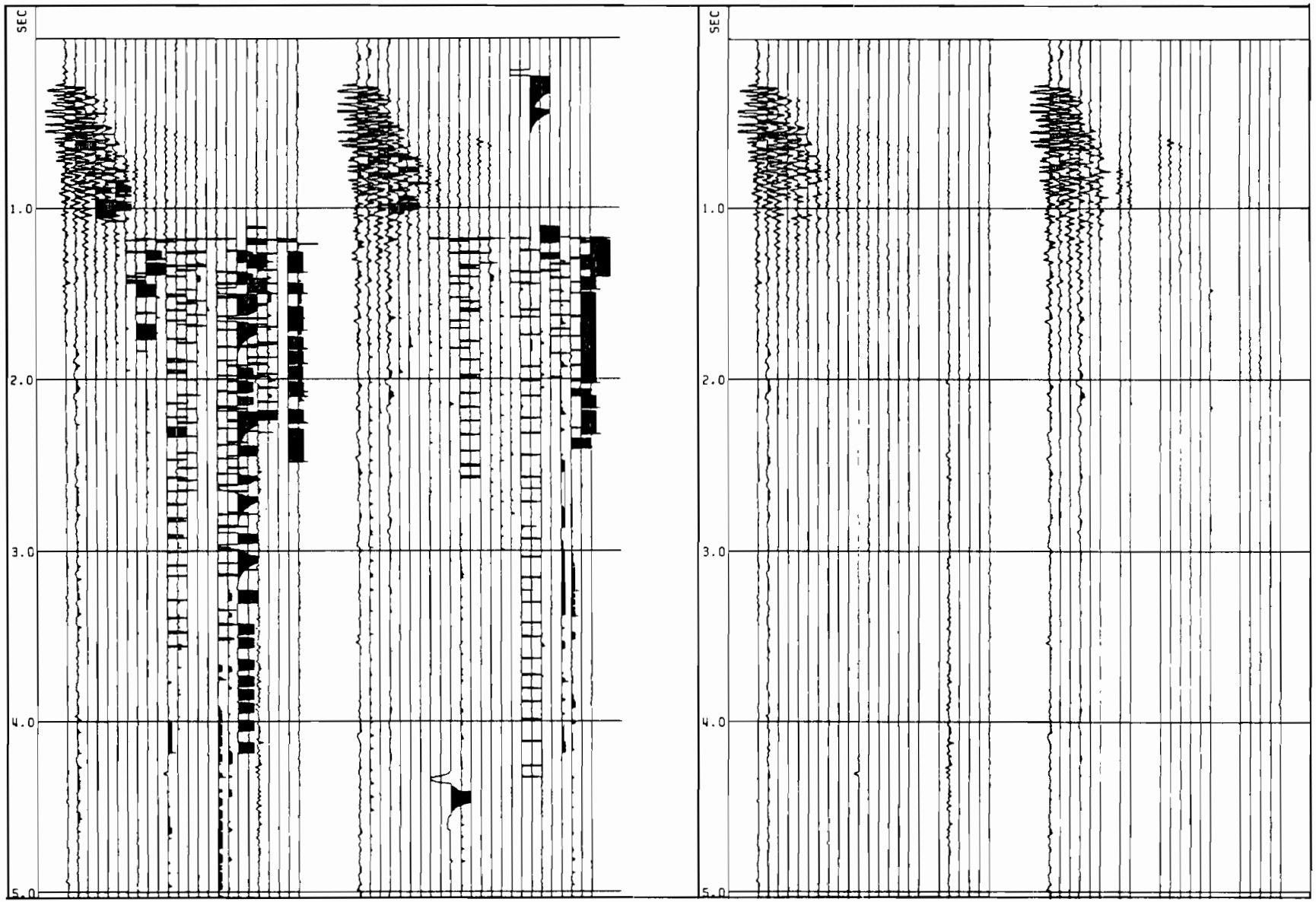

Fig.6.I Two CMP gathers from the Farnella I/8I cruise before and after the removal of recording errors.

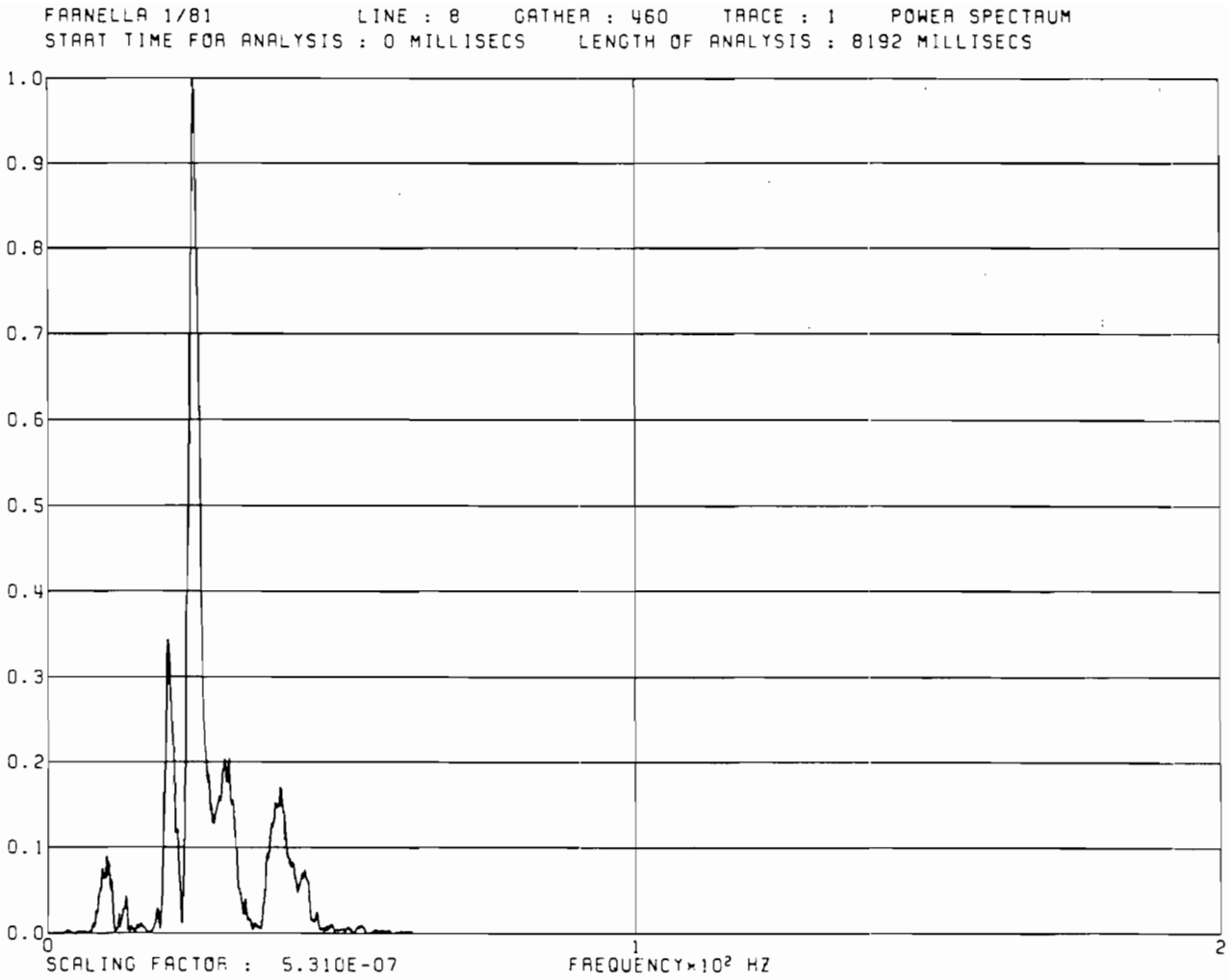

Fig.6.2 Typical power spectrum of the air-gun array used for the Farnella I/8I survey.

samples had been lost from each profile acquired.

6.1.3 Pre-Stack Processing and Stack

Data lost during acquisition cannot be compensated for during processing, but by careful choice of the parameters the effects of the errors may be minimized. All of the data was passed through the steps outlined in table 6.1. The size of the array processor limited the trace length to 4 seconds when using the velocity filter option, step 4, so this was replaced by a deconvolution to obtain 8 second records.

	1.	Time break, source and receiver depth corrections
	2.	Polarity reversal
	3.	Band-pass filter
Either	4.	Velocity Filter
Or	4.	Time ramp Short gapped prediction error deconvolution Removal of time ramp
	5.	Mute
	6.	Velocity Analysis
	7.	Normal move-out correction and vertical stack

Table 6.1 Pre-stack processing applied to the Farnella 1/81 reflection data.

Time-break, source and receiver depth corrections

The source and receiver depth corrections were taken from the watch keepers log. For most of the cruise the two source arrays were towed at two differing depths, 7 metres and 12

metres, except for the last profile when both were towed at 10 metres (section 2.4.1). The receiver array was monitored along its length by sensors which showed that its depth varied between 10 and 14 metres, but at normal profiling speed maintained a depth of about 11 metres. Given the sampling interval of 4 msec the shift of the trace by one sample was equivalent to a depth correction of 10 metres therefore the total correction applied for both the source and reciver was taken to be 2 samples, i.e. 20 metres.

The time-break correction should have been automatically recorded on one of the auxilliary channels, but as this unit was never repaired a fixed correction had to be applied. The SDS 1010 documentation gave figures of 64 or 128 msec. By studying the direct arrival on several shot gathers and knowing the approximate source receiver offset the value of 64 msec was chosen.

The time-break and depth corrections apply in opposite directions the total effective shift on the input traces was equivalent to 14 samples removed at the start of each trace.

Polarity reversal

On connecting the receiver array to the SDS 1010 some of the channels were inadvertantly reversed, i.e. gave the wrong polarity signal to the recorder. To achieve the object of multichannel seismic data stacking it is imperative that all the channels have the same polarity.

For profiles 4, 6, 7, and 8, channels 2, 5, 10, and 12 were

corrected. For profiles 9 and 10, after servicing the SDS 1010, channels 1, 2, 5, 10, 12, and 20 were corrected.

Band-pass filtering

The source array produced frequencies from 10 Hz to 40 Hz with maximum power at 25 Hz (Fig. 6.2). To remove the effect of wave and low frequency ship noise a low-cut of 10 Hz was applied with all frequency components below 5 Hz totally removed. Also frequencies above 40 Hz were suppressed with a cosine taper to 60 Hz, with all frequency components from 60 Hz to the Nyquist frequency of 125 Hz removed. This was to filter out high frequency noise.

Figure 6.3a shows a gather taken from one of the Farnella profiles from over the Sea of the Hebrides Trough without any processing applied. Figure 6.3b shows the same gather after the application of the above processes.

Velocity Filter

It was stated in section 4.3.7 that the velocity filter was not an effi-cient method for the removal of multiple energy during pre-stack filtering. However, this technique did offer two distinct advantages for the Farnella 1/81 data set. Firstly, it did not compromise the signal to noise ratio that is inherent with Wiener filtering, and also it tended to smooth out the gaps left by the recording errors. The disadvantages of this process were that the noise was "coloured" at the cut-off velocity function and would produce coherent events on the final stacked

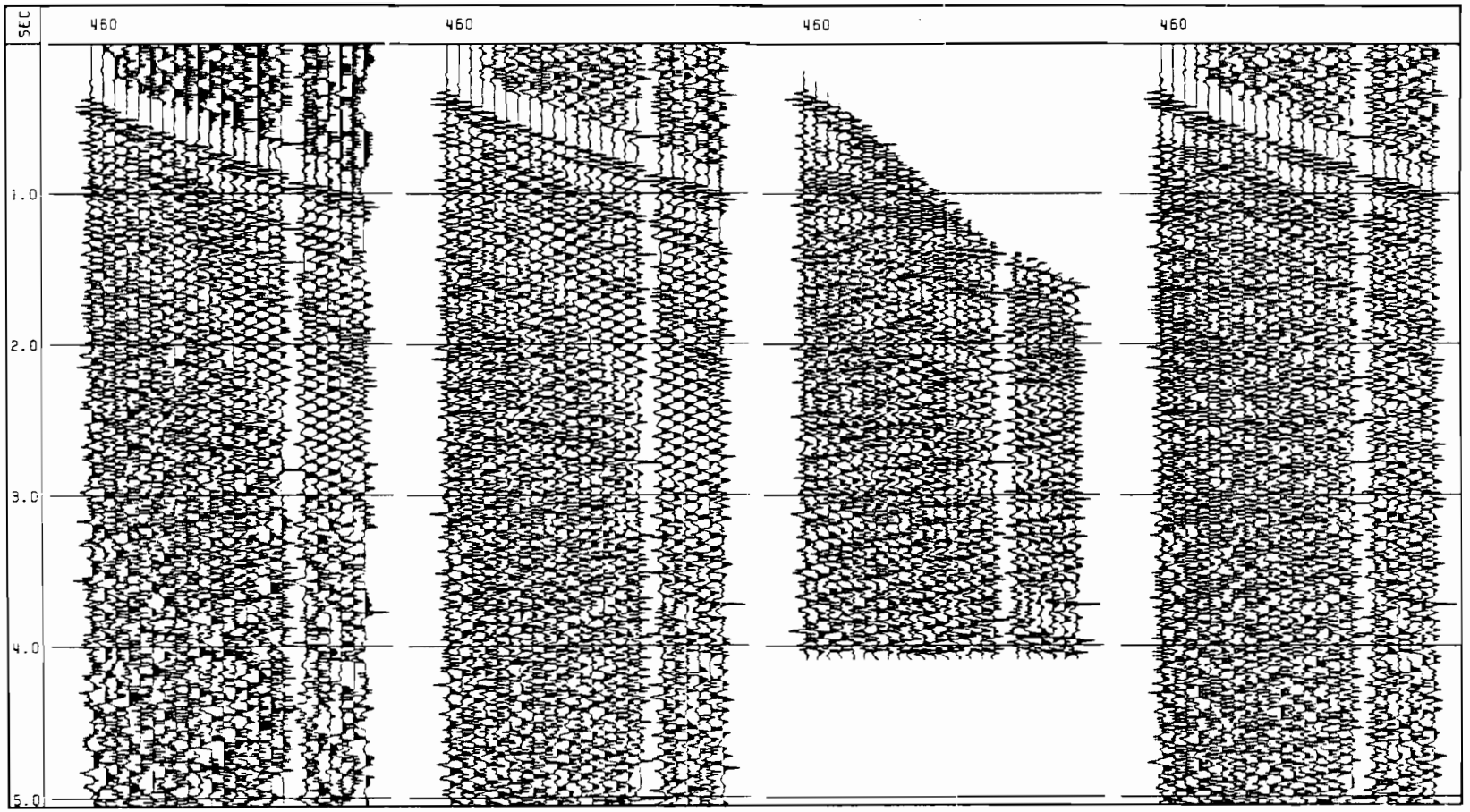

Fig.6.3 Effects of pre-stack processing on a CMP gather from the Farnella I/8I survey. (A.G.C. applied).
(a) Unprocessed gather.
(b) Result of static corrections, polarity reversal and band-pass filtering.
(c) After velocity filtering.
(d) After the application of a short gapped prediction error filter.

section, and the filter had no effect on high order multiples where there was little move-out.

The size of the array processor limited the velocity filtered trace length to only 4 seconds. A standard false velocity function was used for the whole data set (table 6.2).

Two-way time msec	R.m.s. velocity km/sec
500	1.4
1000	2.1
2000	3.0
4000	3.0

Table 6.2 False move-out velocity fuction.

This type of filtering was found to be most effective where the data had been collected over sedimentary basins (Fig. 6.3c).

Time ramp, Prediction Deconvolution and Ramp removal

The use of the velocity filter limited the record length to 4 seconds. To provide a final section with an 8 second record length, prediction error deconvolution was applied as an alternative pre-stack filter. The object of deconvolution before stack is to remove the effects of souce signature. Multiples can also be suppressed, but because of move-out effects they do not maintain a constant periodicity, and therefore cannot be properly dealt with at this stage.

To comply with the approximations imposed by Wiener filtering (Robinson 1980), it is necessary to present a stationary series as input to the process. A seismic signal can

in no sense of the word be described as stationary but the effect of loss of signal amplitude may be improved by the application of a time varying ramp. For this data a time ramp of 8.5 dB per second was chosen, i.e. exp(T) where T is the two way time.

As the source was not minimum phase, a spiking filter was felt to be undesirable, therefore a prediction error filter was chosen. The autocorrelation function was calculated from the first 4 seconds of the record, i.e. the part with the best signal no noise ratio. With a prediction gap of 40 msec and and active filter length of 400 msec, the prediction error deconvolution operator was designed to suppress periodicities in the record between 2.5 to 25 Hz. The filter characteristics were as follows:

Autocorrelation design window	4000 msec.
Autocorrelation window start time	0 msec.
Prediction distance	40 msec.
Active filter length	400 msec.
Added white noise	1 %.

Table 6.3 Pre-stack prediction error deconvolution design parameters

To obtain true amplitude traces again the applied time ramp was removed after filtering. Figure 6.3d shows the output from this process.

Mute

The major approximation of multichannnel reflection processing is that of near normal incidence. It is therefore necessary to remove all large offset data which does not conform to that limitation. Muting to zero of the larger offset traces also removes refracted energy which takes no part in this type of processing, removes arrivals which would suffer intolerable pulse stretching during move-out correction, and removes areas where, due to velocity structure, there is ambiguity over which sample contributes to the stacked trace, a form of spatial aliasing. For the Farnella 1/81 data in areas where the crystalline basement was exposed on the sea floor the first arrival on the nearest receiver was already a wide angle reflection, i.e. beyond the critical angle, and should have been muted. This would have meant the loss of all sea floor information. To avoid this, the mute function started on the fourth trace at 400 msec with an increasing severity of 200 msec per trace until trace six, then with an extra 100 msec per trace out to trace 24.

Velocity Analysis

Using both deconvolved and velocity filtered data sets the optimum stacking velocities were determined. Analyses were performed along each profile at approximately constant CMP intervals, about 2 km, the exact position being chosen so as not to coincide with a data gap caused by a tape change. To improve signal to noise ratio, prior summing of groups of three CMP gathers was carried out. Figure 6.4 shows a typical analysis

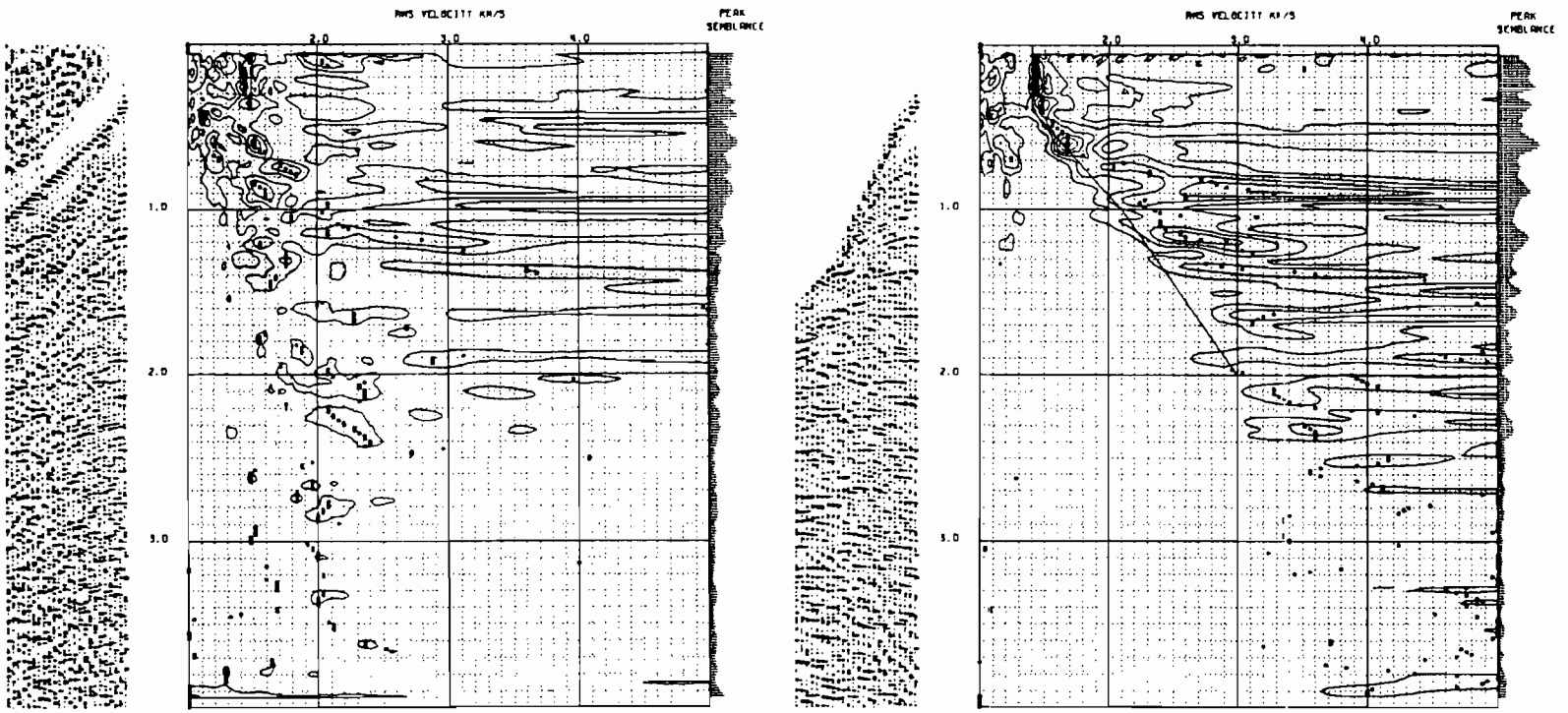

MEAN CMP GATHER NUMBER: 460
VELOCITY ANALYSIS SEMBLANCE CONTOURS

PROCESSING PARAMETERS

NO. OF CHANNELS = 24
SAMPLES PER CHANNEL = 1024
TRACE DELAY MS = 0.0
LEVEL OF INTERPOLATION = 4
CHANNEL 1 OFFSET M = 245.0
CHANNEL SPACING M = 100.0
SAMPLING INTERVAL MS = 4.0
START OF ANALYSIS MS = 0
END OF ANALYSIS MS = 4000
TIME STEP MS = 16.0
OPERATOR GATEWIDTH MS = 128
START VELOCITY KM/S = 1.00
END VELOCITY KM/S = 5.00
VELOCITY STEP KM/S = 0.04
MIN. CONTOUR VALUE = 0.10
CONTOUR INTERVAL = 0.10

VELOCITY FILTERING APPLIED
OPERATOR DIMENSION = 11

Fig.6.4 Velocity analysis from the Farnella I/8I survey before and after the application of a velocity filter.

from the Sea of the Hebrides Trough with and without velocity filtering applied. In cases were the velocity definition was poor, either the result was completely ignored, or, at points where an analysis was needed, e.g. near large offset faults, an ideal structure was imposed assuming a geological model.

Normal move-out correction and vertical stack

The velocity function determined from the velocity analysis files was laterally interpolated to determine the required function at each CMP. Using this function the normal move-out correction was made to the gather and all the non-dead traces summed together. To preserve amplitude information the stacked trace was then normalized by the number of contributing traces, taking into account the effect of the mute function applied at the start of the traces.

6.1.4 Post-Stack Processing

Table 6.4 lists the processing steps applied to the stacked sections.

1. Band-pass filter
2. Geometrical spreading correction
3. Prediction error deconvolution
4. Trace energy equalization
5. Cosmetic time ramp or automatic gain control ramp

Table 6.4 Post-stack processing applied to the Farnella 1/81 reflection data.

Band-pass filtering

To remove the effect of pulse stretching lowering the frequency of the upper part of the section, and the introduction of high frequency noise by the stacking process, a repeat of the previous band-pass fuction was applied.

Geometric spreading correction

Having determined a velocity function for each stacked gather it was now possible to apply a time varying gain function which compensated for the loss of reflected energy because of geometric considerations. For sedimentary basins this produced a reasonably stationary signal, but where the basement was exposed at the sea-floor the large acoustic impedance meant most of the input energy appeared as multiples. As little information was expected from these areas no further time ramp was added so the optimum filter could be designed for the sedimentary basin areas.

Prediction error deconvolution

During the process of stacking most of the strong sea-floor multiples should have been suppressed, but because of the severe mute function used, multiples still obscured much of the primary data. This deconvolution was designed to remove this unwanted energy. As considerable pulse stretching had taken place in the upper section, in particular the sea-floor reflection, the primary and its multiples had little in common, but the deconvolotion did help suppress the unwanted events even if it did not remove them totally. The filter parameters used are as

follows:

Autocorrelation design window	2000 msec.
Autocorrelation window start time	0 msec.
Prediction distance	100 msec.
Active filter length	400 msec.
Added white noise	1 %.

Table 6.5 Post-stack prediction error deconvolution design parameters

Trace energy equalization

To minimise the effect of changes in the trace characteristics along a profile, each trace was normalized to unit energy. These changes would have been caused by alterations in the air-guns used, air pressure variations or reflectivity of the sea bed.

Cosmetic time ramp or automatic gain control

For the profiles where velocity filtering had been applied prior to stack, the geometrical spreading correction proved to be sufficient to compensate for signal amplitude loss with increasing time. This was not found to be true when the data was deconvolved before stack. On these longer records the lack of source power meant it was necessary to apply an extra gain function prior to final display. The most convenient was that which maintains a constant energy over a given window, automatic gain control (A.G.C.). The window length was chosen to be 200

msec as this was found to give the most consistent final picture. Other longer widows were tried but these gave a poor result near the sea floor because of the large amplitude of the sea floor reflection.

6.1.5 Display

Two modes of final display were chosen: the first showing the section to 8 seconds two-way travel time with the pre-stack deconvolution applied, the second shows the first 4 seconds with velocity filtering applied in expanded detail. The time scale and trace spacing were chosen to give 1:1 scaling ratio for a seismic velocity of 6 km/sec.

Figure 6.5a shows a section of a profile as a monitor record. Figure 6.5b and 6.5c show the same section after stacking and processing for the deconvolved 8 second record and the velocity filtered 4 second record respectively.

6.1.6 Summary

Figure 6.5a is taken from the near offset receiver without any processing. The section is totally dominated by multiples and low frequency noise. The section with velocity filtering applied before stack (Fig. 6.5c) shows the structure in the upper two seconds more clearly than when deconvolution has been applied as a pre-stack filter (Fig. 6.5b). In the later case severe multiples still obscure the primary arrivals. Below two seconds primary energy from deeper reflectors can be seen in Fig. 6.5b. This energy is not so clear in the lower part of the velocity

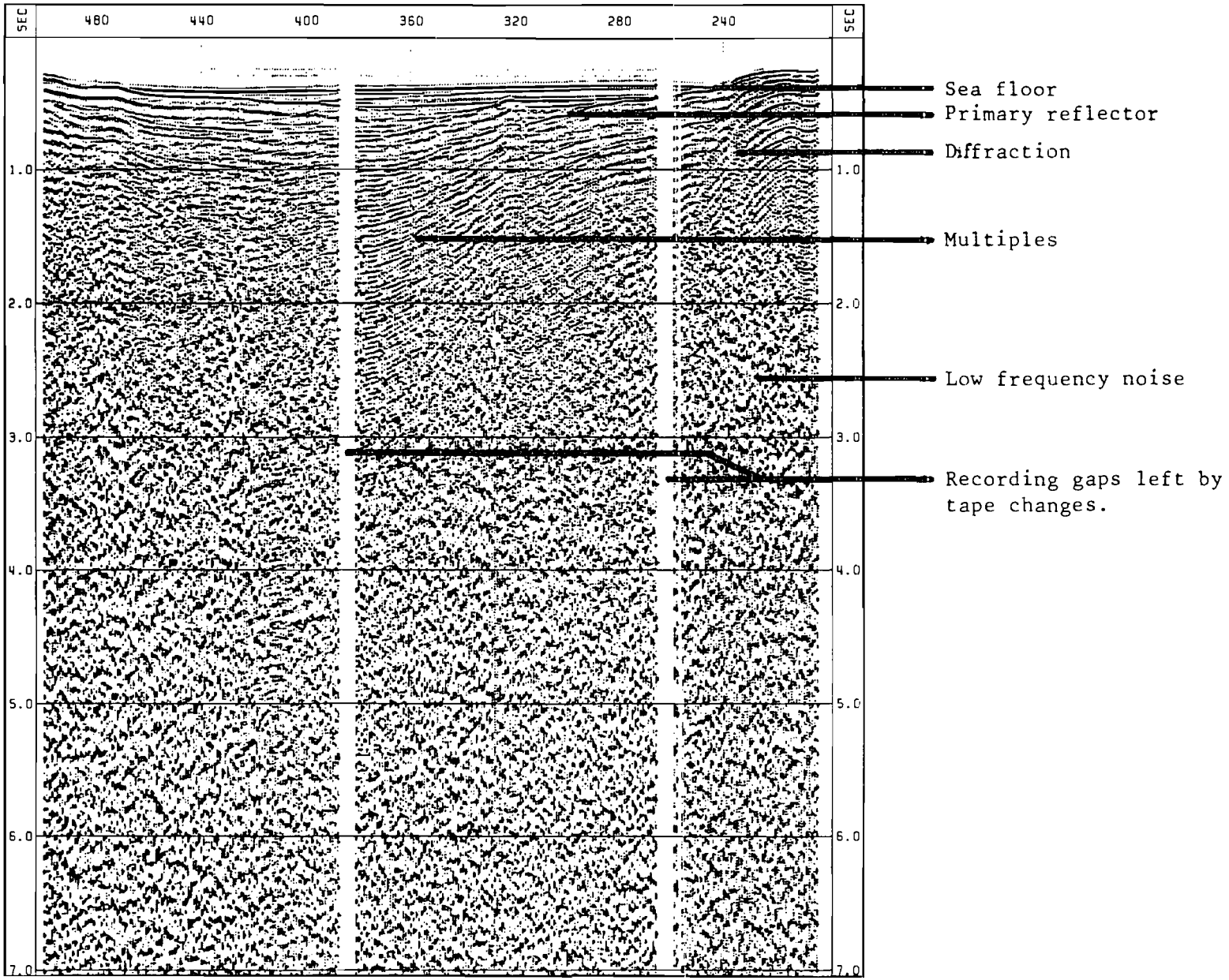

Fig.6.5a Unprocessed near trace monitor record. (A.G.C. applied).

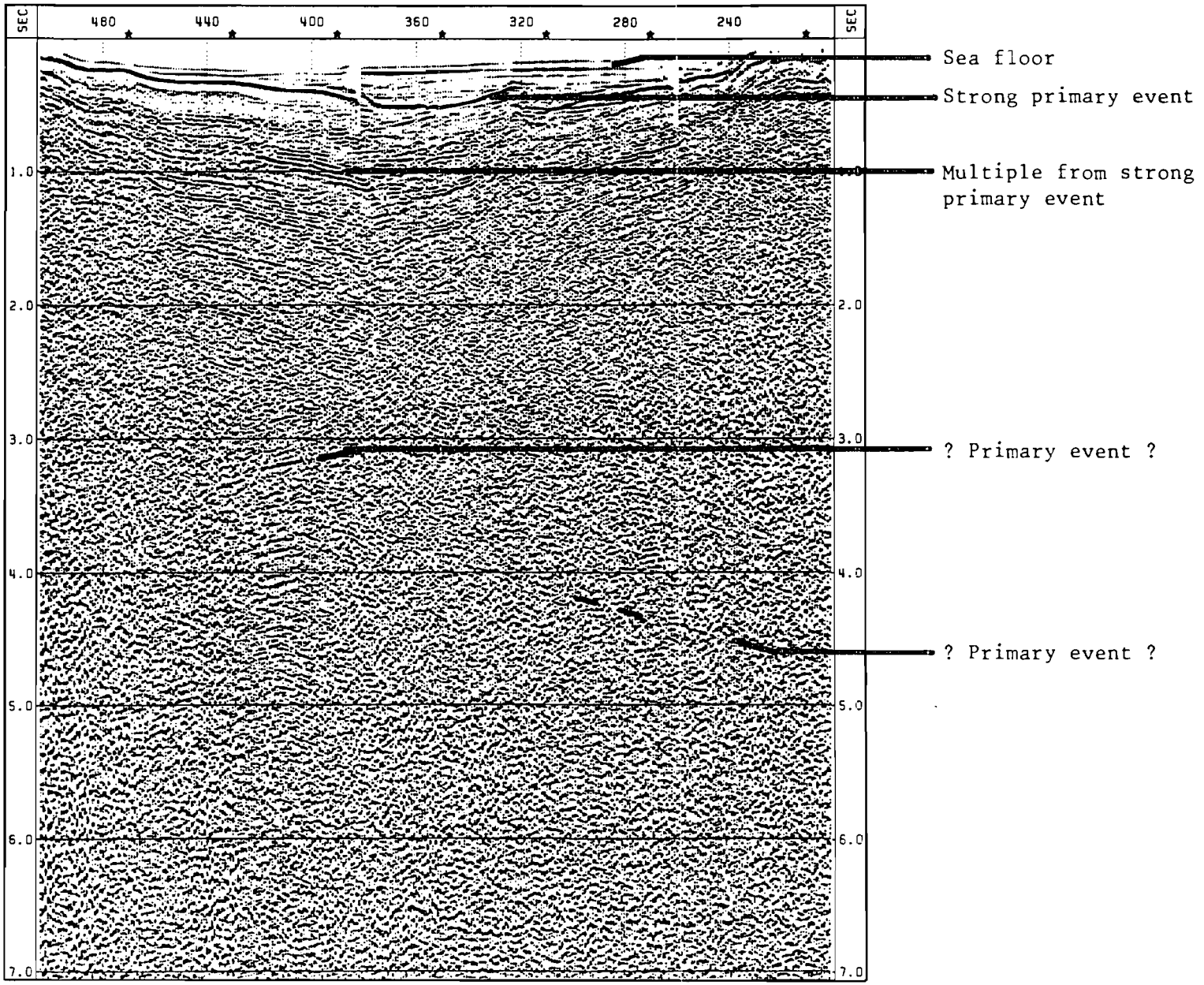

Fig.6.5b Processed section with prediction error filtering applied before stack. (A.G.C. applied).

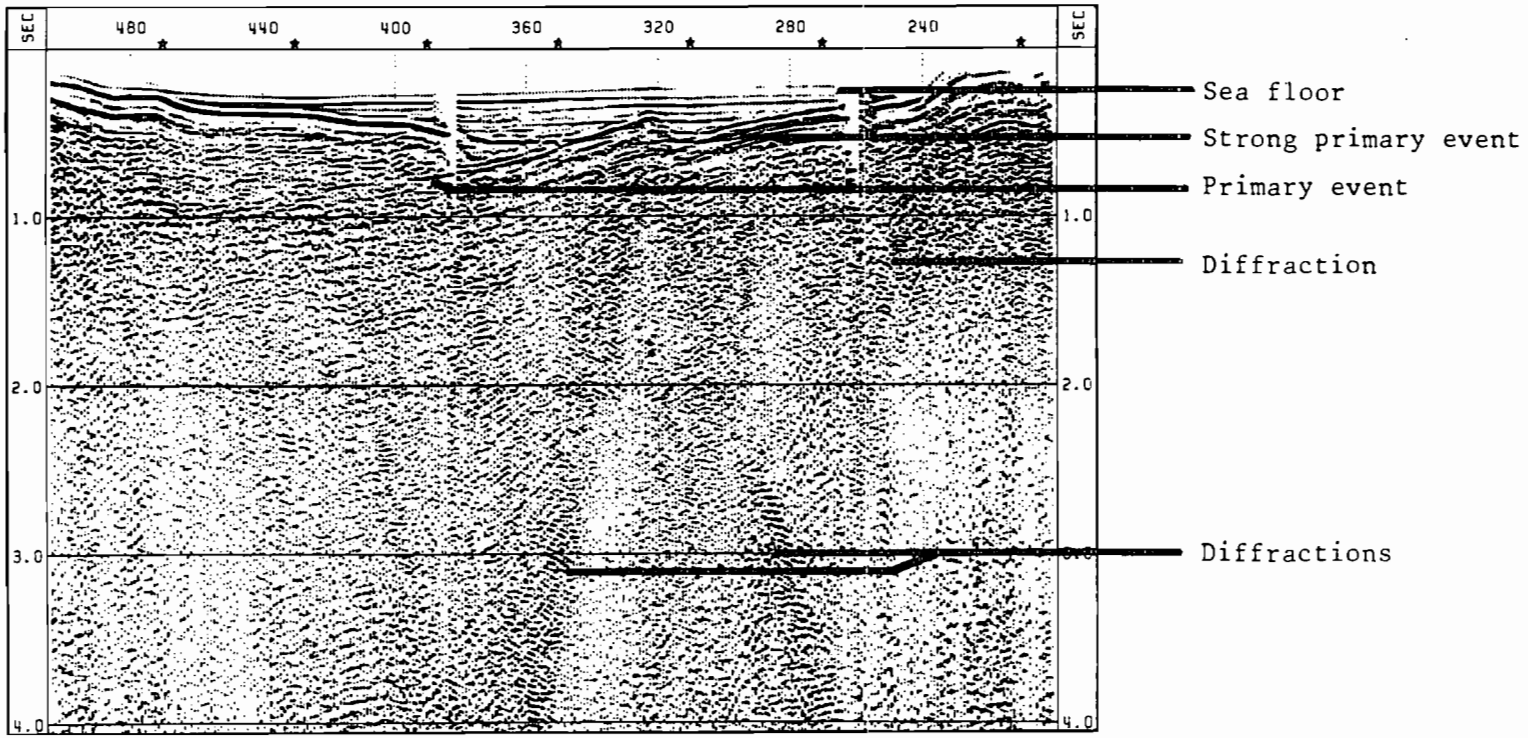

Fig.6.5c Processed section with velocity filtering applied before stack. (True amplitude plot).

filtered section (Fig. 6.5c). This is for two reasons: the first is that the velocity filtered section has not had an automatic gain control function applied, so as the signal amplitude diminishes with increasing time it falls below the minimum plot threshold; secondly interference from noise caused by shallow diffractions has not been removed by the velocity filter and appears as the darker regions along the plot.

6.2 Processing of the Commercial 1973 Data

The tapes obtained from the British Geological Survey, B.G.S., were the original field tapes recorded in 1973 by Seismic Explorations Int..

6.2.1 Demultiplex

The format was a form of SEG-C (Meiners et al. 1982) which necessitated the writing of a special demultiplex routine which produced Durham SEG-Y format which could be used by the rest of the processing software. The form of this program was considerably easier than the SEG-A demultiplex routine, as the data had been recorded in real floating point numbers so the new program only had to read the long field block and sort the numbers without complex mantissa and exponent manipulations. The forty-eight trace common shot gathers had been amplified prior to recording, so that the 11 channels nearest the ship had unit amplification, channels 12 to 39 had a gain of two, and channels 40 to 48 had a gain of four. Problems with the tape-read routine caused the occasional spurious burst of large data samples, the

effect of this may be found on the final output sections. The resulting shot gathers consisted of 48 channel data recorded to 6.144 seconds at a 4 msec sampling rate. The source shot interval was 25 metres and the receiver group spacing was also 25 metres.

6.2.2 Common Mid-Point Sort

The sorting of the data produced 24 fold CMP gathers at a spacing of 12.5 m. The trace spacing in the CMP gather increased by only 50 m as opposed to 100 m for the Farnella 1/81 data. As no navigational information was available the ship was assumed to have kept to the ideal speed so the ideal sort was performed.

6.2.3 Pre-Stack, Stack, Post-Stack Processing and Display

Processing of the data set followed the same pattern as that used for the Farnella 1/81 data. Table 6.6 lists all the steps used to produce the final processed section. As the signal to noise ratio was far better in the Seismic Explorations Int. data set and there were no missing samples, the use of the velocity filter as a pre-stack process was not required. Instead, a 6 dB per second time ramp was applied with the same pre-stack deconvolution as used in the Farnella 1/81 data (table 6.3). Velocity filtering was still used in the velocity analysis to ensure an accurate stacking velocity function from the primary events. There was no need of the polarity reversal routine. However an extra routine was added at the start to identify and remove the unwanted spikes introduced by the demultiplex program.

1. Spike indentification and removal
2. Band-pass filter
3. Time ramp
4. Short gapped prediction error deconvolution
5. Removal of time ramp
6. Mute
7. Velocity analysis
8. Normal move-out correction and vertical stack
9. Band-pass filter
10. Geometrical spreading correction
11. Prediction error deconvolution
12. Trace energy equalization
13. 50 metre CMP simulation
14. Cosmetic time ramp or automatic gain control ramp
15. Display

Table 6.6 Processing applied to the Seismic Explorations Int. 1973 reflection data

The acquisition geometry meant a less severe mute function could also be applied, starting from trace 4 at 200 msec and increasing at a rate of only 50 msec per trace. The band-pass filter remained the same as for the Farnella 1/81 data (section 6.1.3) as Fig. 6.6 shows the power spectrum of the source has a similar band-width but has more power in the higher frequencies.

The filters used in the post-stack processing were the same as used for the Farnella 1/81 data (section 6.1.2) (Fig. 6.7). An extra routine was added to horizontally sum four stacked traces

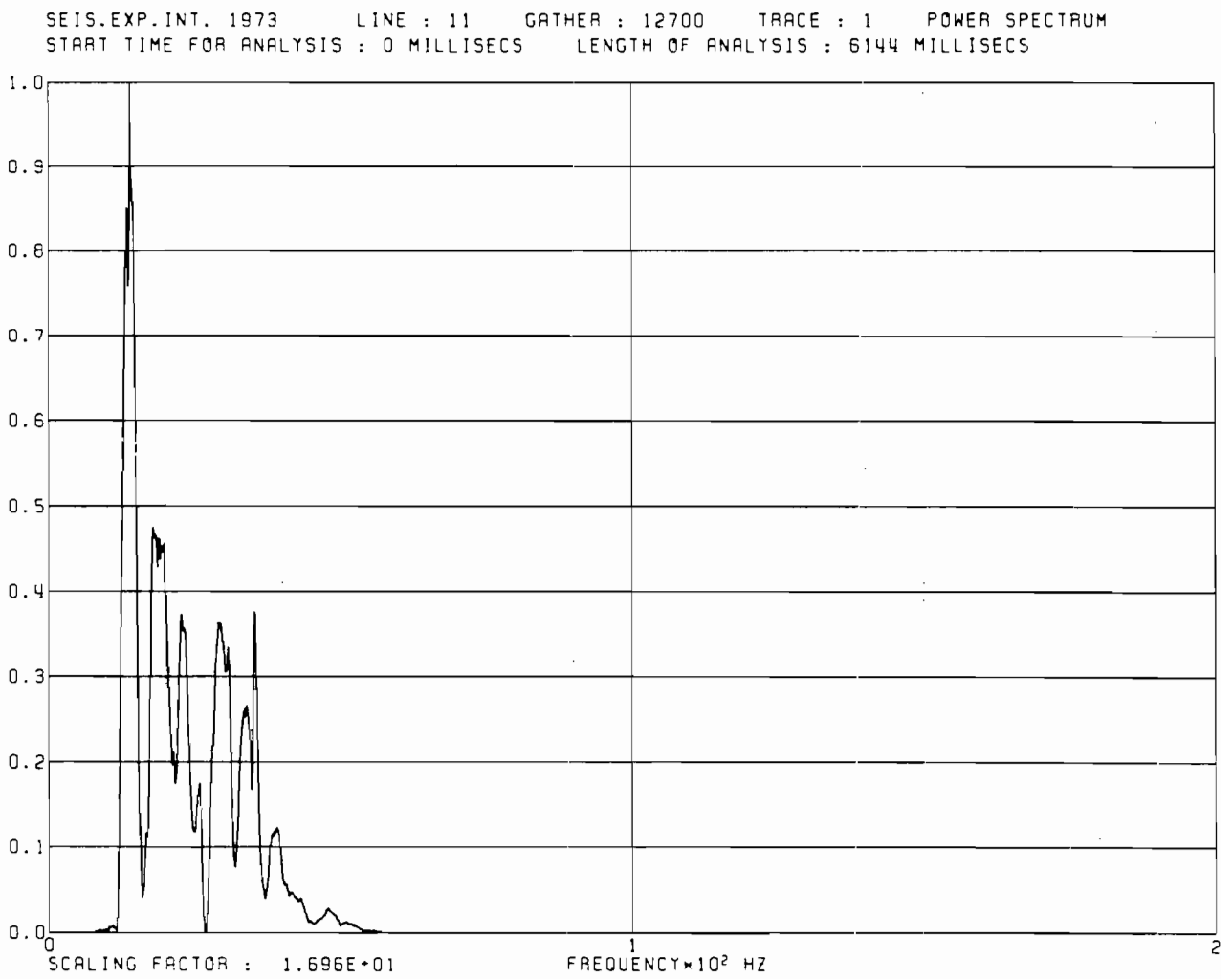

Fig.6.6 Power spectrum of the air-gun array used by Seismic Explorations Int. for their I973 survey.

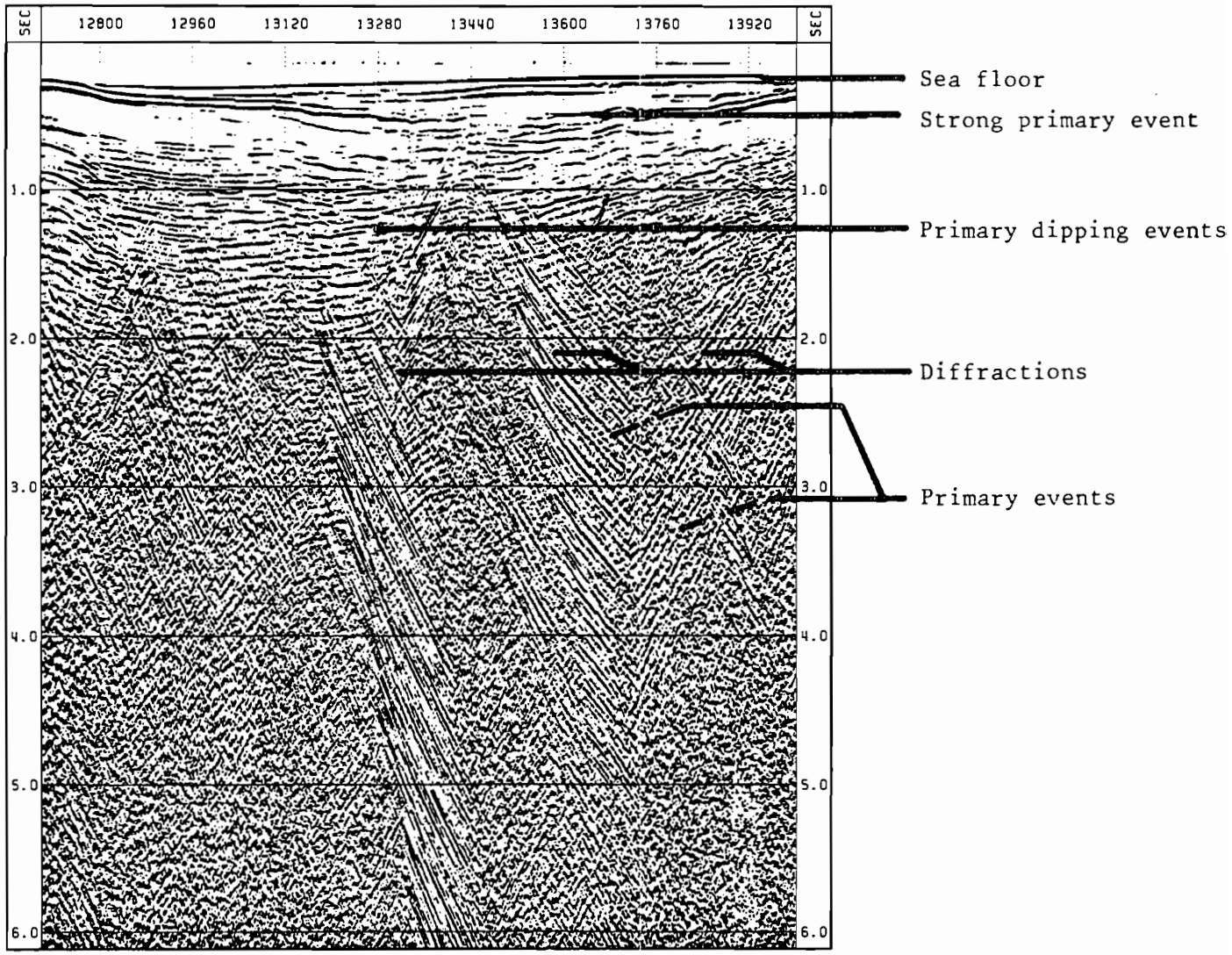

Fig.6.7a Processed stacked section from the Seismic Explorations Int. I973 survey with I2.5 m CMP spacing.

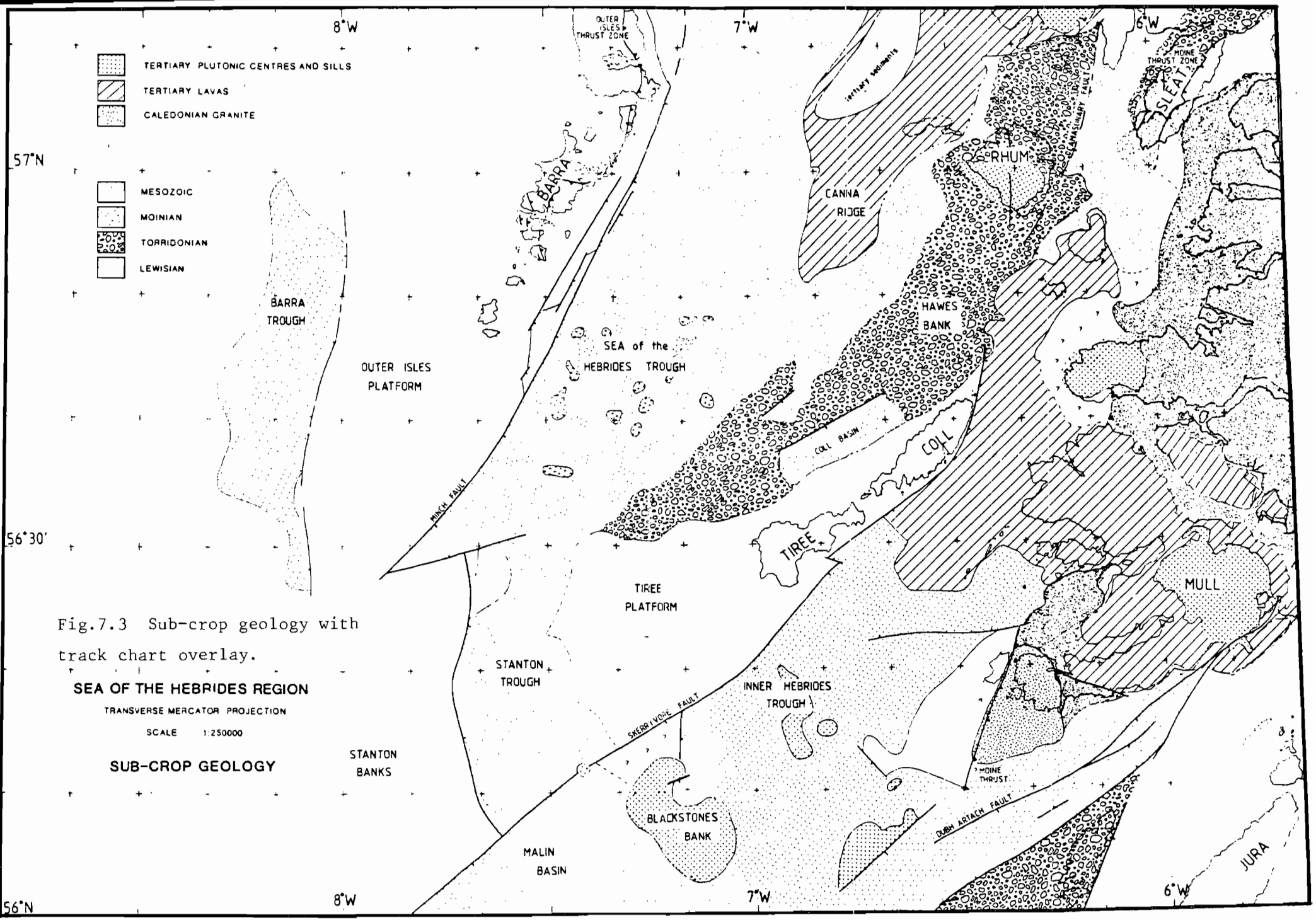

Fig.7.3 Sub-crop geology with track chart overlay.

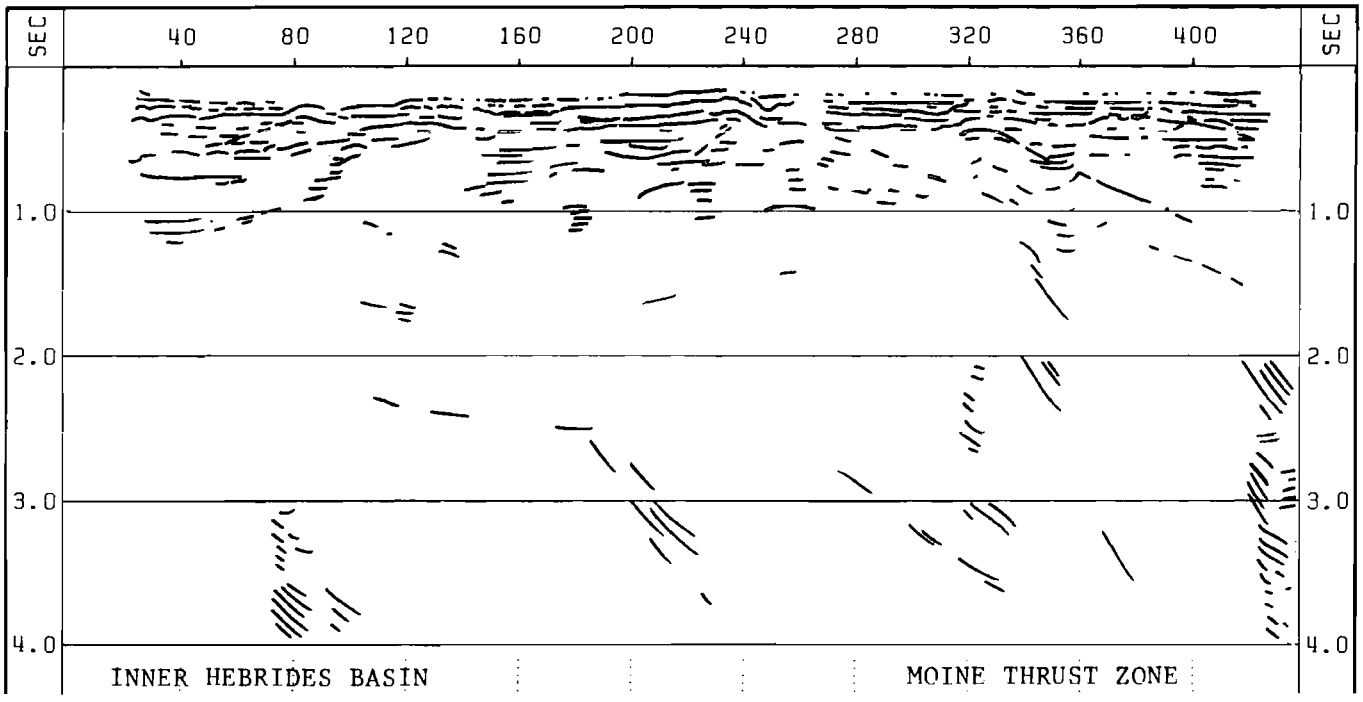

Fig.7.4 Farnella 1/81 reflection profile 4.

one sub-cropping at CMP number 320, and possibly another at CMP number 240. These define the Moine Thrust zone. The eastern most reflector being the Moine Thrust itself with either Moinian metamorphic rock or a southward extension of the Ross of Mull granite giving the higher refraction velocities on its eastern side. The westward event could be identified with the Kishorn Thrust, but this is uncertain. No clear events can be identified between two thrust faults and is possibly made up of imbricated Torridonian and lower Palaeozoic sediments. The eastern end of the profile is probably underlain by Torridonian sediments, the refraction velocity of 4 km/s being too low for Lewisian basement. The average interval velocity of the near surface sediments, calculated from the stacking velocities, indicate a Mesozoic sequence with a thin cover of Quaternary, not the 200 metre thickness of Quaternary deposits suggested by Lunn (1984).

Farnella 1/81 line 6 CMP numbers 1 to 600

The ship's course runs south west from the Ross of Mull to Blackstones Bank over the southern end of the Inner Hebrides Basin. The Bouguer gravity map does not suggest the presence of a deep basin. Refraction velocities of 4.0 to 5.0 km/sec indicate that up to CMP number 300 there is not a significant thickness of Mesozoic. After that point, velocities of 3.5 km/sec are seen. A similar interpretation can be obtained from the reflection profile (Fig. 7.5a) where a layer of interval velocity 5.0 km/sec, Torridonian, is lying on a reflector which dips away westwards, to the higher CMP numbers. This is then covered from

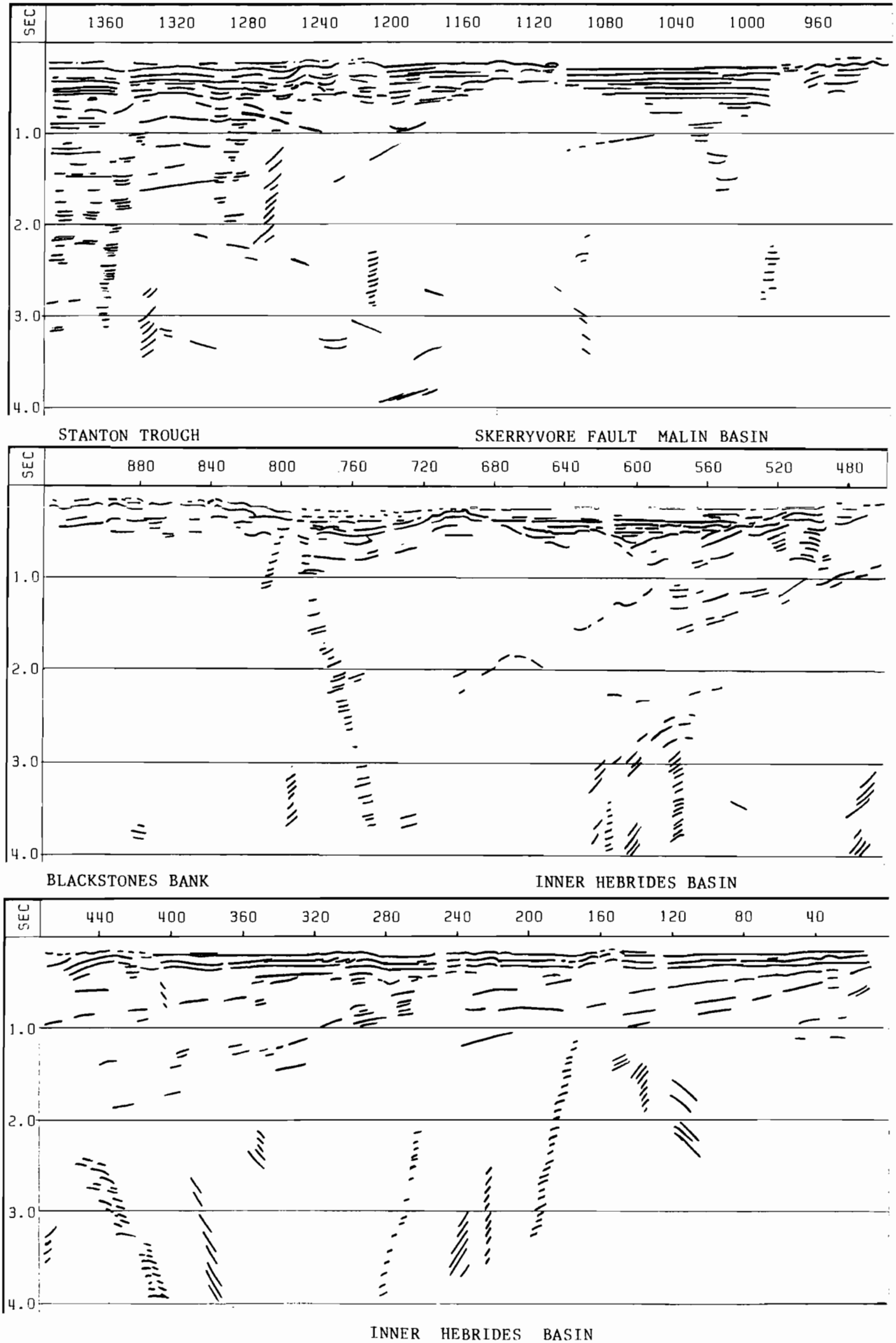

Fig.7.5a Farnella 1/81 reflection profile 6. CMP numbers 1 to 1400.

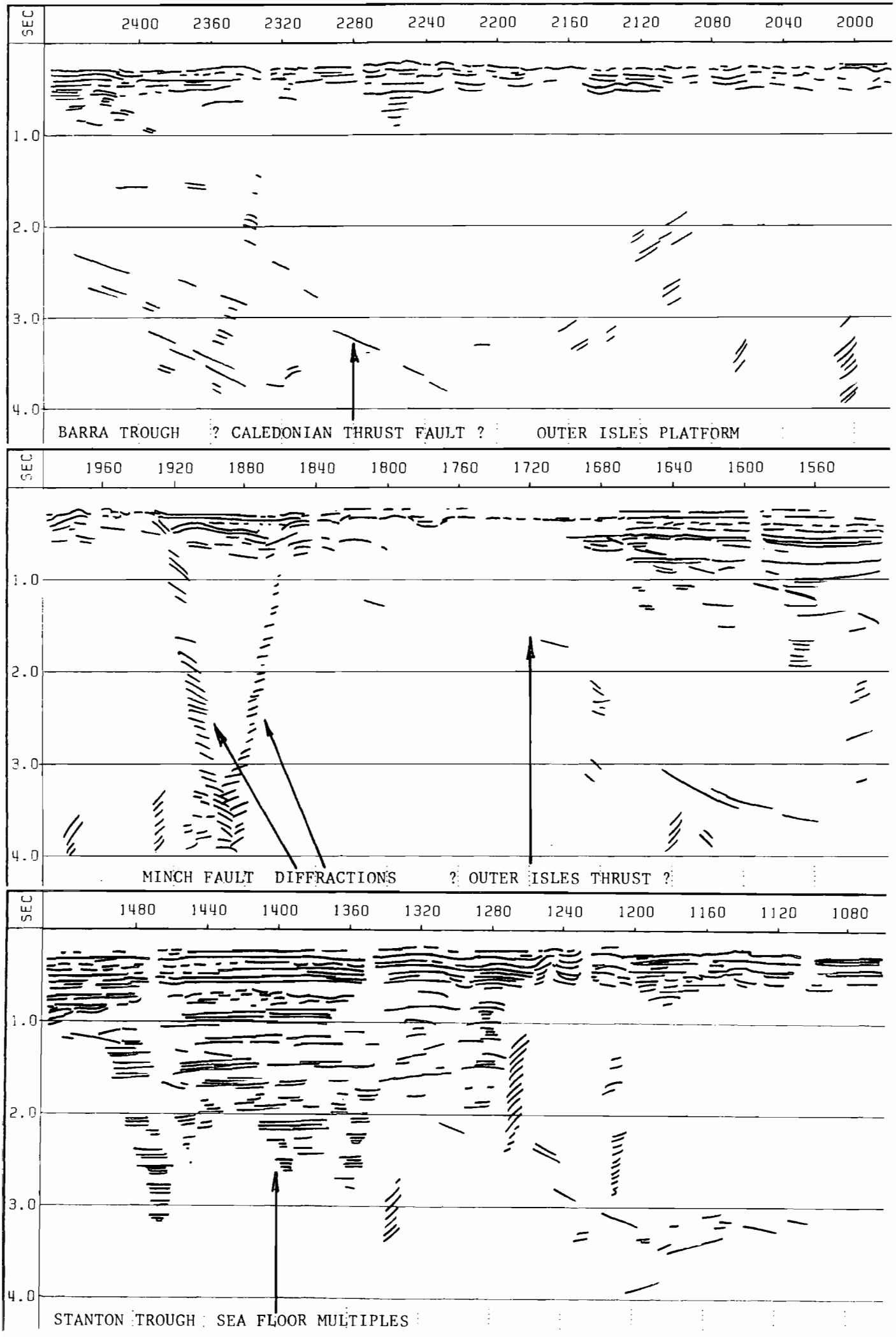

Fig.7.5b Farnella 1/81 reflection profile 6 CMP numbers 1053 to 2452.

CMP 310 by Mesozoic sediments. To the north where I.G.S. line 2 crosses the Skerryvore Fault a much deeper basin is present with up to half a second of Mesozoic sediments. Between CMP points 150 to 160 and again between CMP points 410 and 510 a high velocity refractors, 6 km/sec, appear at the surface. These are interpreted as sills.

Summary

The Inner Hebrides Basin deepens to the north-west where it is truncated by the Skerryvore Camasunary fault against the Tiree Platform. On the downthrown side of the fault the Mesozoic sediments are about 1 km thick, these thin rapidly to the south-east and are no longer present 7 km away from the fault. To the south, the basin is not so deep with little or no Mesozoic present. The thrust fault which passes between the Ross of Mull and Iona can be identified further south along with some evidence for another thrust fault nearly 5 km to the west.

7.2.2 Blackstones Bank Igneous Complex

Farnella 1/81 line 6 CMP numbers 600 to 970

Line 6 (Fig. 7.5a) runs due west over the northern end of the Blackstones Bank complex (Fig. 7.3). The eastern margin of the main body is obscured by extensive sills which can be traced back to CMP point 410. From CMP point 520 to 680 and from CMP point 720 to 800 two sedimentary basins overlie the igneous rocks, both are filled with Mesozoic sediments overlain by

glacial drift. At CMP point 790 a normal fault downthrows the surface of the igneous complex to the east. Westwards from this point to CMP 970 the pluton sub-crops. At CMP 970 the complex ends and a sedimentary sequence appears. No coherent seismic events can be seen within the complex.

7.2.3 The Stanton Trough and the Outer Isles Platform

Four independent surveys cross this area (Fig. 7.3): the WINCH line shot points 8000 to 10800, I.G.S. line 1, Farnella 1/81 line 6 CMP numbers 670 to 2452 and line 7 CMP numbers 1 to 600, and the Seismic Exploration Int. profile CMP numbers 6000 to 10700.

North-west extension of the Malin Basin

The I.G.S. line 1 indicates that there is half a second of Mesozoic sediment to the east of the Skerryvore fault. Further to the south-west Mesozoic refraction velocities are found from the Farnella 1/81 data (Fig. 7.5a) with reflectors dipping towards the fault. On both the Farnella line and the WINCH line it is not possible to discern the bottom of these sediments but as there is Torridonian to the east of Blackstones Bank it seems reasonable to assume that they also underlie the Mesozoic here.

Stanton Trough

The Farnella 1/81 line 6 now turns to the northwest crossing the Skerryvore fault and passes over the Stanton Trough (Figs. 7.5a and 7.5b). The Skerryvore fault downthrows to the south-

east, on crossing it at CMP number 1120 the refraction velocity increases to 3.5 to 4.5 km/sec which is indicative of a Torridonian sub-crop. Binns et al. (1974) identify this basin as filled with late Pre-Cambrian and lower Palaeozoic. This was later modified by Binns et al. (1975) to a Mesozoic basin, which is also supported by work by C. Uruski. The depth of the basin is uncertain and is limited by the size of the negative gravity anomaly. A possible interpretation is that a thin layer of Mesozoic sediments, 500 metres thick or less, lies on a Torridonian base of a maximum thickness of 5 km with the Lewisian beneath. Patches of high velocity material can be seen occasionally on or near the surface of the trough, e.g. CMP point 1240, these are sills emplaced by the Tertiary igneous activity. As the profile moves up the trough, a possible deep reflector is seen dipping towards the lower CMP numbers. This event is seen more clearly on the WINCH data between shot point numbers 10020 and 10300 (Fig. 7.6) where the dip can be calculated to be 12^{o}. Following this event to the surface at CMP number 1720 on the Farnella 1/81 data conincides with a marked increase of refraction velocties to 6.0 km/sec. These velocities indicate the presence of crystalline basement sub-cropping below the glacial drift.

Between CMP numbers 1850 and 1930 (Fig. 7.5b) a small graben-like structure occurs, with the north west fault as the southern extension of the Minch fault. Mesozoic velocities are recorded at the centre of the structure under a thick layer of glacial drift. At CMP number 2000 there is a suggestion of a

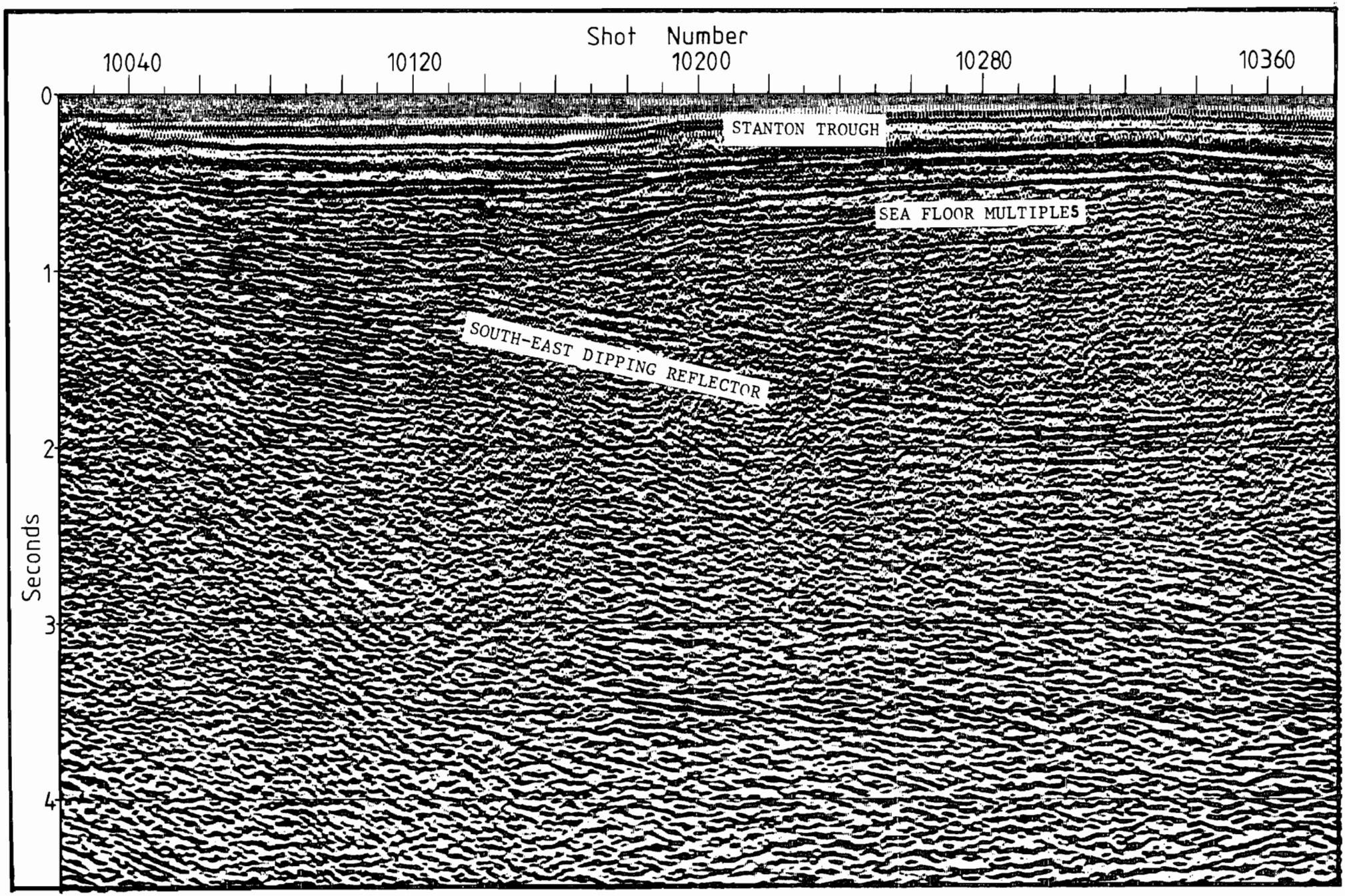

Fig.7.6 Detail from the B.I.R.P.S. WINCH profile, shot point numbers 10020 to 10380.

south eastward dipping reflector which could indicate the offshore line of the Outer Isles Thrust, a similar feature can be seen in the WINCH line at shot point 9660. The seaborne magnetometer profile presented in the I.G.S. report (Binns et al. 1974) shows a magnetic anomaly of 400 gamma at this point (Fig. 7.7). This is a similar to the anomaly which crosses the isles of Barra and South Uist further to the north where the anomaly follows the line of the Outer Isles Thrust.

The Outer Isles Platform and Barra Trough

The refraction velocity maintains a value of 5.5 to 6.0 km/sec across the Lewisian platform. With either Mesozoic or Quaternary sediments filling isolated lows in the Lewisian surface. From 8^{o} west there is a continuous cover of Quaternary over the rock head. Binns et al. (1974) suggest the presence of a Mesozoic basin from the gravity anomaly. At the end of Farnella 1/81 line 6 (Fig. 7.5b) and the start of line 7 (Fig. 7.8) changes in reflection character indicate the presence of sediments but refraction velocities of 4.5 to 5.0 km/sec suggest a Torridonian origin. From the Seismic Exploration Int. profile (Fig. 7.9a) a refractor of 3.5 km/sec is found futher into the basin. The WINCH line shows what appears to be a considerable fault on the eastern margin (Fig. 7.10) but the velocity function used to stack the data imposes an upper limit of half a second for Mesozoic sediments beneath the sea-floor.

On all the reflection profiles in this region eastwardly dipping events may be followed in the Lewisian basement. These

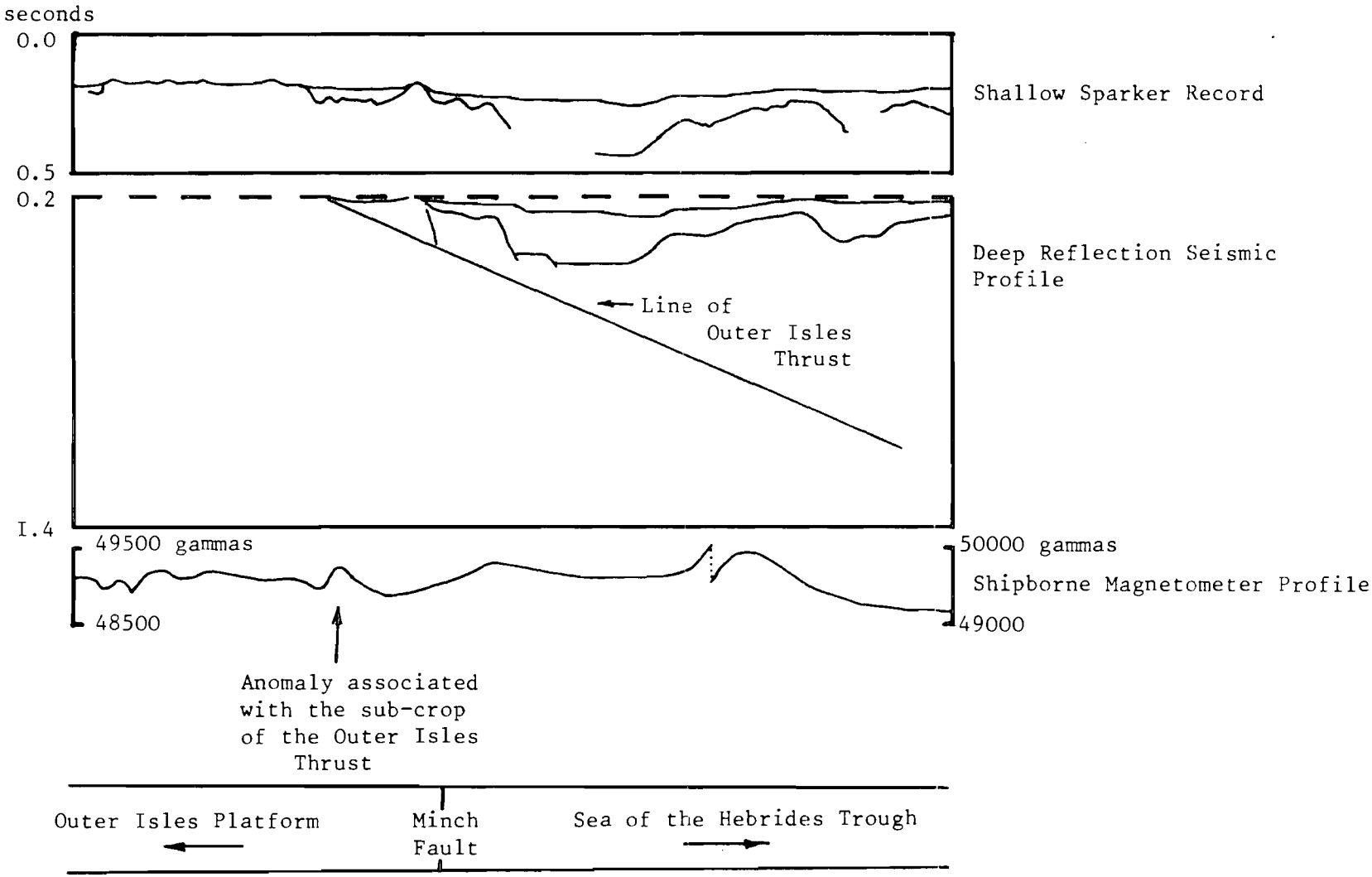

Fig.7.7 Seaborne magnetometer profile over the line of the Outer Isles Thrust fault. After Binns et al. (I974).

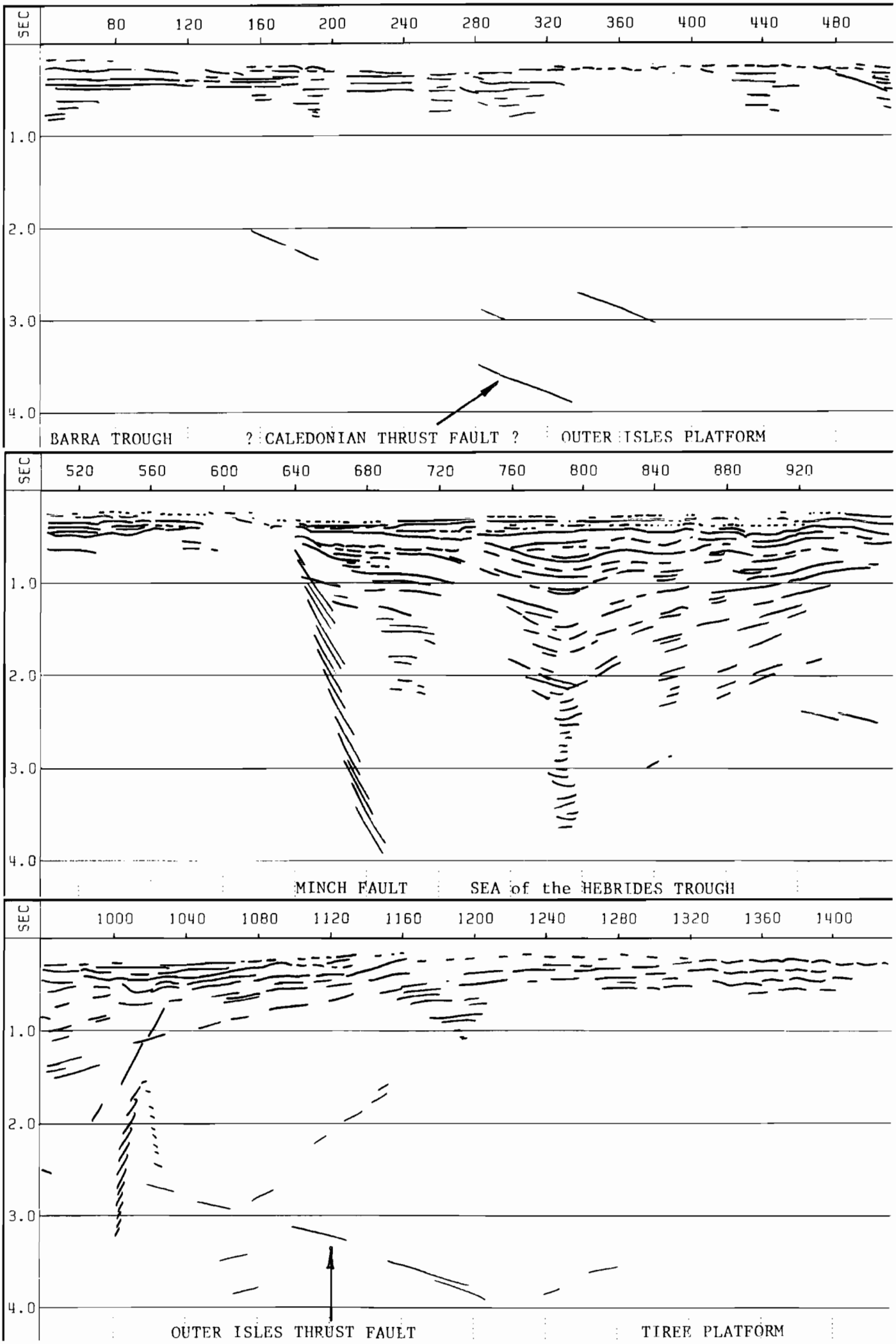

Fig.7.8 Farnella 1/81 reflection profile 7.

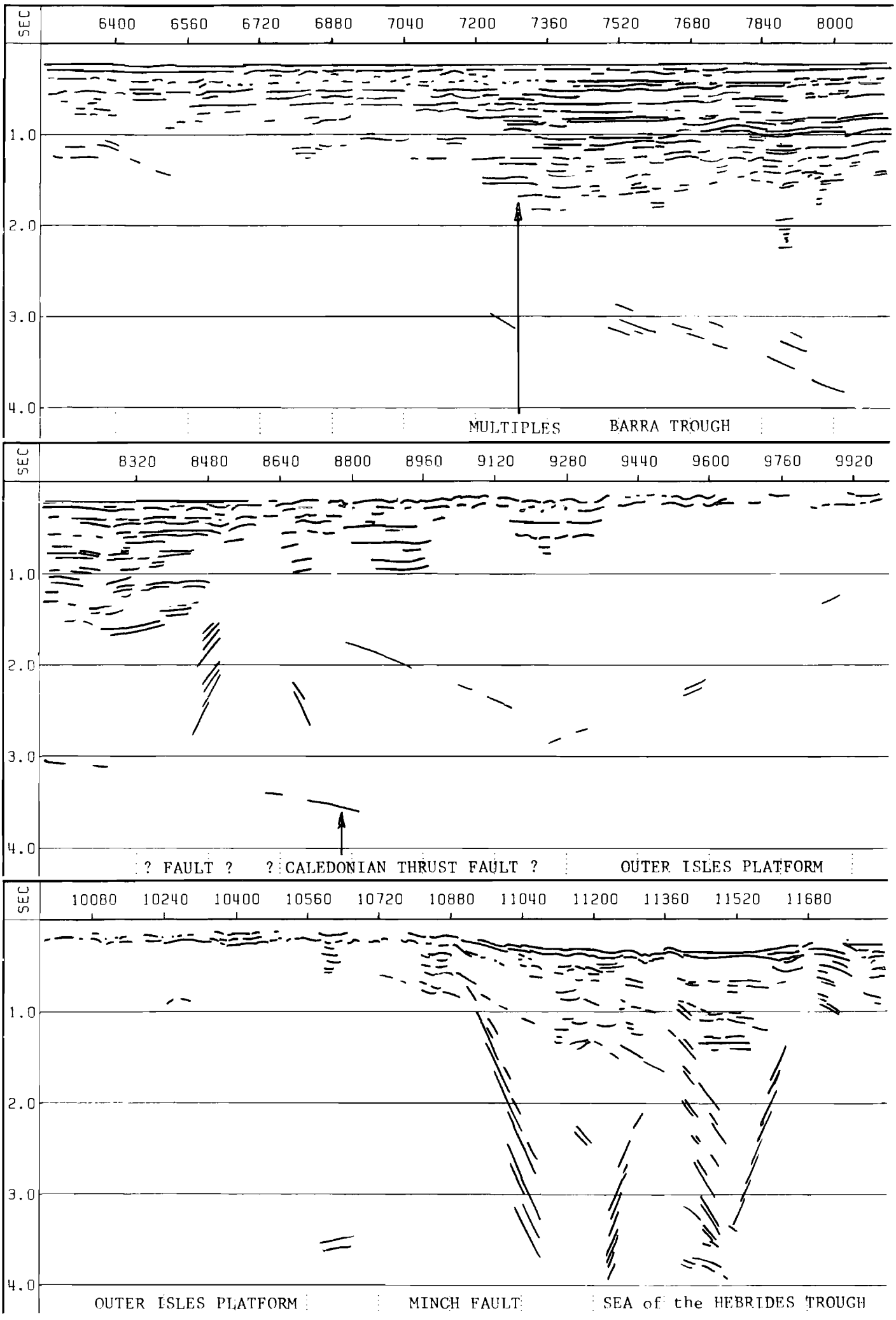

Fig.7.9a Seismic Explorations Int. profile. CMP numbers 6244 to 11843

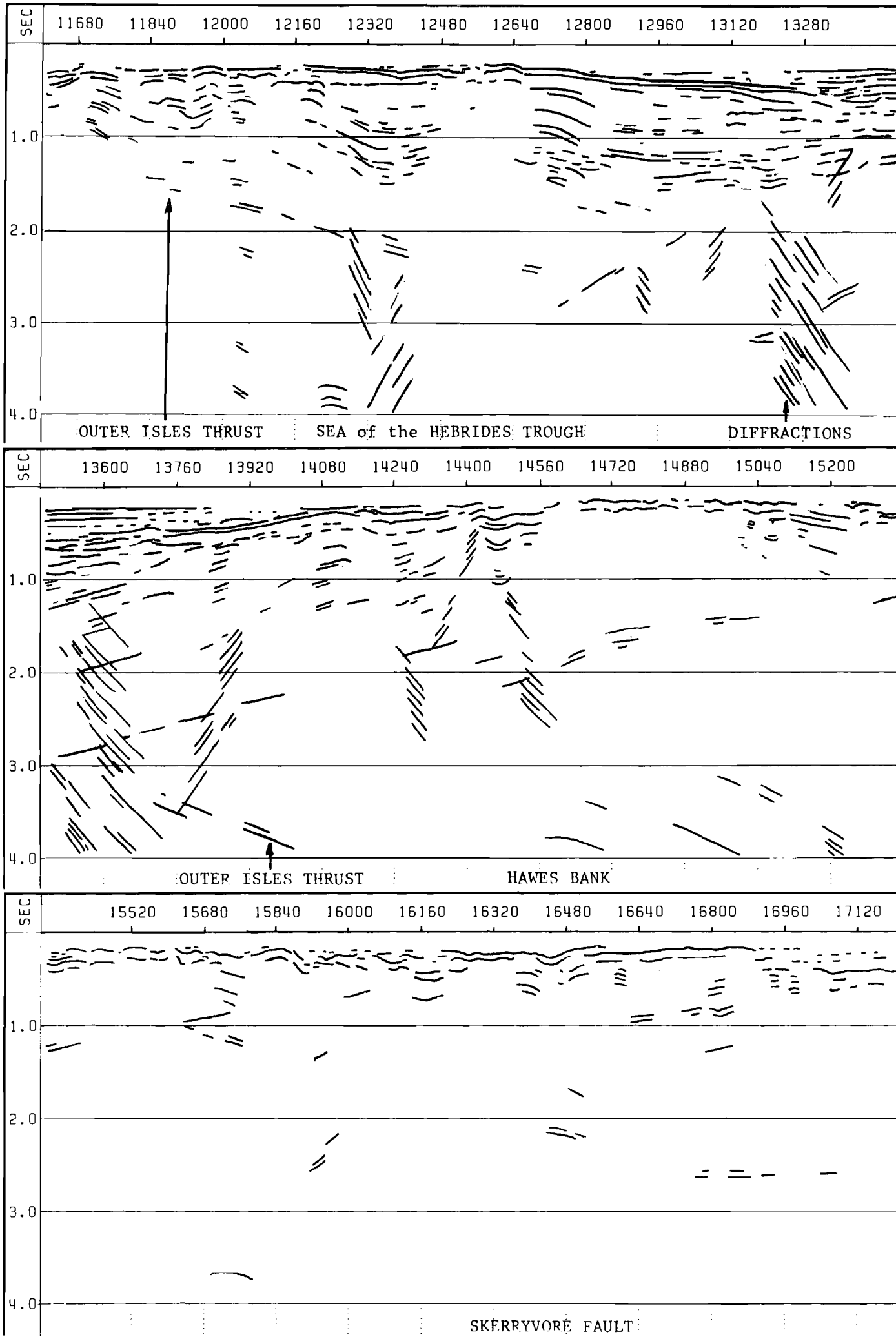

Fig.7.9b Seismic Explorations Int. profile. CMP numbers 11612 to 17211

Lewisian

Beneath the western margin of the Trough the top of the Lewisian is taken as being the plane of the Outer Isle Thrust. On all the profiles processed at Durham the line of this thrust may be traced down into the upper crust as a series of disjointed events with a dip angle of 15°. The interpretation to the east is constrained by the outcrop of Lewisian rocks on the sea floor. On the eastern margin of the trough the Lewisian surface dips westwards at an angle of 15° under the Torridonian. For Farnella 1/81 line 7 (Fig. 7.8) the profile passes onto the Tiree Platform at CMP number 1320, on line 8 (Fig. 7.11) the Lewisian does not outcrop, and on the Seismic Exploration Int. profile (Fig. 7.9b) the northern tip of the platform can be identified at CMP number 16450. On line 7 the maximum depth to the Lewisian surface is 1.9 seconds two-way time at CMP number 850. Further north, this depth is greater, at nearly 3.0 seconds close to the point where the Farnella line 8 and the Seismic Explorations Int. profiles intersect. On the I.G.S. line 3/8 a fault down thrown to the north at shot point 148800 lies between the two readings but it is not possible to identify the Lewisian reflector on this section.

Torridonian

The subcrop of the Torridonian on the eastern margin can be determined from the refraction velocity data. No evidence for Torridonian is found on the western margin. On Farnella 1/81 line 7 (Fig. 7.8) the top of the sequence can be traced across the

are particularly clear in the WINCH data between shot points 8000 and 8130 (Fig. 7.10) and on the Seismic Exploration Int. profile between CMP numbers 7500 and 8000 (Fig. 7.9a). The event appears to have the same dip, 20° to the east, as the Outer Isles Thrust and therefore is probably of Caledonian origin.

7.2.4 Sea of the Hebrides Trough

Most of the rock head of the Sea of the Hebrides Trough is obscured by glacial drift. From work by Binns et al. (1974) the sub-crop geology is predominantly Mesozoic with the appearance of Torridonian and Lewisian on the eastern margin (Fig. 7.3).

The Minch Fault

At the point where the Farnella 1/81 line 7 (Fig. 7.8) profile crosses the Minch Fault, at CMP number 640, a steep scarp feature is shown on the bathymetry map and the refraction velocity falls to 3.5 km/sec. Futher north, where the Seismic Exploration Int. profile crosses, there is no significant bathymetric feature and the refraction velocity only falls to 4.0 km/sec. On the reflection seismic section (Fig. 7.9a) the area is very confused and appears to indicate the presence of some igneous rocks. The sub-crop geology map also shows the presence of a number of igneous bodies in this area. Yet no anomalies appear on either the gravity or aeromagnetic maps. This effect lasts for 7 km before Mesozoic velocities appear.

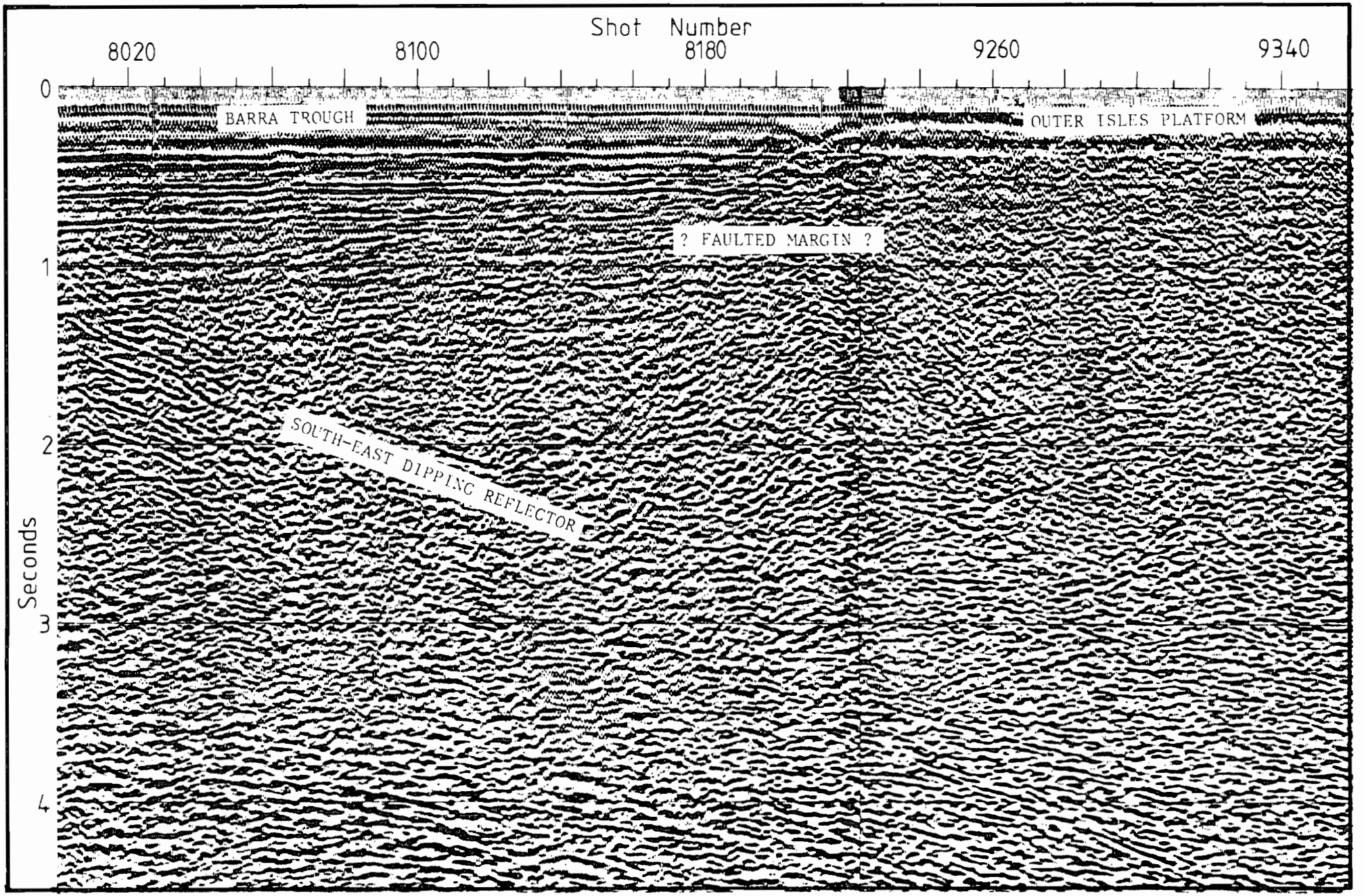

Fig.7.10 Detail from the B.I.R.P.S. WINCH profile, shot point numbers 8000 to 9360.

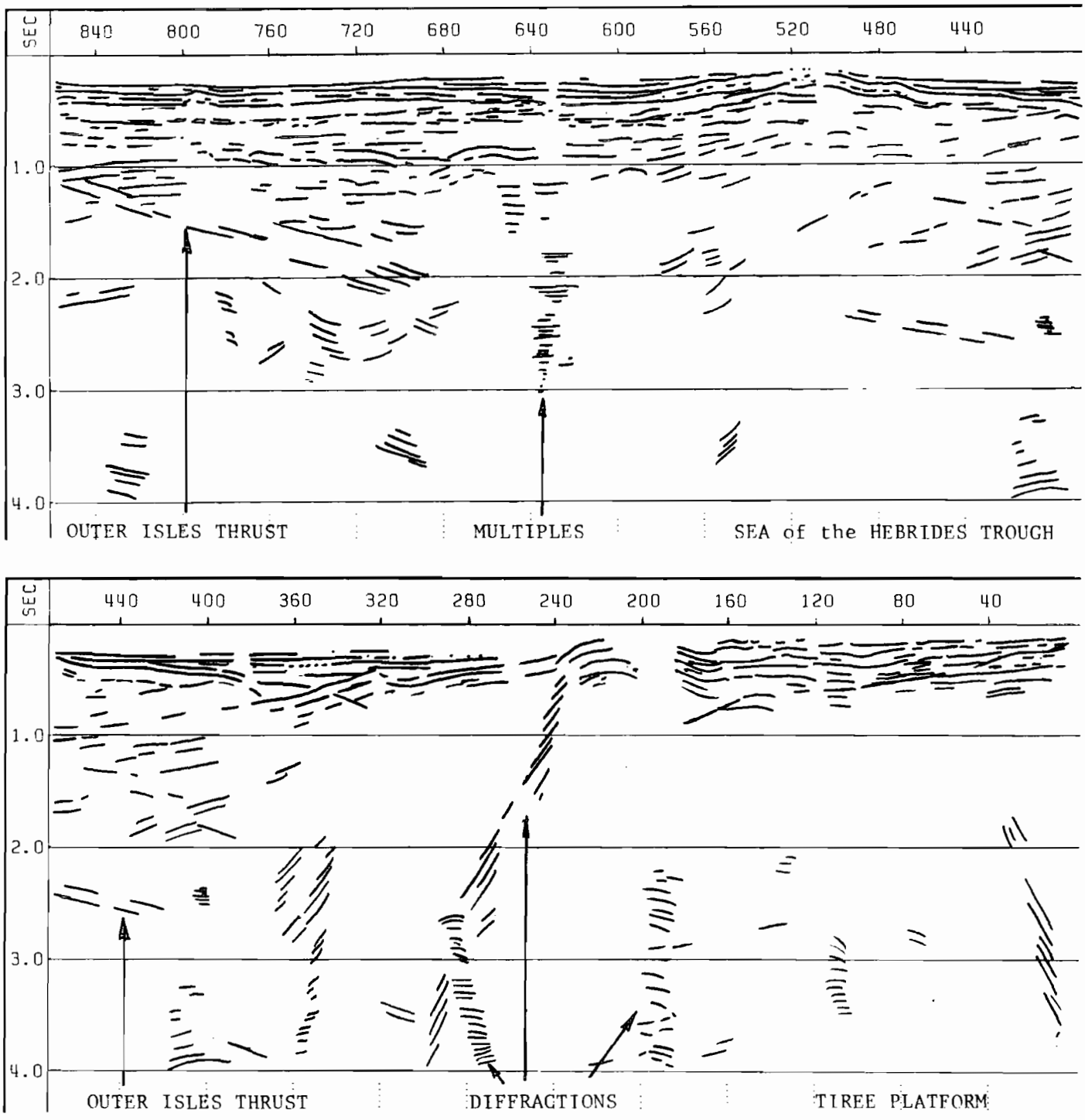

Fig.7.11 Farnella 1/81 reflection profile 8.

whole basin, attaining a thickness of 1.5 km over the lowest point of the Lewisian, then thinning westwards against the Outer Isles Thrust. On Line 8 (Fig. 7.11) thickness of the Torridonian is much greater being 4 km at CMP number 300. At CMP number 320, on the same section, a discontinuity in the Torridonian surface is found, this may be due to glacial erosion but is more likely to be a fault. The surface of the Torridonian under the Mesozoic to the west is unclear but a suggested interface has been indentified. On the Seismic Explorations Int. profile (Fig. 7.9b) a thick sequence is found again but tracing the upper surface across the whole basin is difficult because of igneous intrusions in the rocks above. The Torridonian exposure to the west of CMP number 14400 forms Hawes Bank. Occasional coherent events can be seen dipping westwards which probably indicate the top of the Lewisian. Eastward dipping events can be traced within the basement and are probably of Caledonian age.

Mesozoic

The remaining sediments in the basin have been assigned to the Mesozoic era. On all the sections evidence of sill intrusion can be seen, particularly in the Seismic Exploration Int. profile (Fig. 7.9b). This profile also shows the best example of the unconformity between the Mesozoic and Torridonian sequences.

On this line also, to the east of the line of the Camasunary Fault, CMP number 16480, lies the Inner Hebrides Trough. At this point the sediments are covered by Tertiary lavas extending north from Mull but at the edge of the profile a short section of

Mesozoic sediments can be seen.

Quaternary

As stated at the start of this section most of the geology is covered by glacial drift and more recent deposition. Glacial erosion has cut deep channels in the suface of the sediments in the basin. The effect of this erosion can be seen on line 8 between CMP numbers 280 and 400 (Fig. 7.11).

Gravity Modelling

The gravity profile is presented by Shaw (1978) as a part of a larger profile along the whole of the WISE refraction line. The portion across the basin has been expanded by the inclusion of more data points. Using the reflection data as a control, a simple model is proposed (Fig. 7.12). This model includes both the regional anomaly and the effects of the deep Quaternary glacial channel mentioned above. The model shows that the regional anomaly can be explained by structure within the Lewisian basement. The Tiree platform having a 10 km thickness of the lower density amphibolite Laxfordian overlaying the higher density granulite Scourian, whereas the Outer Isles has only a thin cover of the Laxfordian facies. The line of contact between these two facies follows the plane of the Outer Isles Thrust. The general shape of the negative anomaly can fitted by Mesozoic and Torridonian bodies. The Mesozoic attaining a maximum thickness of 2.5 km at 9 km from the line of the Minch Fault. The Torridonian being up to 5 km thick 32 km from the line of the Minch Fault.

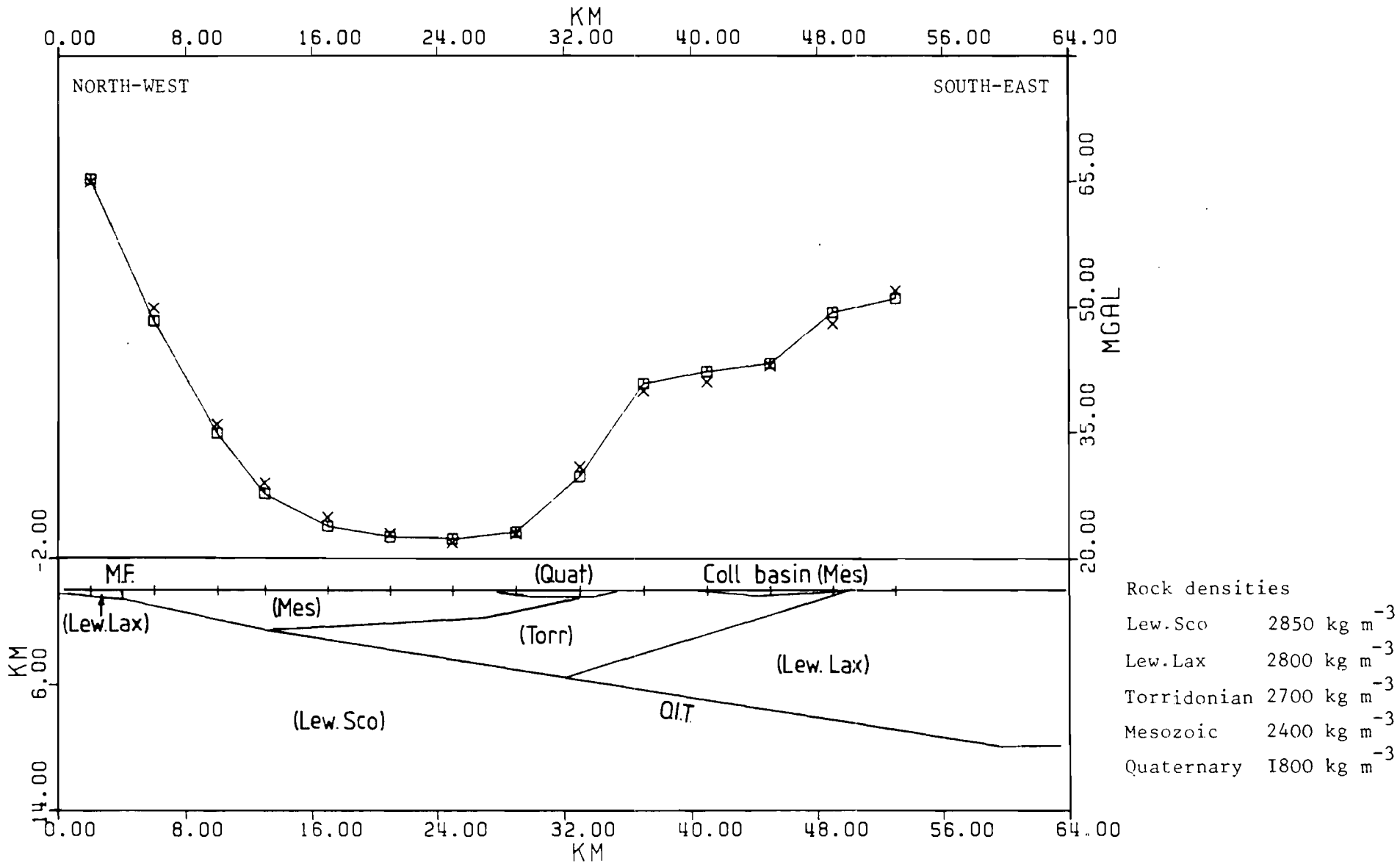

Rock densities

Lew.Sco	2850 kg m^{-3}
Lew.Lax	2800 kg m^{-3}
Torridonian	2700 kg m^{-3}
Mesozoic	2400 kg m^{-3}
Quaternary	I800 kg m^{-3}

Fig.7.I2 Gravity model along the line of the Farnella I/8I and WISE profiles.
M.F. Minch Fault, O.I.T. Outer Isles Thrust.

Fine tuning of the model is achieved by the inclusion of the Quaternary glacial channel and the Mesozoic filled Coll Basin. The fit of the model is good confirming the general shape, density and thicknesses of the sediments involved.

Comparison to the WISE Experimental Results

The course of Farnella 1/81 line 8 was chosen to follow the profile used in the WISE refraction experiment. With the seismometer stations on Barra, Tiree and Iona placed on Lewisian basement, and the Ross of Mull station placed on the Caledonian granite, most of the time term delays must be due to the sediments under the shots set off in the Sea of the Hebrides. Some time term delay under the seismometer stations should be expected, as there is a reduction in the basement refractor velocity where the Lewisian is exposed on the surface. As shown by Hall (1978) the refraction velocity rapidly rises to 6 km/sec within a depth of 1 km, so the time term delays for the stations will be small compared to those from the shots. Using the reflection profile and average interval velocities, the expected delay can be calulated for each shot position and compared to those presented by Summers (1982) (table 7.2).

WISE shot No.	Isotropic Time Term	Anisotropic Time Term		Calculated Time Term
		North	South	
20	0.18 (5)	0.47 (1)	0.07 (4)	0.51
21	0.42 (5)	0.78 (1)	0.27 (4)	0.75
22	0.41 (7)	0.76 (1)	0.26 (6)	0.65

Table 7.2 Comparison of experimental and calculated time term delays in seconds for the WISE shots in the Sea of the Hebrides Basin. The number in brackets represents the number of measurements contributing to the previous value.

The isotropic case assumes that the geology directly below the shot is uniform in all directions. The anisotropic case allows for any dip and velocity structure which may cause the time term delay to be directionally dependent. Those to the north are calculated from the arrival time at the Barra seismometer station, those to the south are a least squares fit for all the stations to the south of the shot on which the basement refractor P_g arrival can be identified. The calculated time terms assume an isotropic state and as can be seen the results are significantly different to the computed delays from the experimental data. The calculated results are similar to the anisotropic case to the north, which suggests that the least squares fit to the travel times to the south has not given the correct results. This can be explained by the variation of refractor velocity as the distance from the shot point increases.

An alternative approach is to assume a P_g velocity, then by subtracting the basement refractor time from the total travel

time, the individual shot delay terms may be calculated for each station (Table 7.3).

SHOT No.	Station location				
	BARRA	TIREE	IONA	MULL	Calculated Time Term
20	0.34	-	0.31	0.17	0.51
21	0.67	0.60	-	0.36	0.75
22	0.62	0.59	0.41	0.44	0.65

Table 7.3 Difference in seconds between the observed travel times and the basement refractor times, assuming a basement velocity of 6 km/sec.

The correlation between the calculated time term delays and the observed delay times assuming a basement refractor velocity of 6 km/sec is good for the two nearest stations on Barra and Tiree. The results for the stations on Iona and Mull show that the basement refractor must have a higher velocity of 6.01 to 6.02 km/sec.

Summary

The Sea of the Hebrides Trough has been interpreted as a half gaben basin filled with 2.5 km of Mesozoic and 5 km of Torridonian sediments. The north-western margin is bounded by the Minch and Outer Isles Thrust faults. The Outer Isles Thrust fault also marks the change in the basement from the Laxfordian above the fault plane to the Scourian below. The basin has been extensively intruded by sills during the Tertiary. Evidence of

glacial erosion features are clearly seen with up to 200 m of Quaternary deposits filling them. The interpretation of the reflection data fits the known sub-crop geology and measured gravity anomaly. The results from the WISE refraction survey can also be fitted to the interpretation provided the correct basement refractor velocity is chosen.

7.2.5 The Region Between the Isle of Skye and Rhum

Farnella 1/81 line 9

This profile (Fig. 7.3) approximately follows the same course as that presented in the I.G.S. report (Binns et al. 1974). The gravity in this region is dominated by the igneous centres on Rhum and the Isle of Skye and yields little information besides that the two centres appear to be seperate. The aeromagnetic map shows the lava flows which extend south from Skye over the Canna Ridge, by the high amplitude and frequency anomolies they produce (Fig. 7.2). Away from this effect the rest of the profile appears to be magnetically quiet. Refraction velocities give a mostly uniform value of 4.5 to 5.0 km/sec except for two short areas of 3.5 km/sec.

The reflection profile (Fig. 7.13) starts over the lava field to the west, the multiple energy from which obsures all other arrivals. At the edge of the lavas a small Mesozoic basin is found (Binns et al. 1974) which passes into a 15 km wide bank of Torridonian. The contact is covered by over 100 metres of glacial drift making it difficult to identify if the basin is

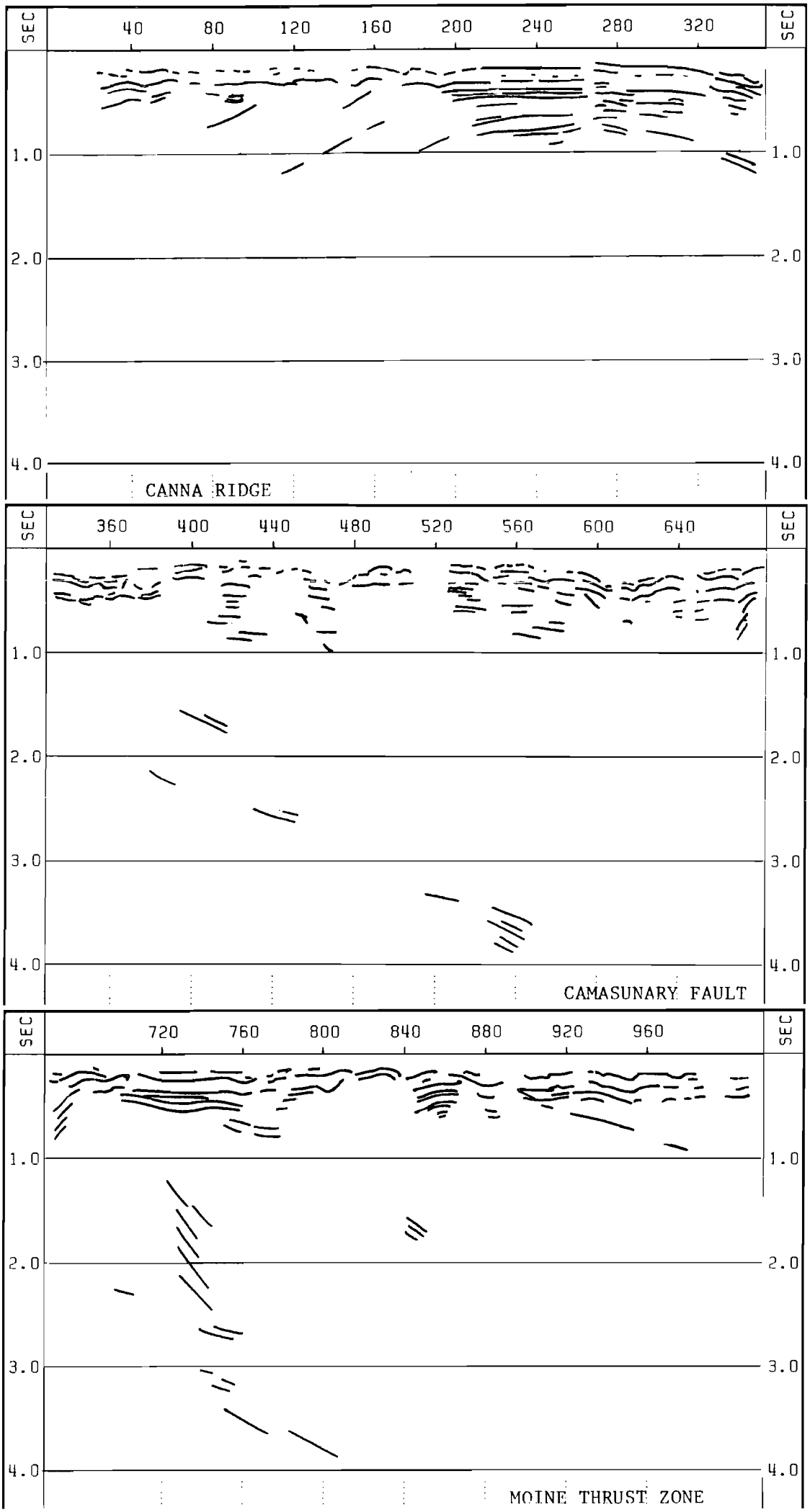

Fig.7.13 Farnella 1/81 reflection profile 9.

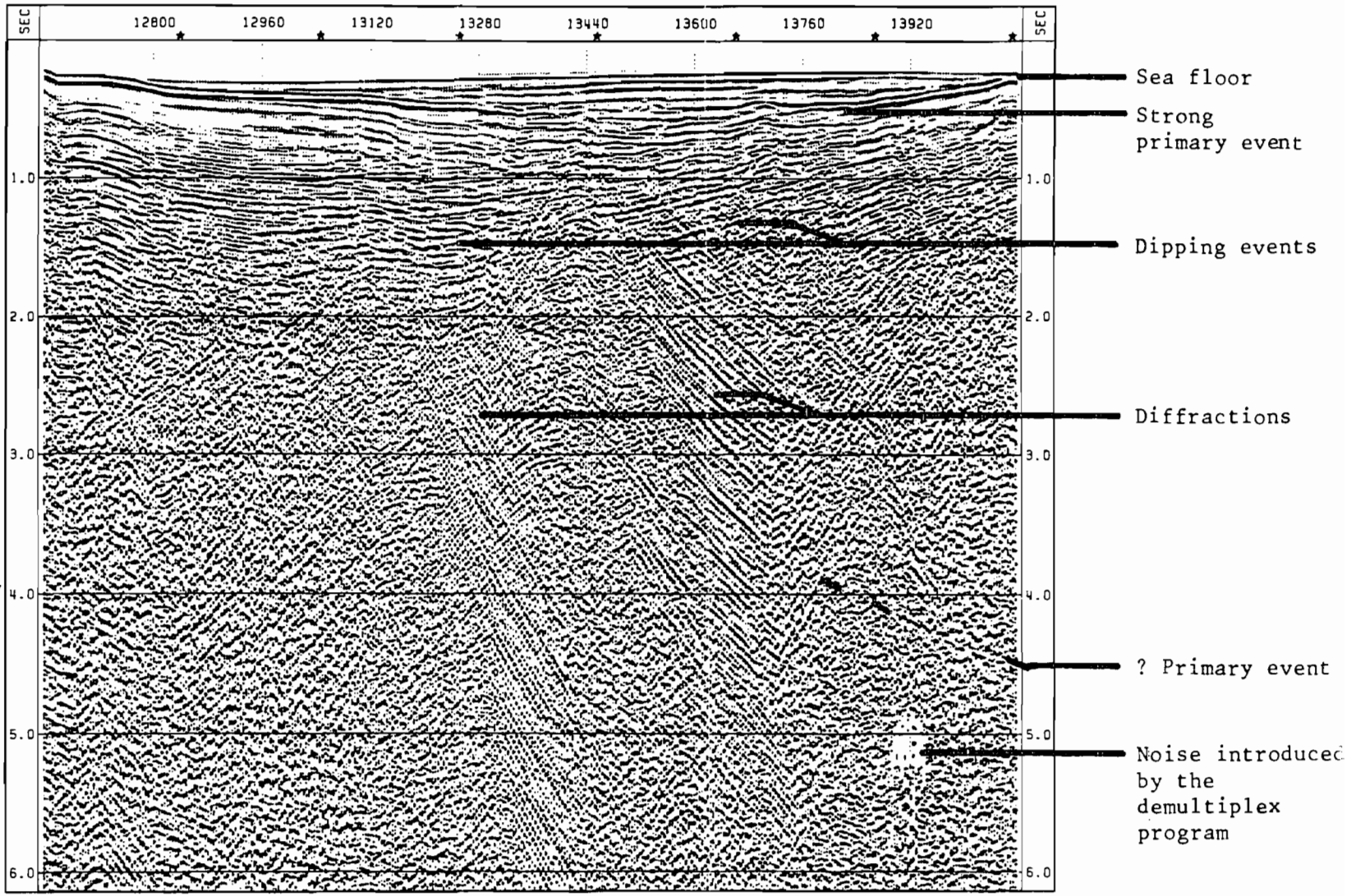

Fig.6.7b Processed stacked section from the Seismic Explorations Int. 1973 survey with 50 m CMP spacing.

together to simulate a 50 metre CMP spacing (Fig. 6.8). This effectively dip filtered the section to suppress diffractions which covered much of the lower part of the section with 12.5 metre CMP spacing.

6.2.4 Summary

The final section presented in Fig. 6.8 comes from the same region of the Sea of the Hebrides Trough as used in the examples of the Farnella 1/81 data (Figs. 6.5b & 6.5c). The velocity filtered Farnella 1/81 section (Fig. 6.5c) compares well with the commercial results (Fig. 6.8) particularly in the first second of record. However, the section from the Seismic Explorations Int. survey showes more detail than either of the Farnella 1/81 sections in the lower part of the record. This can be explained by the use of a more powerful broad band-width source (Figs. 6.2 & 6.6) and the higher density of coverage.

CHAPTER 7

INTERPRETATION

This chapter covers the interpretation of the reflection data acquired on the Farnella 1/81 cruise and that of the Seismic Explorations Int. profile which has been reprocessed in Durham. Other available data from this region include: reflection profiles obtained by I.G.S. processed by Seismograph Service Ltd. in 1969, the British Institutions Reflection Profiling Syndicate WINCH line processed by GECO in 1983 (Brewer et al. 1983), gravity and magnetic data presented by Shaw (1978), and the WISE refraction profile (Summers 1982).

The chapter contains all the interpreted sections using the colour code given in table 7.1. All the profiles, except for the Seismic Explorations Int. section, have been velocity filtered before stack. Appendix 1 contains the sections without the interpretation on an expanded scale. For the Farnella 1/81 cruise sections are also included which have been deconvolved before stack and plotted to 8 seconds two-way time. A composite track chart, with all the reflection profiles used in this interpretation and the WISE refraction line marked, is supplied with a sub-crop geology map drawn to a scale of 1 to 250 000.

Rock Type	Colour
Top of Lewisian	Purple
Top of Torridonian	Blue
Top of Mesozoic	Green
Top of Quaternary	Yellow
Igneous bodies	Red
Faults and reflecting events in Lewisian	Black

Table 7.1 Colours used to identify interfaces between rock types on the interpreted seismic sections.

7.1 Physical Properties of the Rocks

7.1.1 Precambrian Metamorphic Rocks, Lewisian.

These form the acoustic basement over the whole region. They have a high acoustic velocity of 6.0 km/sec at the near surface, modelling suggests that this rises to 6.5 km/sec at depth (Summers 1982). Where this rock is exposed on the sea-floor, refraction velocities are found to be in the range 5.0 to 6.0 km/sec calculated from the common mid-point records from the Farnella 1/81 survey, these agree with the findings of Hall and Al-Haddad (1976). Despite the metamorphic nature of these rocks the B.I.R.P.S. project has shown that it is possible to obtain coherent reflected arrivals from fault planes which pass through to the deep crust (Smythe et al. 1982). Reflections from deep crustal structures, e.g. the Moho, have not been found in the sections processed at Durham, but it is possible to see discontinuous events in the upper basement which correlate with known geological features, e.g. the Outer Isles Thrust. Stacking velocities from the B.I.R.P.S. data gives a mean interval velocity of 6.0 km/sec for the Lewisian, but this will not be as

accurate as velocity structure derived from the WISE refraction survey. From the final processed sections in areas of exposed Lewisian, the record of the sea-floor has a broken character with no apparent multiple. This is explained by the uneven surface scattering the energy preventing the formation of a coherent reflected wavefront. With the large source-receiver offset the refracted energy also interferes with the reflected arrivals. In areas with a thin layer of more recent sediments covering the basement a multiple may be seen, but the sea floor record still has a broken appearance because of the interference from the refracted arrivals. Where the Lewisian is covered by a thick sequence of later sediments, as under the Sea of the Hebrides Trough, only intermittent coherent arrivals may be seen from its surface.

The density of this rock is very high 2800 to 2850 kg m^{-3} (Telford et al. 1973, Westbrook et al. 1978). Shaw (1978) modelled the basement as two layers; an upper amphibolite gniess layer, Laxfordian, of density 2800 kg m^{-3}; and a lower granulite layer, Scourian, of density 2850 kg m^{-3}. On the Bouguer anomaly map (Fig. 7.1) areas of Lewisian outcrop are associated with gravity highs, e.g. the Outer Isles. The Tiree Platform also shows a positive anomaly except to the south west of Tiree where a cicular low probably indicates the presence of a granitic body emplaced within the Lewisian (Shaw 1978).

The aeromagnetic map (Fig. 7.2) shows broad moderate amplitude anomalies indicating that the Lewisian has some significant magnetisation. Modelling by Shaw (1978) suggests the

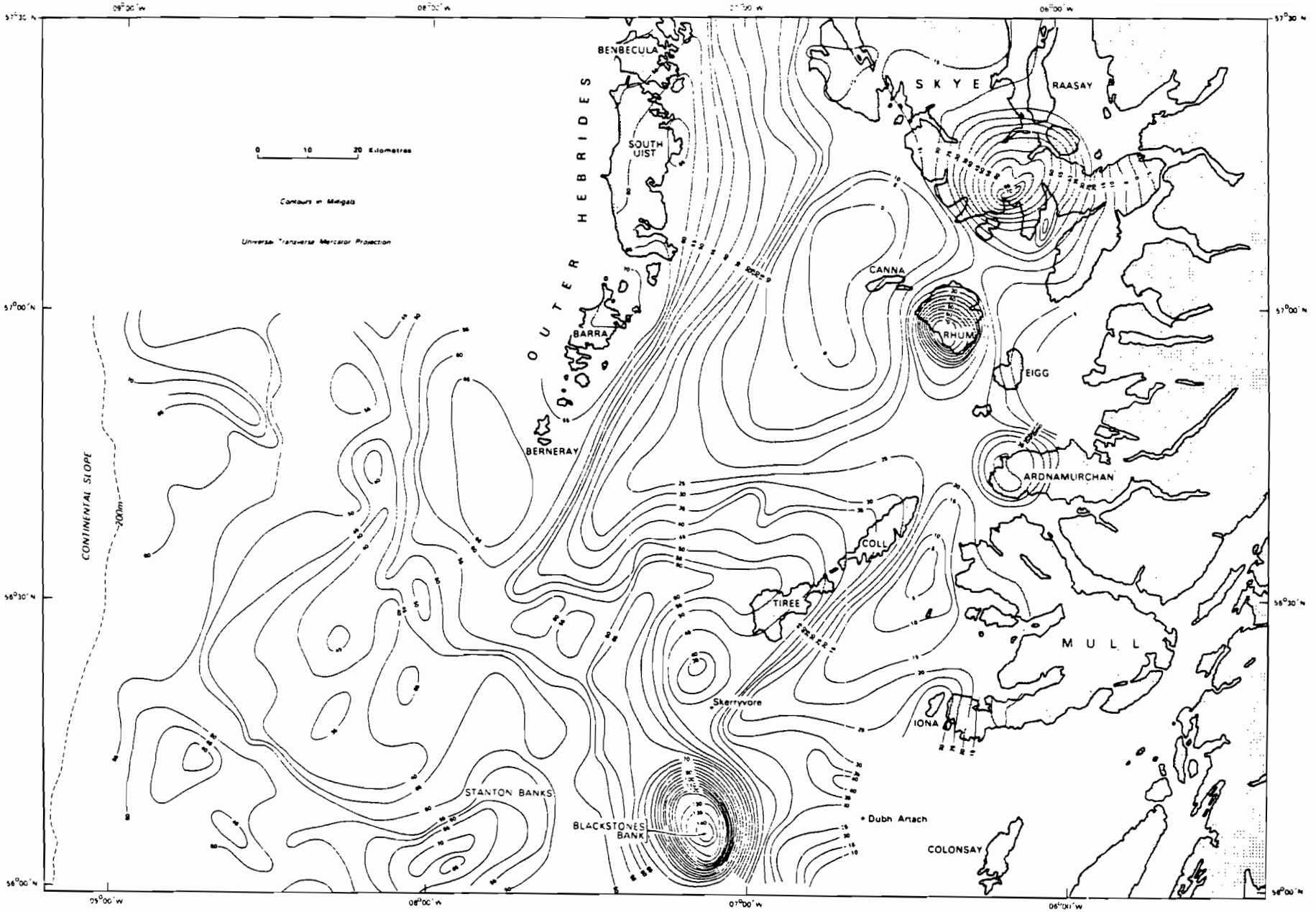

Fig.7.1 Bouguer anomaly map. After Binns et al. (1975).

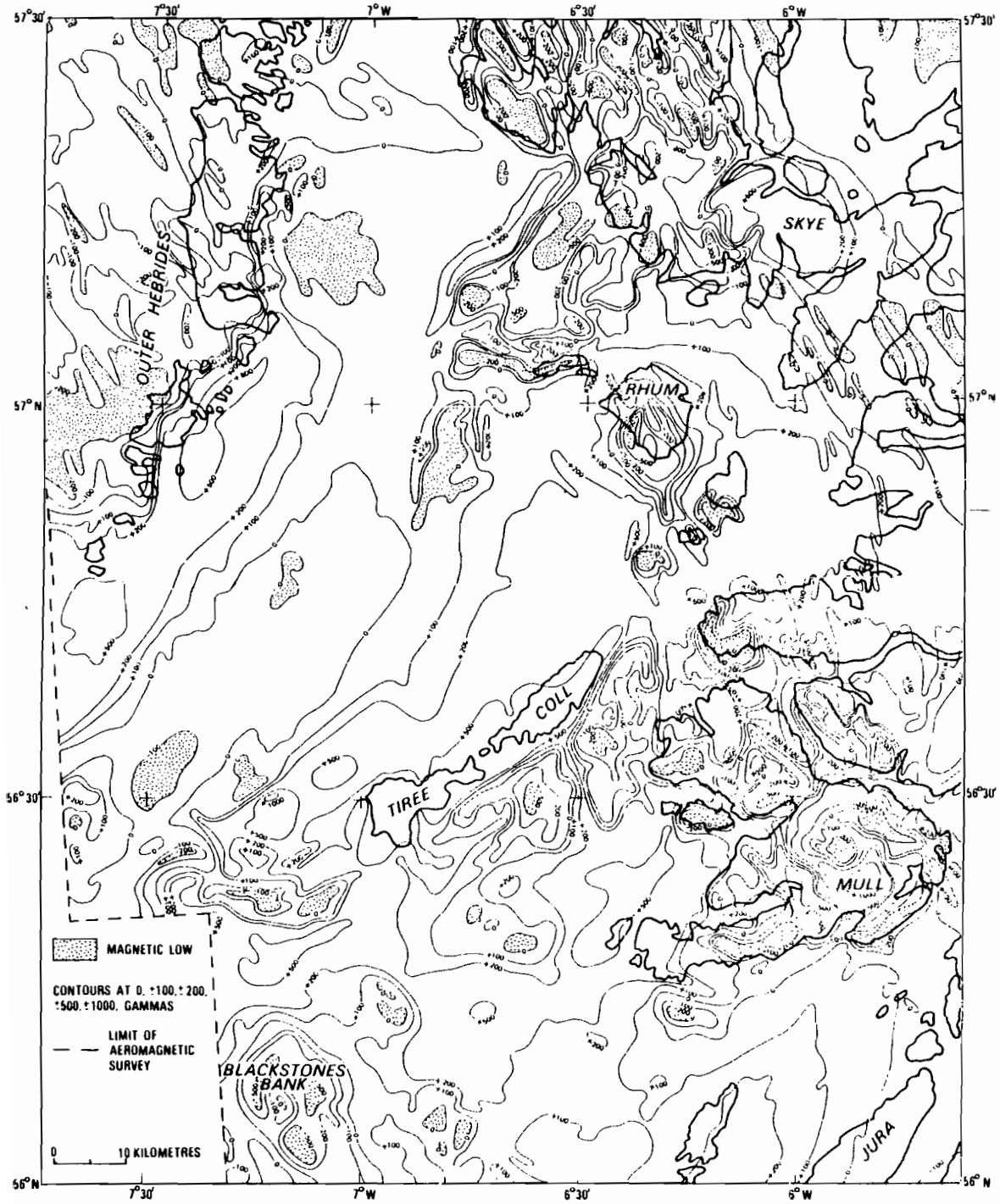

Fig.7.2 Aeromagnetic anomaly map.

Laxfordian facies has a magnetisation of 0.23 A m^{-1} and Scourian rocks have a magnetisation of 1.9 A m^{-1}. C. Uruski has recognized the linear anomaly passing through South Uist and Barra which follows the line of the Outer Isles Thrust but is quickly lost to the south of Pabbay and to the north of South Uist. As will be shown later, this anomaly can be identified on the shipborne magnetometer profile passing to the south of the Outer Isles.

7.1.2 Pre-Caledonian Orogeny Sedimentary Rocks, Torridonian

This group includes the Torridonian and a thin sequence of Lower Palaeozoic rocks. The group is predominantly made up of sandstones with some limestones and shales (Harris 1983).

The refraction seismic velocity lies in the range of 4.0 to 4.5 km/sec calculated from the Farnella 1/81 CMP gathers. The interval velocity, calculated from stacking velocities using the Dix formula (1955), give a mean value of 4.5 km/sec. The signal character on the processed sections again shows the effect of interference between the reflected and refracted arrivals where this group form the sea-floor. When covered by later sediments the uncomformity can be indentified on the Seismic Exploration Int. profile and traced on the Farnella 1/81 data. There are occasional events imaged from within the sequence but no geological significance can be implied.

This density of this group of rocks is in the range of 2650 to 2700 kg m^{-3} (Allerton 1968, Westbrook et al. 1978). This produces a negative density contrast with the Lewisian basement and in areas where there is a thick sequence an appreciable

gravity anomaly can be expected.

Magnetically they present no major anomalies and are assumed to have little magnetization.

7.1.3 Post Caledonian Orogeny Sediments, Mesozoic

These are much younger softer rocks made up of sandstones, shales and clays. They consequenty have a lower average density in the range 2300 to 2680 kg m^{-3} (Tuson 1959, Allerton 1968). As can be seen from the Bouguer anomaly map the gravity lows correlate with the major basins. Modelling by Shaw (1978) confirmed this.

Refraction seismic velocities range from 3.0 to 3.5 km/sec., with a typical average interval velocity of 3.0 km/sec as calculated from stacking velocities. The reflection character is good, clearly showing sea-floor and internal interfaces. Where the Mesozoic sequence outcrops very strong multiples are seen. On the Seismic Exploration Int. profile the structure within these sediments is seen, particularly on the eastern margin of the Sea of the Hebrides Trough.

No magnetic anomalies appear to be associated with Mesozoic sediments.

7.1.4 Tertiary Igneous Rocks

Both gravity and magnetics provide abundant evidence for presence of the Tertiary igneous rocks. The plutonic centres are clearly marked by gravity highs and large magnetic anomalies on Figs. 7.1 and 7.2, e.g. Rhum, Blackstones. Modelling by Bott et

al. (1973) and others indicate that the centres must have a density above 3000 kg m^{-3}. Farnella 1/81 line 6 crosses Blackstones Bank pluton where refraction velocities in excess of 6.0 km/sec are recorded, but no detail can be obtained from within the body.

The lava flows though not thick enough to present a significant gravity anomoly do create a range of short wavelength anomalies in the aeromagnetic survey (Fig. 7.2). Where seismic reflection profiles cross over the lavas, little coherent information can be seen below. Examples can be seen in the Farnella 1/81 line 9 south Skye. A refraction velocity of 4.0 to 4.5 km/sec is typical in this region.

Where intrusive sills have been emplaced within the sedimentary sequence a strong reflection and multiple sequence can be seen. These bodies are not sufficiently thick to give any interval velocity information, but in areas where refraction data can be determined the sills have a velocity of about 6.0 km/sec.

7.1.5 Quaternary

The recent drift has been formed by glacial action leaving behind silts, boulder clays and fluvio-glacial sands. The density is low, typically 1700 to 2200 kg m^{-3} (Telford et al. 1973). Acoustic velocities are also low at about 1.8 km/sec. In places the glacier, or its outflow, has gouged deep channels in the earlier rocks which has since been filled by later sediments.

7.2 Interpretation of the Seismic Reflection Data

The interpretation of the reflection data will be done on an area basis drawing on other data and experimental results for support as necessary.

7.2.1 South-West of Mull

The area covers the Inner Hebrides Trough south-west of Mull to the Blackstones Bank complex (Fig. 7.3). Of the reflection lines collected in this region only two have been processed, line 4 and the first part of line 6. Lunn (1984) used lines 3, 4 and 5 in an interpretation of this area based on the refraction data. The I.G.S. reflection lines 1 and 2 also extend into the basin.

Farnella 1/81 line 4

This profile crosses from west to east, starting in the Inner Hebrides Trough, passing over the projected line of the Moine Thrust south of Mull, and ending over the Dubh Artach Fault. The whole area is covered with a layer of Quaternary sediments which should not be more than 20 metres thick according to Binns et al. (1974), whereas Lunn (1984) predicts that the Quaternary sediments may be up to 200 metres thick. The detailed refraction interpretation by Lunn (1984) shows that to the west the predominant refractor velocity is 4.0 km/sec rising to 5.0 km/sec after CMP number 340. The reflection profile (Fig. 7.4) shows a well developed sequence of multiples which is consistent with the smooth sea-floor expected from glacial drift. Coherent events with angles of dip to the east of 14^{o} may be identified,

fault bounded. On crossing the Camasunary Fault a Mesozoic sequence is again expected from the geology on Skye but the refraction velocities remain high. As in the Stanton Trough, this suggests only a thin cover over Torridonian beneath. By CMP point 900 to the end of the line an eastward dipping reflector may be identified with the Moine Thrust zone. Elsewhere in the section short disjointed eastward dipping events may be seen but none can be positively identified as another thrust plane.

The Farnella 1/81 line 10 (appendix 1) follows the same course as above but in a reverse sense and with a different air-gun array. For the first part of the line a double reflection is seen of the sea-floor possibly caused by one of the air-guns firing some 800 msec late but no record of this is found in the log. Despite using a different air-gun array no further detail could be seen on this profile which has not already been mentioned above.

Summary

The structure of the basin obscured by the lavas is unclear but for the rest of the profile no other major basins are evident, to the east of the Camsunary fault some 500 metres of Mesozoic may be present. A tentative thrust plane is suggested to the east of the profile which would intersect the off shore extension of most westerly arm of the Moine Thrust Zone.

CHAPTER 8

REVIEW OF THE FARNELLA 1/81 EXPERIMENT AND THE DURHAM PROCESSING SYSTEM

This chapter presents a summary of the results obtained from the Farnella 1/81 cruise and their geological implications. A critical review of the experiment and suggestions for further work are made. The first section briefly reviews the current state of the Seismic Reflection Processing System at Durham, both hardware and software, and the possible future expansion of the facility.

8.1 The Durham Seismic Processing System

With the expansion of the facility in Durham by the purchase of extra hardware and the improvements to the software package, Durham now has a viable reflection processing facility. This may be used for the processing of small reflection surveys or the reprocessing of parts of larger surveys. During this project the hardware has been rationalized, and work by Dr. Wellby and the author on the software package has produced a suite of advanced processing programs with a high level of user documentation.

However, there is a danger that if demand increases for the facility then the system would quickly be overwhelmed. As stated in section 3.4 a throughput of 40 km per week can currently be expected. Provided the system runs continuously this would result

in 2000 km of multichannel seismic reflection profile being produced each year. This figure makes no allowance for hardware failures or time used for further software development; hardware failures should only lose a few weeks per year, but the writing of new or improved processing algorithms could easily reduce the total throughput by a significant amount. This could be alleviated by the further expansion of the system, or by having some of the processing done by outside commercial companies. The following recommendations are made.

(a) Purchase a larger more powerful host computer, such as one of the Digital Equipment Corporation VAX range. Even the Micro-VAX machine could be considered provided the system is not multi-tasked with other computational requirements. This does not mean that the system should not be networked to other computers to allow the sharing of facilities, but while reflection processing is underway the demands are such that it would not be possible to execute other jobs.

(b) Network an up-graded system or the current system with the other computers in the department and the main computer system of the university, NUMAC. This would allow the passing of data between systems to be by direct transfer rather than using magnetic tape. The writing of software could be done on a remote computer, but because of the configuration, the testing and de-bugging will have to be done on the processing system.

(c) Purchase an optical disc drive (LASER) for the storage of seismic data. The advantage of an optical disc over a

magnetic disc or tape is the increase of storage capability. Figures in the region of 20 Gbytes are quoted for a single disc that can be removed and stored away from the system. This compares with 2.5 Mbytes for the removable disc from the current Pertec drive or about 34 Mbytes on a 1600 b.p.i. tape. A single LASER disc can store all the data from a profile, along with the processing parameters and the processed sections. As the disc is a random access device, the need for permanent sorting of the common shot gathers to common mid-point gathers would be removed. The CMP gather could be generated at any required spacing or fold of cover directly from the shot records. Bulk long term storage of data then ceases to be a problem as these discs are virtually indestructable under normal conditions.

(d) Purchase a colour raster plotter. This need not be of the high resolution used for seismic sections, but sufficient to enable the display of velocity analysis, reflection strength and instantaneous frequency plots. This would aid the interpretation as well as increasing the speed of the processing.

(e) Expansion of the array processor by the addition of more memory. At present the system is well balanced but if a VAX host computer is purchased then a further increase in array processor memory size would enable better use of the increased computer power. An alternative could be the replacement of the device with a current version, which even in its smallest configuration contains more memory than

presently available.

(f) Demultiplexing of field tapes and, for single ship profiles, the CMP sorting of the data set to be done by a commercial company. For large data sets there may even be a case for the production of stacked sections by an outside company. The system at Durham could then be used to reprocess the more interesting features identified on these sections. This would also allow the research worker more time to either examine in detail a small sub-set of the data or develop new routines.

(g) If the main host computer is changed to one of the VAX family then serious considerations should be made of the software package available on the current system. The new machine would work under a different operating system, VMS, as opposed to the PDP 11/34 RT-11 system. As the operation of the seismic processing package is dependent on modifications made to the computer operating system, the software developed on the current machine could not be easily tranferred to a new computer. Therefore, the purchase of a pre-written commercial software suited to the new machine must be seriously considered.

(h) The improvement of the array processor software by the inclusion of a Fortran compiler that will take programs written in the high level language and produce array processor routines without the need of future students having to learn the machine code instructions before they can make full use of the speed of the device.

However, the most immediate requirement to ensure continued reflection processing at Durham is the commitment to keep the hardware which is currently installed under maintenance contracts.

8.2 Marine Geological Structure of the Western Isles

The interpretation presented is in general agreement with that produced by Binns et al. (1974) with Mesozoic basins lying uncomformably on lower Palaeozoic and Torridonian sediments or directly onto the Lewisian basement.

Considerable thicknesses of Torridonian sediments have been found underlying two of the four basins covered by this survey: the Stanton Trough where the Torridonian is up to 5 km thick, and the Sea of the Hebrides Trough where again over 5 km of Torridonian sediments underlie the eastern margin. Evidence is also seen for Torridonian in the Inner Isles Basin south-west of Mull and in the Barra Trough west of the Outer Isles.

Binns et al. (1974) suggest that the post-caledonian orogeny sediments are predominently Jurassic in age. This is consistent with the seismic velocities found during this experiment and Jurassic sediments found in the North Sea (Brown 1984). In the Inner Hebrides Basin these sediments are 1 km thick against the Skerryvore-Camasunary Fault to the east of Tiree and against the eastern margin of the Blackstones Bank igneous complex. The lack of Mesozoic refraction velocities over the Stanton Trough limits the thickness of Mesozoic sediments to less than 500 m. The Farnella 1/81 profile that crosses the Sea of the Hebrides Trough

between Tiree and Barra shows over 2 km of Mesozoic sediments. This is supported by gravity modelling and the results of the refraction survey presented by Summers (1982). Accurate modelling from the refraction data has not been possible as there were only three shots over the basin. The presence of Mesozoic sediments can also be seen on the I.G.S. profiles that cross the basin. On the line 3/8 that passes down the centre of the basin several major faults are crossed suggesting some east west structure. The Sea of the Hebrides trough narrows to the south because of the convergence of the Minch and Skerryvore faults .

Quaternary sediments cover much of the region normally reaching thicknesses of 100 m but as is shown north-west of Tiree a deep glacial channel has been eroded. Here the Quaternary sediments reach 200 m in thickness.

Off-shore continuations to the Moine Thrust Zone and the Outer Isles Thrust have been identified (Fig. 8.1). The Moine Thrust Zone has been found to the south of Mull and to the south of the Sleat Peninsular on Skye. From magnetic evidence and by extrapolating the plane of the thrust underlying the Sea of the Hebrides Trough, the southward line of the Outer Isles Thrust has also been mapped. Evidence for another thrust further to the west underlying the Barra Trough is shown on both the Seismic Explorations Int. profile and on the WINCH data. This is similar to the structure found on the B.I.R.P.S. MOIST profile to the north of Scotland (Brewer et al. 1984).

The eastward dipping feature seen to the south-west of the Stanton Trough is probably the basement reflector under the

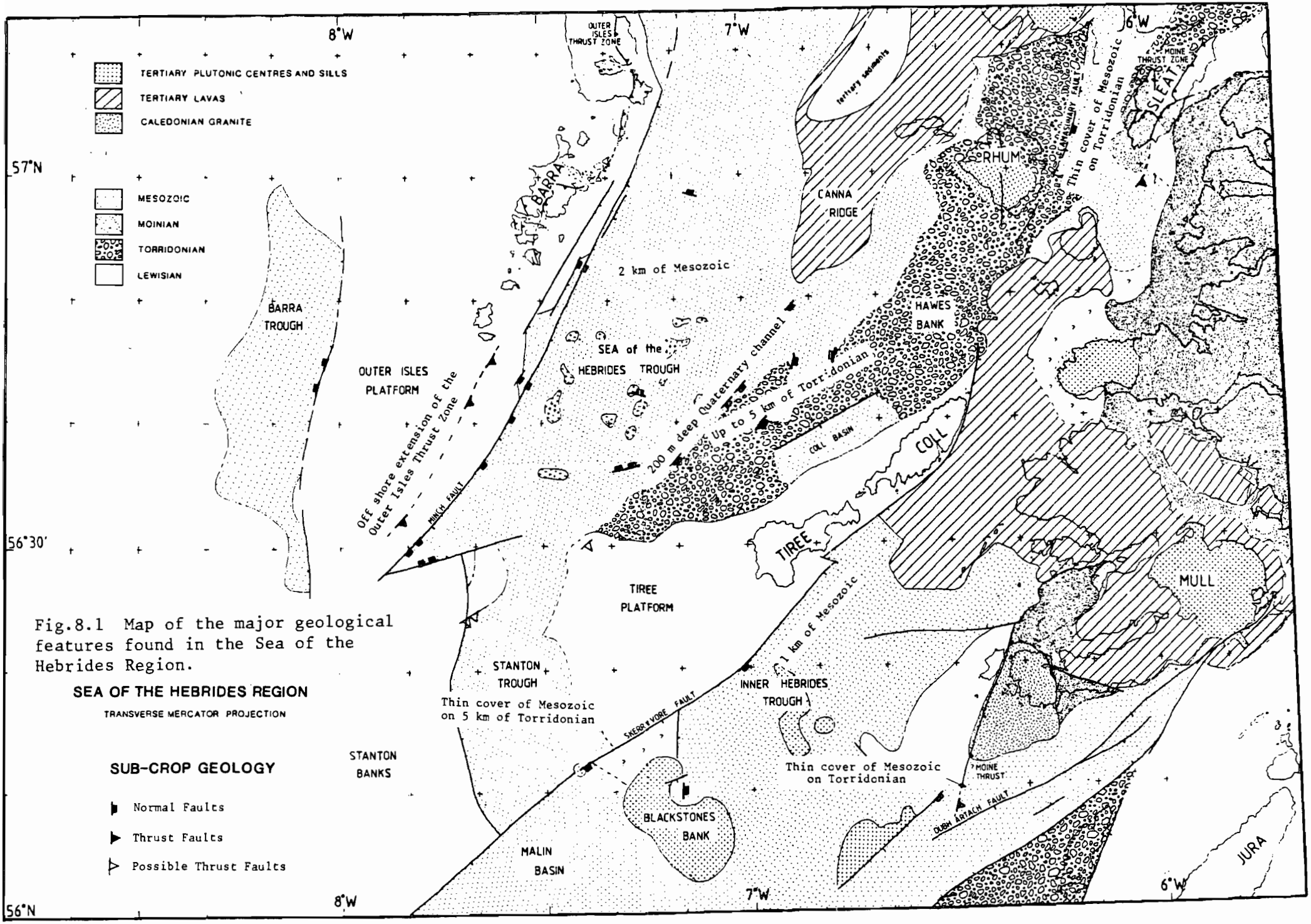

Fig.8.1 Map of the major geological features found in the Sea of the Hebrides Region.

Torridonian sequence. The other margin has a less clear westerly dipping event with it. Assuming a 100 kg m^{-3} density contrast between Lewisian and Torridonian rocks, it would need a 5 km basin to produce the observed gravity anomaly. The eastward dipping feature that is seen to the west of the trough may be evidence for a thrust plane which would run to the west of the Tiree Platform and then pass up between Canna and Rhum. Eastward dipping events in the upper crust can be seen on profiles further to the north to the west of Tiree. The existence of such a fault would enable similarities to be drawn between the Inner Isles Basin and the Sea of the Hebrides Trough; both are half graben features bound to the west by a normal fault and formed by the reactivation of a thrust fault beneath. The top of the granitic body implied by gravity south of Tiree may also be limited by this proposed thrust fault. If the granite is of the same Caledonian age as that on the Ross of Mull, it will have been emplaced towards the end of the Caledonian orogeny.

8.3 Tectonic Model for the Sea of the Hebrides Trough

With the plane of the Outer Isles Thrust forming the floor of the basin on the western margin, the shape of the Sea of the Hebrides Trough must be linked to the reactivation of Caledonian faults during the opening of the North Atlantic. The presence of 5 km of Torridonian sediments underl-ying the eastern margin of the Sea of the Hebrides Trough posed the major problem when defining a tectonic model for the basin. Assuming the Lewisian basement was a stable platform up until the Caledonian orogeny,

then creating the whole trough by reactivating the Caledonian thrust faults as low angle normal faults during the Permo-Triassic, would mean that there must have been 5 km of Torridonian sediments on top of the Lewisian at this time. Also it would have been necessary for a minimum of 30 km of movement along the Outer Isles Thrust plane to open the basin enough to accommodate this quantity of Torridonian. This hypothosis is unreasonable. Firstly, the extension of 30 km is excessive. Secondly, as the total thickness of the Torridonian and Lower Palaeozoic sediments deposited was about 7 km, this would only allow 2 km to have eroded between uplift during the Caledonian orogeny and the formation of the trough (about 200 Ma). After the formation of the trough, it would be necessary to erode the remaining 5 km from the Outer and Inner Hebridean islands in the same period of time. An alternative model is to allow the Torridonian to be deposited in a subsiding basin (Fig.8.2). This Pre-Cambrian basin was probably fault bounded, and this raises the possibility that these earlier faults may have influenced the formation of the Outer Isles Thrust during the Caledonian orogeny. As in the previous hypothesis the Mesozoic basin was formed by the reactivation of the Caledonian Outer Isles Thrust as an low angle normal fault. The second model is more realistic, as this removes the need to erode 5 km of Torridonian from Barra and Tiree since the Mesozoic, and the movement necessary on the Outer Isles Thrust to create the basin is reduced from a mimimum of 30 km to a minimum of 10 km. As the Stanton Trough and the Inner Hebrides Basin are also underlain by Torridonian

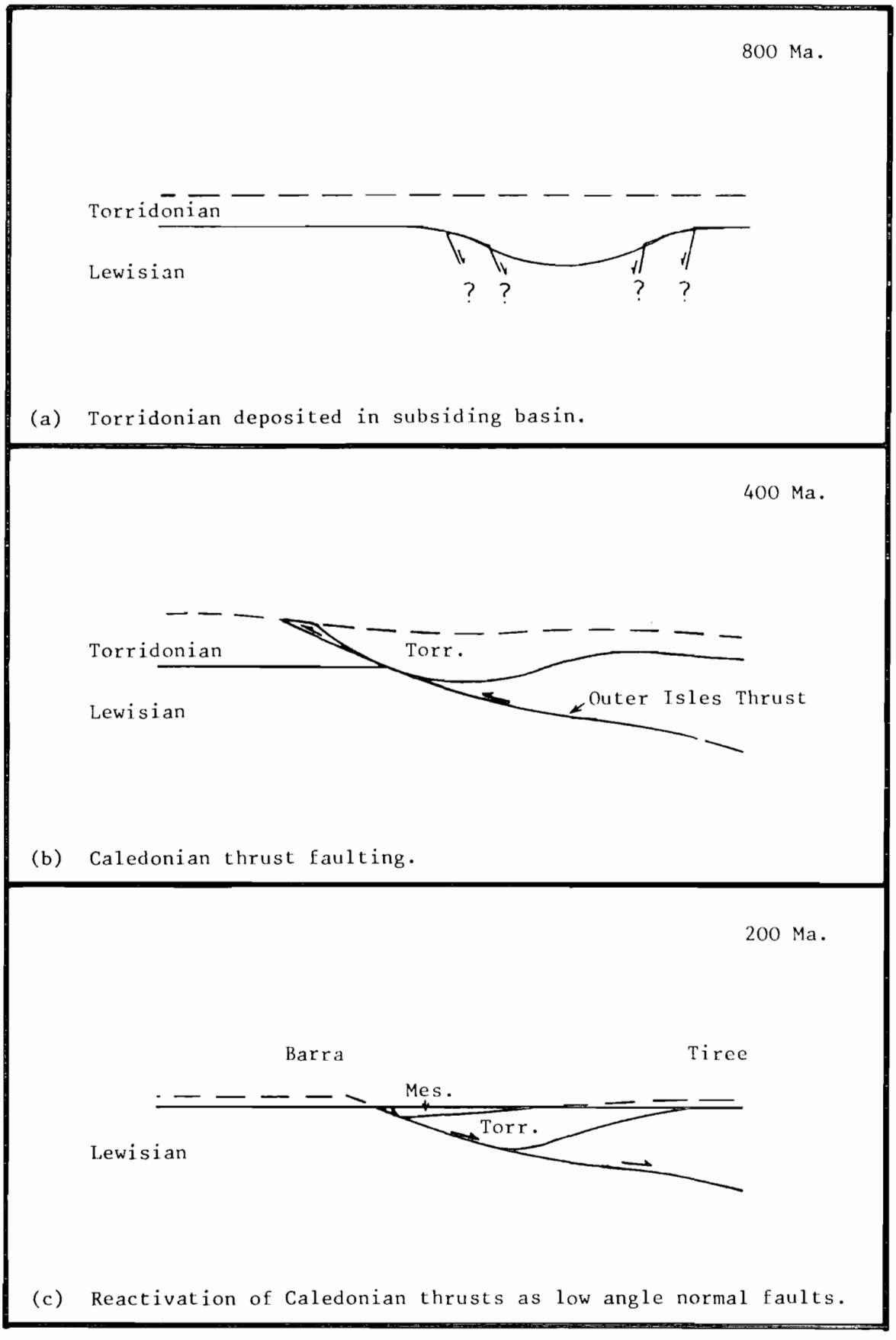

Fig.8. 2 Model for the tectonic evolution of the Sea of the Hebrides Trough.

sediments, these may also have been active basins during the Pre-Cambrian.

Problems of differential opening along the length of the Sea of the Hebrides Trough may be explained by considering the combined effect of both the Sea of the Hebrides Trough and the Inner Isles Basin. In the north, there is a large basin in the Minch, but only a narrow extension of the Inner Isles Basin off of the south coast of Skye. In the south, the situation is reversed with the wide basin to the east of the Skerryvore fault while the Sea of the Hebrides basin disappears completely. The stress in this area, and therefore the resulting extension, could have been shared between the two basins, with either all the movement occurring along the Outer Isles Thrust or sharing the movement with the thrust proposed earlier which underlies Tiree and Rhum. In either case the existence of transfer faults (Gibbs 1984b) must be postulated to share the movement between the two basins.

8.4 Critical Review of the Farnella 1/81 Experiment and recommendations for futher work

The consistent complaint throughout this thesis is the poor quality of the original data set. As is shown in section 5.3 it is important to design the reflection experiment to match the area in which the data are to be acquired. The monochromatic nature of the source shows that more thought must be given to the deployment of a source array that will give a broad frequency response. This may be done by using 6 or more guns with a

selection of air chamber sizes. In particular chambers with sizes as small as 40 in^3 should be included to increase the high frequency content. This will give better resolution of the sediments directly under the sea floor. The air supply should be from at least three independent compressors, so that in the event of one failing, or being taken out of service for repair, only a small part of the source array need be shut down. The receiver array used for the Farnella 1/81 cruise with 100 m between receiver groups was too long for the power of the source array used. When profiling over the sedimentary basins useful data from the shallow structure were only recorded on the near offset channels.

The interpretation of the reflection data acquired on the Farnella 1/81 cruise would have also been improved had both gravity and magnetics been availiable. For normal multichannel work both systems may be run without interference to the reflection work.

The time availiable for the recording of reflection seismic data on the Farnella 1/81 cruise limited the amount of profiling that could be done. Of the areas covered, the Sea of the Hebrides Trough gave the best results because of the sedimentary structure. For a more complete interpretation of this area extra profiles are needed, in particular a tie line down the axis of the basin, as the I.G.S. 1969 survey was not sufficiently processed to reveal the structure. Similarly the extension of the profiles to fully cross the Barra Trough west of the Outer Isles Platform may have revealed more information on the upper crustal

structure, in particular the dipping reflectors subsequently discovered in the Seismic Explorations Int. and the WINCH data (section 7.2.3.)

Interest by the oil industry in the area has meant that over the past six months several commercial surveys have been carried out. Results from these are as yet not available but, as has happened in the North Sea over the past twenty years, if oil reserves are found in exploitable quantities then a detailed picture of the basin geology will be built up. Even so, the following work will help with the interpretation of the region.

(a) The detailed mapping of the off-shore line of the Outer Isles Thrust to the south of Barra using a shipborne magnetometer.

(b) A detailed reflection survey over the Stanton Trough and the western edge of the Sea of the Hebrides Trough to verify the existance of an intermediate thrust between the Moine and the Outer Isles Thrust zones.

(c) A reflection survey over the Barra Trough to determine accurately its limits, structure and how the underlying thrust fault has influenced its formation.

(d) A refraction survey over the Sea of the Hebrides Trough to determine the velocity structure.

(e) The drilling of a borehole in the middle of the Sea of the Hebrides Trough to identify the strong reflectors seen on the seismic sections with particular geological horizons.

For future work in continental shelf regions a source array of at least 6 air-guns should be used with chamber sizes ranging from 40 to 400 in^3, with a total capacity of over 1000 in^3.The

receiver array should have 48 channels at a maximum spacing of 50 m between active sections. The 25 m spaced array used by Seismic Explorations Int. in their 1973 survey would be ideal. This configuration should be capable of fully resolving the near surface structure and providing evidence of deeper reflectors. With 48 active channels some resolution of deeper velocity structure would be possible. The knowledge of the deep velocity structure could be improved by the use of sonar buoys and tau-p inversion techniques (Diebold and Stoffa 1981). In areas subject to strong tidal currents like the Western Isles, the buoys would have to be anchored and have their own recorder, as disposable buoys would drift and the frequency band of their transmitters is not allowed in British coastal waters. An alternative is to use Ocean Bottom Seismometers (OBSs) (Sinha et al. 1981) or Pull-up Sea-bed Seismometers (PUSSes) (Smith et al. 1977) which would record the shots and remain on the sea-bed until recovered. Another technique is the use of the expanding spread profile (ESP) (Stoffa & Buhl 1979), where two ships move apart in opposite directions at a constant velocity keeping a common mid-point. One ship provides a powerful source signal, e.g. a large air-gun array of at least 2000 in^3 capacity or small explosive charges, while the other ship tows a standard multichannel array. The disadvantages of this technique are that it does not give good results in areas where there are dipping reflectors or faults within the ESP aperture and the expense of using two ships. For areas like the Sea of the Hebrides Trough the determination of an accurate velocity structure should be

possible using reverse refraction line techniques. As the trough is bounded on both sides by island chains, a network of stations on the Outer and Inner Hebridean Islands may be set up, supplimented by OBSs or PUSSes on the sea-bed in the trough. Several reverse refraction lines would then be shot aross the basin using a large air-gun array, 3000 in^3 or more, fired every two minutes. End to end time for each profile could be measured using explosive charges dropped from the ship close to the shore based seismometer station at either end of the profile. The results from the Caledonian Suture Seismic Project (Bott et al. 1983, Green 1984) show that accurate structure can be obtained from a seismic refraction survey.

8.5 Summary

The results from the Farnella 1/81 survey have shown the presence of significant quantities of Torridonian sediments underlying most of the basins in the region. These sediments reach 5 km thick and the model is proposed that the sediments were deposited in active basins during the Pre-Cambrian. The area was then involved in the Caledonian orogeny during which several eastward dipping thrust faults were formed, e.g. the Moine and the Outer Isles. Reactivation of these thrusts as normal faults during the period at the start of the opening of the North Atlantic created the Mesozoic basins in their present form. There is also evidence for a deep glacial erosion channel which has since been filled by thick sequences of fluvio-glacial deposits.

BIBLIOGRAPHY

ALLERTON, H.A., 1968. An interpretation of the gravity of the North Minch, Scotland. M.Sc. Thesis, University of Durham.

BARFORD, N.C., 1967. Experimental Measurements: Precision, Error and Truth. Addison-Wesley Publishing Co. Inc., 143pp.

BARRY, K.M., CAVERS, D.A., & KNEALE, C.W., 1982. SEG-C - Recommended standards for digital tape formats. Digital Tape Standards. Society of Exploration Geophsicists, 1-12.

BINNS, P. E., McQUILLIN, R., & KENOLTY, N., 1974. The Geology of the Sea of the Hebrides. Rep. Inst. geol. Sci. London, 73/14, 43pp.

BINNS, P.E., McQUILLIN, R., FANNIN, N.G.T., KENOLTY, N., & ARDUS, D.A., 1975. Structure and stratigraphy of the sedimentary basins in the Sea of the Hebrides and the Minches. In Petroleum and the continental shelf of North-West Europe. Vol. 1, (ed WOODWARD, A.W.) Applied Science Publishers Ltd. 93-102.

BOTT, M. H.P., LONG, R.E., GREEN, A.S.P., LEWIS, A.H.J., SINHA, M.C., & STEVENSON, D.L., 1985. Crustal structure south of the Iapetus suture beneath northern England. Nature London, 314, 724-727.

BOTT, M.H.P., & TUSON, J., 1973. Deep structure beneath the Tertairy Volcanic regions of Skye, Mull and Ardnamurchan, north-west Scotland. Nature Phys. Sci., 242, 114-116.

BREWER, J. A., & SMYTHE, D.K., 1984. MOIST and the continuity of crustal reflector geometry along the Caledonian-Appalachian orogen. J. geol. Soc. London, 141, 105-120.

BREWER, J.A., MATTHEWS, D.H., WARNER, M.R., HALL, J., SMYTHE, D.K., & WHITTINGTON, R.J., 1983. BIRPS deep seismic reflection studies of the British Caledonides. Nature London, 222, 206-210.

BRIDEN, J.C., TURNELL, H.B., WATTS, D.R., McCLELLAND BROWN, E. & EVERETT, S., 1982. Palaeomagnetism of the Scottish Highlands and the question of the magnitude of displacement on the Great Glen Fault. Paper presented at Symposium, Geophys. Soc. and Eur. Seismol. Comm., Leeds, United Kingdom.

BRITISH GEOLOGICAL SURVEY, 1984. Tiree Solid Geology, Sheet 56°N-08°W, 1:250 000 Series. (Compiled by EVENS, D.). Ordnance Survey Southampton.

BROWN, S., 1984. Jurrasic. In Introduction to the Petroleum Geology of the North Sea (ed GLENNIE, K.W.). Blackwell Scientific Publications, 103-132.

BUHL, P., DIEBOLD, J.B., & STOFFA, P.L., 1982. Array length magnification through the use of multiple sources and receiveing arrays. Geophysics, 47, 311-315.

BUTLER, R. W.H. & COWARD, M.P., 1984. Geological constraints, structural evolution and deep geology of the northwest Scottish Caledonides. Tectonics, 3, 347-365.

DEC, 1978a. Processor Handbook. Digital Equipment Corporation, Maynard, Mass..

DEC, 1978b. RT-11 Users Guide. Digital Equipment Corporation, Maynard, Mass..

DEC, 1978c. RT-11 System Generation Manual. Digital Equipment Corporation, Maynard, Mass..

DEC, 1978d. RT-11 Advanced Programmer Guide. Digital Equipment Corporation, Maynard, Mass..

DEWEY, J.F., 1969. Evolution of the Appalachian/Caledonian orogen. Nature London, 222, 124-129.

DEWEY, J.F., 1982. Plate tectonics and the evolution of the British Isles. J. geol. Soc. London, 139, 317-412.

DEWEY, J.F. & SHACKLETON, R.M., 1984. A model for the evolution of the Grampian tract in the early Caledonides and Appalachians. Nature London, 312, 115-121.

DIEBOLD, J.B., & STOFFA, P.L., 1981. The traveltime equation, tau-p mapping and inversion of common midpoint data. Geophysics, 46, 238-254.

DIX, C.H., 1955. Seismic velocities from surface measurements. Geophysics, 20, 68-86.

DOBRIN, M.B., 1976. Introduction to Geophysical Prospecting, 3rd edition. McGraw Hill, 630pp.

DURANT, G.P., DOBSON, M.R., KOKELAAR, B.P., McINTYRE, R.M., & REA, W.J., 1976. Preliminary report on the nature and age of the Blackstones Bank Igneous Centre, western Scotland. J. geol. Soc. London, 132, 319-326.

EMELEUS, C.H., 1983. Tertiary igneous activity. In Geology of Scotland 2nd edition, (ed CRAIG, G.Y.). Scottish Academic Press, 1-22.

FLOATING POINT SYSTEMS, 1982. Software Users Guide and associated manuals. Floating Point Systems Inc., U.S.A..

GEOQUEST INTERNATIONAL INC., 1979. AIMS Avanced Interpretive Modelling System, version 3. GeoQuest International Inc., Houston.

GIBBS, A.D., 1984a. Structural evolution of extentional basin margins. J. geol. Soc. London, 141 609-620.

GIBBS, A.D., 1984b. Structural Interpretation with emphasis on Extensional Tectonics (part 2). Joint Association for Petroleum Exploration Courses (United Kingdom), Geological Soc. London.

GREEN, A.S.P., 1984. The crustal structure beneath Northern England and ajacent marine areas. Ph.D. Thesis, University of Durham.

HALL, J., 1978. 'LUST' - a seismic refraction survey of the Lewisian basement complex in NW Scotland. J. geol. Soc. London, 135, 555-563.

HALL, J., & AL-HADDAD, F.M., 1976. Seismic velocities in the Lewisian metamorphic complex, northwest Britain - 'in situ' measurements. Scott. J. Geol., 12, 305-314.

HARRIS, A.L., 1983. The growth and structure of Scotland. In Geology of Scotland 2nd edition, (ed CRAIG, G.Y.). Scottish Academic Press, 1-22.

HOLGATE, N., 1969. Palaeozoic and Tertiary transcurrent movements on the Great Glen Fault. Scott. J. Geol., 5, 97-139.

JEHU, T.J., & CRAIG, R.M., 1925. Geology of the Outer Hebrides, Part 1 - The Barra Isles. Trans. R. Soc. Edin., 53, 419-440.

JIFON, F., 1984. Processing and modelling of seismic reflection data acquired off the Durham coast. Ph.D. Thesis, University of Durham.

JOHNSON, M.R.W., 1983. Torridonian - Moine. In Geology of Scotland 2nd edition, (ed CRAIG, G.Y.). Scottish Academic Press, 49-75.

KENT, P.E., 1975. The tectonic development of Great Britain and the surrounding seas. In Petroleum and the continental shelf of North-West Europe. Vol. 1, (ed WOODWARD, A.W.) Applied Science Publishers Ltd. 93-102.

LOVERIDGE, M.M., 1981. Residual Static Corrections. M.Sc. Thesis, University of Durham.

LU, C.H., & GUPTA, S.C., 1978. A multirate digital filtering approach to interpolation. - Application to common depth point stacking. Geophysics, 43, 877-885.

LUNN, S.F., 1984. The use of refracted arrivals from multichannel seismic reflection data to investigate the geological structure of the Iona Platform. M.Sc. Thesis, University of Durham.

LYNN, P.A., 1977. An Introduction to the Analysis and Processing of Signals. MacMillan Press Ltd., 222pp.

McKERROW, W.S., 1982. The northwest margin of the Iapetus Ocean during the early Palaeozoic. Mem. Am. Assoc. Petrol Geol., 34, 521-533

MEINERS, E.P., LENZ, L.L., DALBY, A.E., & HORNSBY, J.M., 1982. SEG-C - Recommended standards for digital tape formats. Digital Tape Standards. Society of Exploration Geophsicists, 1-12.

MITCHELL, J.G., JONES, E.J.W. & JONES, G.T., 1976. The composition and age of basalts dredged from the Blackstones igneous centre, Western Scotland. Geol. Mag., 113, 523-533.

NEIDELL, N.S., & TANER, M.T., 1971. Semblance and other coherency measures for multichannel data. Geophysics, 36, 482-497.

NIKOLIC, Z.J.,1975. Short note on a recursive time-varying band-pass filter. Geophysics, 40, 520-526.

NORTHWOOD, E.J., WEISINGER, R.C., & BRADLEY, J.J. 1982. SEG-A, SEG-B, SEG-X - Recommended standards for digital tape formats. Digital Tape Standards. Society of Exploration Geophsicists, 1-12.

NUNNS, A.G., 1980. Marine Geophysical Investigations in the Norwegian-Greenland Sea between the latitudes of 62°N and 74°N. Ph.D. Thesis, University of Durham.

PHILLIPS, W.E.A., STILLMAN, C.J. & MURPHY, T., 1976. A Caledonian plate tectonic model. J. geol. Soc. London, 132, 579-609.

POULTER, M.J., 1982. The design and implementation of the Durham University Seismic Processing System. Ph.D. Thesis, University of Durham.

RADER, C.M., & GOLD, B., 1967. Digital filter design techniques in the frequency domain. Proc. I.E.E.E., 55, 149-171.

RESEARCH VESSELS SERVICES, 1980. Report on visit to MV NORTHELLA 24th November 1980. R.V.S. Report No. 10.

ROBINSON, E.A., 1980. Physical applications of stationary time-series. London Griffin,

RYU, J.V. , 1982. Decomposition (DECOM) approach applied to wave field analysis with seismic reflection records. Geophysics, 47, 869-884.

SHERIFF, R.E., & GELDART, L.P., 1893. Exploration seismology. Vol. 1, History, theory, and data acquisition, Vol. 2, Data-processing and interpretation. Cambridge University Press, 474pp.

SHARP, R.J., PEACOCK, J.H., & GOULTY, N.R., 1985. Ultrasonic seismic modeling system. Paper presented at Eur. Assoc. of Exp. Geophysicists, 47th meeting, Budapest, Hungary.

SHAW, B.H., 1978. The structure of the crust between Jura & Barra. M.Sc. Thesis, University of Durham.

SIBSON, R.H., 1977. Fault rocks and fault mechanisms. J. geol. Soc. London, 133, 191-214.

SINHA, M.C., OWEN, T.R.E., & MASON, M., 1981. An ocean-bottom hydrophone recorder for seismic refraction experiments. Marine Geophysical Researches, 5, 173-187.

SMITH, W.A., & CHRISTIE, P.A.F., 1977. A pull-up shallow water seismometer. Marine Geophysical Researches, 3, 235-250.

SMYTHE, D.K., DOBINSON, A., McQUILLIN, R., BREWER, J.A., MATTHEWS, D.H., BLUNDELL, D.J., & KELK, B., 1982. Deep structure of the Scottish Caledonides revealed by the MOIST reflection profile. Nature London, 299, 338-340.

SOPER, N.J. & HUTTON, D.H.W., 1984. Late Caledonian sinistral displacements in Britain: implications for a three-plate collision model. Tectonics, 3, 781-794.

STANSELL, T.A., 1978. The Transit Navigation Satellite System. Magnavox Goverment and Industrial Electronics Company, 83pp.

STOFFA, P.L., & BUHL, P., 1979. Two-ship multichannel seismic experiments for deep crustal studies. J. geophys. Res., 84, 7645-7660.

SUMMERS, T.P., 1982. A seismic study of crustal structure in the region of the Western Isles of Scotland. Ph.D. Thesis, University of Durham.

TANER, M.T., & KOEHLER, F., 1969. Velocity spectra - Digital computer derivation and applications of velocity functions. Geopysics, 34, 859-881.

TELFORD, W.M., GELDART, L.P., SHERIFF, R.E., & KEYS, D.A., 1976. Applied Geophysics. Cambridge University Press, 860pp.

TOPPING, J., 1978. Errors of Observation and Their Treatment. Science Paperbacks, 119pp.

TUSON, J., 1959. A geophysical investigation of the Tertiary volcanic districts of Western Scotland. Ph.D. University of Durham.

VAN DER VOO, R. & SCOTESE, C.R., 1981. Palaeomagnetic evidence for a large (2000 km) sinistral offset along the Great Glen Fault during Carboniferous time. Geology, 9, 583-589

VERSATEC, 1976. Versaplot-07. Graphics Programming Manual. Versatec, Santa Clara, California.

WATSON, J., 1983. Lewisian. In Geology of Scotland 2nd edition, (ed CRAIG, G.Y.). Scottish Academic Press, 23-47.

WATSON, J., 1984. The ending of the Caledonian orogeny in Scotland. J. geol. Soc. London, 141, 193-214.

WESTBROOK, G.K., & BORRADAILE, G.J., 1978. The geological significance of magnetic anomalies in the region of Islay. Scott. J. geol., 14, (3).

WESTERN GEOPHYSICAL, 1971. Technical Manual. Series 1010 Geophysical Digital Recording System. Western Geophysical.

ZIEGLER, P.A., 1982. Geological Atlas of Central and Western Europe. Elsevier, New York.

APPENDIX 1

CONTENTS

CONTENTS OF MAP POCKET

Combined track chart for the reflection and refraction data used in the interpretation

Sub-crop geology map of the Hebrides region

Profile	line number	plot length (secs)	trace spacing (inches)	processing
Farnella	4	4	0.050	Pre-stack velocity filter
Farnella	4	8	0.025	Pre-stack decon. filter
Farnella CMP numbers 1 to 1400	6	4	0.050	Pre-stack velocity filter
Farnella CMP numbers 1053 to 2452	6	4	0.050	Pre-stack velocity filter
Farnella CMP numbers 1 to 1400	6	8	0.025	Pre-stack decon. filter
Farnella CMP numbers 1053 to 2452	6	8	0.025	Pre-stack decon. filter
Farnella	7	4	0.050	Pre-stack velocity filter
Farnella	7	8	0.025	Pre-stack decon. filter

Profile	line number	plot length (secs)	trace spacing (inches)	processing
Farnella	8	4	0.050	Pre-stack velocity filter
Farnella	8	8	0.025	Pre-stack decon. filter
Farnella	9	4	0.050	Pre-stack velocity filter
Farnella	9	8	0.025	Pre-stack decon. filter
Farnella	10	8	0.025	Pre-stack decon. filter
Seismic Explorations Int. CMP numbers 6241 to 10240	11	6	0.015	Pre-stack Decon. 12.5m CMP spacing
Seismic Explorations Int. CMP numbers 9729 to 13728	11	6	0.015	Pre-stack Decon. 12.5m CMP spacing
Seismic Explorations Int. CMP numbers 13217 to 17216	11	6	0.015	Pre-stack Decon. 12.5m CMP spacing

Abridged Watch Keepers Log

DAY	TIME	AIR-GUN PRESSURE p.s.i.	AIR-GUNS IN USE CENTRE 160	CENTRE 300	STBD. 160	STBD. 300	FILES LOST AT TAPE CHANGE	COMMENTS
246	0012	1000	*	*	*	*		Start line 1 Stbd. comp. on Port comp. on Fire int. 20 s.
	0042		*	*	*	*	2	Tape change
	0050		*					
	0130		*				?	Tape change
	0150		*	*		*		
	0205		*	*		*	?	Tape change
	0214		*	*		*	?	Tape scrapped Mount new tape
	0220	1600		*		*		
	0240	2000	*	*		*		
	0250		*	*		*	6	Tape change
	0320	1200		*				Stbd. comp. off
	0326			*		*		Stbd. comp. on
	0340	2000		*		*		Stbd. comp. off
	0400	2000		*		*		Stbd. comp. on
	0409			*		*	12	Tape change
	0413			*		*		End line 1
	0442			*	*	*		
	0457			*	*	*	?	Tape change
	0501	1950		*	*	*	?	Tape scrapped Mount new tape
	0524							Start line 2
	0540	1850		*	*	*	7	Tape change
	0620	1000			*			Stbd. comp. off
	0624	2000			*		6	Tape change
	0630	1900		*	*			Stbd. comp on
	0640	2000	*			*		
	0703		*			*		End line 2
	0707		*			*	13	Tape change
	0720	1850	*			*		Start line 3
	0730	1750	*			*		File counter not working
	0748		*			*	10?	Tape change
	0810	2000	*	*	*	*		
	0835		*	*	*	*		End line 3 All guns off SDS 1010 off Tape change
	1400	2000			*	*		SDS 1010 on

DAY	TIME	AIR-GUN PRESSURE p.s.i.	AIR-GUNS IN USE CENTRE 160	CENTRE 300	STBD. 160	STBD. 300	FILES LOST AT TAPE CHANGE	COMMENTS
								Start line 4
246	1440				*	*	5	Tape change
	1520				*	*	6	Tape change
	1600	1600			*	*	5	Tape change
	1615							End line 4
								All guns off
								SDS 1010 off
	1840	1850			*	*		SDS 1010 on
								Start line 5
	1904				*	*	6	Tape change
	1945	1700			*	*	8	Tape change
	2020				*	*		End line 5
	2027				*	*	8	Tape change
	2029	2000			*	*		Start line 6
	2045				*	*		End turn
	2148	2020			*	*	5	Tape change
	2229	2100			*	*	6	Tape change
	2310	2010			*	*	6	Tape change
	2320				*	*		Start turn
	2335				*	*		End turn
	2351	2020			*	*	7	Tape change
247	0000	2020			*	*		
	0032	2020			*	*	6	Tape change
	0113	2000			*	*	5	Tape change
	0155	2000			*	*	5	Tape change
	0200	2000			*	*		Start turn
	0222				*	*		End turn
	0235	2000			*	*	5	Tape change
	0317	2000			*	*	6	Tape change
	0358	2000			*	*	5	Tape change
	0436	2000			*	*	7	Tape change
	0519	2000			*	*	7	Tape change
	0600	2000			*	*	7	Tape change
	0640	2000			*	*	8	Tape change
	0722	2000			*	*	6	Tape change
	0804	2000			*	*	6	Tape change
	0843	2000			*	*	6	Tape change
	0906				*	*	6	Clock problem
	0908				*	*		Clock O.K.
	0924	2000			*	*	6	Tape change
	0930	1900		*	*	*		
	0950			*	*	*		Start turn
	1004			*	*	*		End turn
	1007			*	*	*		End line 6

DAY	TIME	AIR-GUN PRESSURE p.s.i.	AIR-GUNS IN USE CENTRE 160	CENTRE 300	STBD. 160	STBD. 300	FILES LOST AT TAPE CHANGE	COMMENTS
								Start line 7
247	1045	2000		*	*	*	6	Tape change
	1115	2000		*	*	*	7	Tape change
	1200			*	*	*		Course change
	1209	2050		*	*	*	7	Tape change
	1250	2000		*	*	*	5	Tape change
	1330	2020		*	*	*	6	Tape change
	1350	2020		*		*		
	1415	2100		*		*	7	Tape change
	1453	2020		*		*	6	Tape change
	1533	2100		*		*	5	Tape change
	1615	2100		*		*	4	Tape change
	1654	2050		*		*	5	Tape change
	1735	2050		*		*	4	Tape change
	1740			*		*		Start turn
	1813			*		*		End turn
	1815			*		*		End line 7
							5	Tape change
								Start line 8
	1855	2000		*		*	4	Tape change
	1921	2000		*		*	18	SDS 1010 died
	1927			*		*		SDS 1010 on
	1942	2050		*		*	6	Tape change
	2019	2000		*		*	6	Tape change
	2104	2000		*		*	7	Tape change
	2145	2000		*		*	6	Tape change
	2226	2050		*		*	5	Tape change
	2305			*		*		End line 8
								Air-guns off
								SDS 1010 off
								Tape change
248	1326			*	*			SDS 1010 on
	1405			*	*		6	Tape change
	1420	2030		*	*			Start line 9
	1446	2000		*	*		6	Tape change
	1527	2050		*	*		7	Tape change
	1609			*	*		18	Tape change
	1645	2000		*	*		5	Tape change
	1736	2000		*	*		5	Tape change
	1818			*	*		9	Tape change
	1857			*	*			End line 9
								Tape change

DAY	TIME	AIR-GUN PRESSURE p.s.i.	AIR-GUNS IN USE CENTRE 160	CENTRE 300	STBD. 160	STBD. 300	FILES LOST AT TAPE CHANGE	COMMENTS
248	2003	1800		*	*			Start line 10
								Stbd. comp. off
	2043	2000		*	*		6	Tape change
	2048			*	*			Course change
	2056			*		*		
	2122			*		*	4	SDS 1010 fault
	2125			*		*	10	Tape change
	2206	2020		*		*	6	Tape change
	2249	2000		*		*	4	Tape change
	2315	2150		*		*		SDS 1010 error rate increasing
	2328			*		*	5	Tape change
	2347			*		*		End line 10
								Air-guns off
								Tape change
249	0000							Noise records
	0010							SDS 1010 off

Decca Readings Converted to Latitude and Longitude by Decca Co. Ltd.

DAY	TIME	DECCA POSITION Red	Green	Purple	LATITUDE	LONGITUDE
246	0000	1E17.18		1G73.78	56°17'11.059N	6°54'10.335W
	0400	1G10.34		1I59.08	56° 5'29.622N	6°24' 7.800W
	0530	1G 3.90		1I67.57	56° 3'50.828N	6°29'44.011W
	0700	1F20.16		1H62.36	56°12'18.564N	6°35'36.959W
	0740	1F12.22		1H57.46	56°13'39.130N	6°41'22.392W
	0840	1E22.85		1H58.02	56°14' 0.601N	6°51'19.616W
	1430	1F14.90		1H73.30	56°10' 3.096N	6°40' 3.161W
	1600	1G 8.55		1H79.96	56° 7'45.936N	6°25'50.815W
	1910	1G 6.24		1H75.28	56° 8'58.234N	6°27'49.060W
	2000	1G 3.06		1H54.39	56°13'58.098N	6°30'16.819W
	2100	1F17.01		1G77.76	56°15'41.651N	6°37'27.260W
	2300	1E21.29		1H73.25	56°10'55.211N	6°53'49.117W
247	0000	1E11.30		1I51.62	56° 9'51.143N	7° 2'37.958W
	0200	1D15.89		1I59.14	56°10' 2.799N	7°20' 8.921W
	0300	1D 5.68		1H73.89	56°13'47.220N	7°26'44.475W
	0900	1A21.99		1E70.79	56°37'40.987N	7°59'48.383W
	1100	1A13.85		1D69.66	56°44'17.410N	7°58'25.590W
	1700	1D10.29		1D77.12	56°35'31.177N	7° 2'30.984W
	1900	1D13.47		1D60.93	56°39' 9.257N	7°57'53.954W
	2200	IB10.83		1B66.26	56°49'48.740N	7°15'54.319W
248	1400	1E13.51	1E40.02		56°11'24.537N	7°30'23.150W
	1800	1H10.20	1E40.02		56°11'24.537N	6°30'23.150W
	2000	1H10.80	1E36.92		56°57' 3.865N	6° 3'22.918W
	2300	1F 7.84	1E40.98		57° 8'21.018N	6°21'55.921W

SDS 1010 Specifications

Number of input channels	24 data 6 auxillary
Maximum input signal	250 mV
Input impedance	500 ohms
Minimum gain	32 dB
Automatic gain range	90 dB
Attack rate "burst out"	3000 dB/sec
Release rate	200 dB/sec
Sample rate	4 msec
System resolution (A/D)	15 bits including sign
Data code	15 bits in 2bytes,1's complement
Redundancy check	Odd lateral parity
Accuracy	+/- 1/2 least sig. bit
Tape speed	20 i.p.s.
Tape format	SEG-A (IBM compatible)
Tape packing density	800 b.p.i.
Tape tracks	9